Wavelength Dependence and Picosecond Spectroscopy in the Photochemistry of Co(III) Complexes

Aramice Y. S. Malkhasian

A Thesis

in

The Department

of

Chemistry

Presented in Partial Fulfilment of the Requirments
for the degree of Doctor of Philosophy at
Concordia University
Montréal, Québec, Canada

October 1984

ABSTRACT

Wavelength Dependence and Picosecond Spectroscopy in the Photochemistry of Co(III) Complexes

Aramice Y. S. Malkhasian, Ph.D.
Concordia University, 1984

The work reported in this thesis contain three intereleted areas:

The first area was conventional photochemistry in which we studied the substitution quantum yield in the various region of the visible electronic spectrum for the complexes $Co(NH_3)_5Cl^{2+}$ and $Co(en)_2Cl_2^+$ where X = Cl^- and A = NO_2^-, SCN^-. The results prove without any doubt the wavelength dependence of this yield as well as the possibility of more than one state participating in the reaction.

The second area which was studied was the MCD (magnetic circular dichroism) spectrum of the above complexes. In this case, it reveals two new terms in the spectra . It was clear from these spectra that the spin forbidden bands have an A term as well as a B term. This study also allows us to place the quintate state near the first singlet state. Consequently this means that it excludes any participation of the quintet state near the first singlet state in the mechanism of reaction.

II

The last area of study was the transient absorption spectra of the above complexes whose wavelength dependence implies rapid processes related to vibrational relaxation. Among these compounds only the ones which have a π level revealed a short lived transient. The relaxed excited state was assigned as a triplet state. Reactivity similar to Rh(III)-amine complexes was, in consequence, assigned to Co(III)-amine triplets.

Acknowledgements

I wish to express my thanks to the following people My supervisor Prof. Cooper H. Langford for his guidance and assistance which will always be remebered.

Prof. Bryan Hollebone at Carleton University for running the MCD spectra and his assistance in the theoretical aspect of photochemistry and MCD spectrocopy and also for fruitful discussions.

The government of Iraq for financial support during my three year stay in Canada.

Dedication

I would like to dedecate this thesis to my grandfather Sarkis Malkhasian ,whos survival of the 1914 Armenian masscare made the existence of my family possible.

To my parents, aunt and entire family

List of Contents

List of figures

Chapter 1

Chapter 2

Chapter 3

Chapter 4

Chapter 5

List of tables

Chapter 3

Chapter 4

List of Symbols

CT	Charge Transfer
LF	Ligand field
LMCT	Ligand to Metal Charge Transfer
MLCT	Metal to Ligand Charge Transfer
MCD	Magnetic Circular Dichroism
λ	wavelength
ε	extinction coefficient
Φ	Quantum Yield
Φ_p	Phosphorescence Quantum yield
k	rate constant
k_f	fluorescence rate constant
isc	intersystem crossing
Δ	Octahedral Energy Field splitting
B	Racah parameter
C	Racah parameter
τ	Lifetime of the species
τ_S	Singlet lifetime
η	viscosity coefficient
E_{app}	apparent activation energy
S	Singlet state
T	Triplet state

Chapter I

Overview and Review

1.1 Introduction

1.1.1 Statement of the problem .

This thesis deals with the ligand field photochemistry of low spin $Co(NH_3)_5Cl^{2+}$ and $Co(en)_2XA^+$ complexes where X = Cl^- and A = NO_2^-, SCN^-. These complexes (which are called Werner complexes since they are among those in Werner's classic structure work) have local octahedral approximate geometry, some examples of which are shown in Fig. 1).

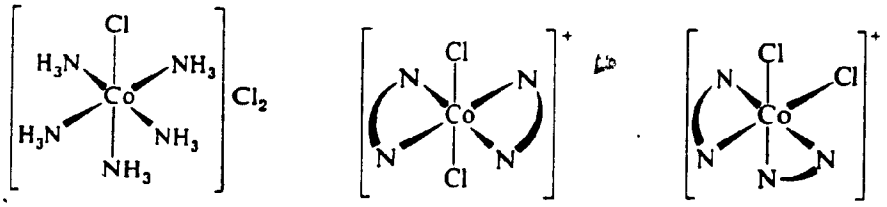

Fig. 1 structure of some Werner Co(III)-amines .

Early photochemical studies were well reviewed in Balzani and Carasitti's book (1) and a recent review has been prepared by Zinato (2). The most fundamental photochemical reactions of metal Co(III) complexes can be divided into 1) photoredox and 2) photosubstitution according to equations (1.1.1) and (1.1.2),respectively.

$$Co(NH_3)_5X^{2+} \longrightarrow Co^{II}(NH_3)_5 + X \cdot \begin{cases} \nearrow Co(NH_3)_5OH_2^{3+} + X^- \\ \searrow Co(II)_{aq} + 5NH_3 + X^- + \text{Amine oxid. prod.} \end{cases} \qquad (1.1.1)$$

$$Co(NH_3)_5X^{2+} \longrightarrow \begin{cases} Co(NH_3)_5H_2O^{3+} + X^- \\ Co(NH_3)_4H_2OX^{2+} + NH_3 \end{cases} \qquad (1.1.2)$$

The first reaction occurs with energy of excitation in the charge transfer (CT) region while the second occurs in the low energy ligand field region (LF) . In contrast to several other metal complex systems, wavelengh (energy) dependence of reaction yields is not limited to the distinction between charge transfer and the ligand field regions. Within each region there is variation of yield. The availability of tunable lasers and picosecond flash photolysis has made the detailed study of of this wavelength dependence possible . It is, therefore, practical to begin asking detailed question about the excited state origins of the various modes of reaction and the lifetimes of the states responsible. Here the focus is on ligand field states. Such questions had naturally to raise question about detailed assignment of spectra . This problem may be open to improved analysis by magnetic circular dichroism (MCD) spectroscopy .

1.1.2 The spectra of Co(III)-amines complexes.

Co(III) has the electronic configuation $[Ar]3d^6$ and forms low spin hexacoordinate complexes with all ligands of greater field strength than F^-. In O_h symmetry, the ground state, $^1A_{1g}$, has the electronic configuratuion t_{2g}^6.The lowest energy spin allowed excited states are $^1T_{1g}$ and $^1T_{2g}$

with the $t_{2g}^5 e_g^1$ configuration. Two bands appear at 472 and 338 nm for $Co(NH_3)_5Cl^{2+}$ which are assigned to these transition(3). The $^1T_{1g}$ splits to $^1E_{1g}$ and $^1A_{2g}$ in C_{4v} and D_{4h} symmetry whereas $^1T_{2g}$ splits to $^1E_{1g}$ and $^1A_{2g}$. The assignment of ligand field parameters has been discussed by Wentworth and Piper (4). The corresponding triplets $^3T_{1g}$ and $^3T_{2g}$ are assigned in $Co(NH_3)_5Cl^{2+}$ to a very weak band near 770 nm and a shoulder at 580 nm. The quintet state which forms by promotion of two electrons to the e_g orbital is difficult to place experimentally. Any absorption band for it would be very weak. The most recent calculation by Solomon and Wilson (5) located it between $^3T_{1g}$ and $^3T_{2g}$.

In the uv region one finds the charge transfer transitions of mononuclear metal complexes of these types fall into two classes (6): I- cases with an electron originally localized on the central metal which is excited to an orbital localized on the ligand (metal to ligand charge transfer, MLCT);

II- complexes with an electron originally in an orbital localized on one or several ligands and excited to an orbital localized on the metal(ligand to metal charge transfer, LMCT). In the same region one often also finds transitions at wavelengths similar to bands of free ligands. These are usually assigned as intra-ligand transitions(often $\pi \longrightarrow \pi^*$). In the case of Co(III) complexes, according to this classification, CT spectra have been discussed by many workers. A good reference is Balzani et al. (3). Also, an important review is by

Balzani et al. (3). Also, an important review is by Adamson et el. (7). Among the latest reviews is that of Endicott. (8).

In the specific case of Co(III)-amines, where the complex contains ligands like halides with π electrons, a band appears which may be assigned as a ligand to metal charge transfer LMCT. In $Co(NH_3)_5X^{2+}$ a higher energy band is the ligand σ to σ^* like the band in $Co(NH_3)_6^{3+}$.

The lower energy band found near 300 nm in $Co(NH_3)_5I^{2+}$ and 260 nm in $Co(NH_3)Br^{2+}$ is assigned as a ligand σ to a metal e_g, ref. (9,10). In the case of ligands with vacant π^* levels, an inverse charge transfer (MLCT) is possible. This transition is well characterized only for complexes of diimine ligands (bipyridine, phenanthroline) (11).

1.1.3 Thermal Substitution reactions:

Substitution reactions of Co(III) complexes occurring without the intervention of a photon have been extensively studied. In acidic media the hydrolysis reaction is the typical mode. It is represented in equation (1.1.3)

$$Co(NH_3)_5X^{2+} + H_2O \underset{k_{anation}}{\overset{k_{hydrolysis}}{\rightleftharpoons}} Co(NH_3)_5H_2O^{3+} + X^- \text{---(1.1.3)}$$

The linear free energy relationship with slope of unity for change of leaving group establishes the notion that every change in metal ligand bond strength is parallel to a change in activation energy. Thus, conversely, the relation implies that the rate of the reverse reaction is

insensitive to the entering X^- anion. These are the tests of a dissociative reaction. In contrast to the photochemistry, loss of NH_3 is slow enough not to be observed.

Related studies (12) support the idea that dissociative substitution characterized the $Co(en)_2AX^+$ family as well (where A and X are as halogen or other monovalent anion, with X the leaving group.) The stereochemistry of substitution in the family cis and trans $Co(en)_2AX^+$ is dominated by cases where retention of geometry is observed. This suggests that the entering ligands attack cis to the leaving group. Any five coordinate structure (transition or intermediate) is square pyramidal in this case. The exception is where the A ligand is a π donor. In this case isomerization (trans attack) is observed. The simplest explanation is based on π donation stabilization of a trigonal bipyramid form of the five coordinate state.

1.2 Review of Co(III)-amine and related photochemistry.

1.2.1 Charge transfer photochemistry.

1.2.1.1- $Co(NH_3)_6^{3+}$: The irradiation of this compound at 254 nm results in only photo redox decomposition yielding Co(II) (5) and an oxidation product

$$Co(NH_3)_6^{3+} \xrightarrow[H_3O^+]{h\nu} Co^{(II)}_{(aq)} + \text{amine oxid. prod.} \quad (1.2.1)$$

$$Co(NH_3)_6^{3+} \xrightarrow[H_3O^+]{h\nu} Co(NH_3)_5H_2O^{3+} + NH_4^+ \quad (1.2.2)$$

A possible mechanism for the above reaction was given by Endicott and Hoffmann (13,14). An intramolecular oxidation-reduction reaction between the central metal and one of ligands is postulated as a consequence of ligand σ orbital to metal e_g charge transfer

$$Co(NH_3)_6^{3+} \xrightarrow{h\nu} Co(NH_3)_5^{2+} + {}^{\cdot}NH_3 \quad (1.2.3)$$

According to this interpretation, the redox products follow from the dissociation of the radical from the Co(II) fragment and the completion of the oxidation of the amine radical by reaction with the solvent. On the other hand, a solvent separated radical pair state regenerates NH_3 and an aquated Co(III) complex.

1.2.1.2- $Co(NH_3)_5Cl^{2+}$: Endicott and Hoffman (14) reported that 254 nm irradiation corresponded to the $\sigma(Cl) \longrightarrow e_g(Co)$ charge transfer band. An acid solution of this complex undergoes a photoredox reaction. The rate of Co(III) disappearance was equal to the rate of Co(II)

formation. Consequently, no photoaquation occurs by irradiation at 254 nm.

According to Moggi et al. (16) 254 and 313 nm irradiation caused two simultaneous photoreactions. During irradiation the spectral changes below 300 nm were remarkably different from those expected on the basis of the sole photoredox reaction. The changes in absorbance showed that one product is trans-$Co(NH_3)_4(H_2O)Cl^{2+}$, which actually absorbs more than $Co(NH_3)_5Cl^{2+}$ below 300 nm. They concluded that substitution also occurs beside the oxidation-reduction photodecomposition. Consequently, they suggest the following mechanism:

$$Co(NH_3)_5Cl^{2+} \begin{cases} \rightarrow Co(II) + \text{other product} \\ \rightarrow \text{trans-}Co(NH_3)_4(H_2O)Cl^{2+} + NH_4^+ \end{cases} \qquad (1.2.4)$$

The quantum yield for Co(II) formation was found to increase from 0.13 to 0.34 with decreasing acidity of the medium from 0.93 N to 4.4 10^{-3} N acid. Temperature (37°C - 60°C) and absorbed light intensity (53×10^{-4} — 8.9×10^{-4} Einstein l^{-1} min^{-1}) were found to have no effect on quantum yield. These observations are consistent with the model proposed for $Co(NH_3)_6^{3+}$ above.

1.2.1.3- $Co(NH_3)_5I^{2+}$: Haim and Taube (15) irradiated solutions of $Co(NH_3)_5I^{2+}$ in 0.1 N $HClO_4$ with 254 nm radiation corresponding to $\sigma(I) \longrightarrow e_g(Co)$ CT band. On the basis of the observed 1:2 ratio between I_2 and Co(II)

formed, they proposed the following overall reaction

$$2Co(NH_3)_5I^{2+} + 10H^+ \xrightarrow{h\nu} 2Co(II) + 10NH_4^+ + I_2 \text{-----(1.2.5)}$$

This reaction was found to obey zero order kinetics. A quantum yield 1.94 for Co(II) formation was calculated. Later, Endicott and Hoffman (14) observed that the quantum yield of the photodecomposition of $Co(NH_3)_5I^{2+}$ at 254nm was not very reproducible and was strongly dependent on the intensity of absorbed light. This intensity dependence was explained by Haim and Taube (15) according to the following mechanism. The reaction (1.2.5) :

$$Co(NH_3)_5I^{2+} \xrightarrow[H^+]{h\nu} Co(II) + 5NH_4^+ + I^\cdot \text{ ----------(1.2.6)}$$

is rapidly followed by the reaction (1.2.6):

$$Co(NH_3)_5I^{2+} + I^\cdot + 5H^+ \longrightarrow Co(II) + I_2 + 5NH_4^+ \text{----(1.2.7)}$$

which is in competition with recombination of I atoms

$$2I^\cdot \longrightarrow I_2 \text{ ----------(1.2.8)}$$

In such an hypothesis, as the light intensity increases the rate of reaction (1.2.8) increases more than the rate of (1.2.7) so that a decrease in Co(II) quantum yield is expected.

1.2.1.4- cis and trans-$Co(en)_2Cl_2^+$: The photoredox of trans $Co(en)_2Cl_2^+$ was investigated by Endicott and Hoffman (14) by irradiating at 254 nm which corresponds to the $\sigma(Cl) \longrightarrow e_g(Co)$ charge transfer band. The Co(II) quantum yield was found to be 0.09 and 0.07 independent of the acidity of the medium, absorbed light intensity and addition of $NaClO_4$. Moggi et al. (16) found the presence of formaldehyde as an oxidation product of

ethylenediamine while no evidence for the existence of chlorine was found. For cis complexes, irradiation at 254 nm gave rise only to oxidation - reduction decomposition; on the other hand, 313 nm light caused, in addition to the redox decompostion simultaneous Cl^- aquation ($\Phi \simeq 10^{-2}$) without a change in geometrical configuration. For example:

$$cis\text{-}Co(en)_2Cl_2^+ \xrightarrow[H_2O]{h\nu} cis\text{-}Co(en)_2(H_2O)Cl^{2+} + Cl^- \text{--(1.3.9)}$$

For trans isomers irradiation at 254 and 313 nm caused the oxidation-reduction decomposition as well as Cl^- aquation reaction leading to cis products ($\Phi \simeq 10^{-2}$).

1.2.1.5 trans-$Co(en)_2(NCS)Cl^+$: The emphasis on this compound as investigated by Vogler and Adamson (17) in both the CT and LF regions, was mainly on two points.

1- Was there any spectrospecificity to photoaquation of Co(III)amine? (This can be studied using a complex of the type CoA_4XY^+ for which two relatively similar aquations are possible). Should the ratio of photoaquation of group X to that of group Y be spectrospecific?

2- The thermal reaction chemistry of the aqueous ion has been studied in detail, and only chloride aquation occurs (the observed product being a 50-50 mixture of isomers of $Co(en)_2(H_2O)NCS^{2+}$.) The irradiation of the first LF band of trans-$Co(en)_2(NCS)Cl^+$ in aqueous solution results in a very low quantum yield, with a ratio of thiocyanate to chloride aquation of 1:6. Photoredox

reaction was negligible at this wavelength. Irradiation of the first CT band leads to a reaction with a total quantum yield of 0.013, of which 66% comprises Co(II) production and the remainder aquation. The ratio of the two aquations is 6:3. The results confirm qualitative photolysis rules for Co(III)amines (7). The pathway for irradiation of the first CT band were discussed by using the following homolytic bond fission mechanism :

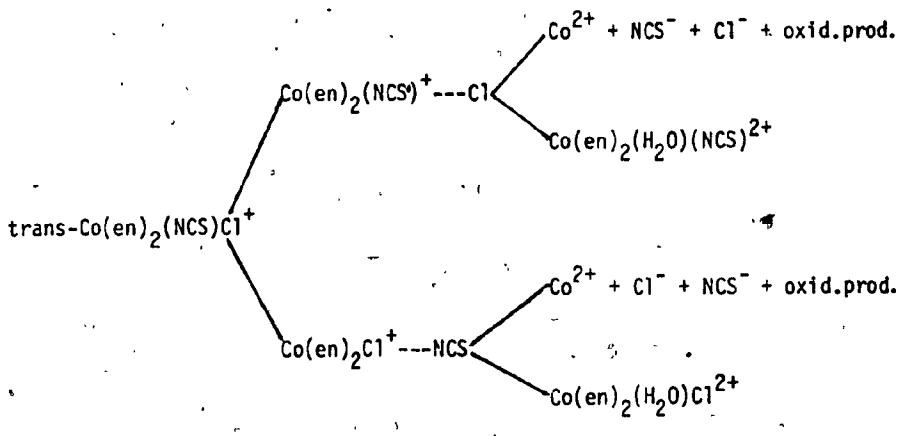

1.2.2 Visible region low yield substitution:

As we have seen in the previous section, the photochemical reaction in the CT region is mostly photoredox with some associated aquation. The photochemical feature which dominates the visible, ligand field band, region is photosubstitution reaction (and photoisomerization). Any remaining oxidation-reduction processes are assigned to tails of charge transfer bands under the ligand

field bands. Attention will focus on the following complexes; $Co(NH_3)_6^{3+}$, $Co(NH_3)_5X^{2+}$, cis and trans $Co(en)_2X_2^{2+}$.

1.2.2.1- $Co(NH_3)_5Cl^{2+}$ and trans $Co(en)_2Cl_2^{+}$:

Pribush et al.(18), thoroughly studied with a high resolution laser the $Co(NH_3)_5Cl^{2+}$ and trans- $Co(en)_2Cl_2^{+}$, complexes using the Ar-ion line at 488 nm. Later Langford and Vuik (19) extended the work on $Co(NH_3)_5Cl^{2+}$ to the wavelengths 514 and 647 nm. their results and conclusions, consistent with earlier less high resolution work, were:

1- a small value of Co(II) yield is attributable to a small component of CT in the transition where photoaquation is the dominant mode of reaction.

2- Both halide ligands and ammonia are replaced by water. This contrasts with thermal chemistry where halide ligands are much more labile than ammonia. At 488 and 514 nm the reactivity pattern is similar to the pattern of photolabilties discovered for Cr(III) complexes which Adamson labeled "antithermal".

3- The spectra of solutions of trans-$Co(en)_2Cl_2^{+}$ which are irradiated to progressively greater extents of photolysis, indicate mostly trans-$Co(en)_2(H_2O)Cl^{+}$. This means the reaction is stereoretentive.

4- For irradiation of $Co(NH_3)_5Cl^{2+}$ at 488 nm and 514 nm the quantum yields for the aquation of both ligands are $\Phi_{NH_3} \cong 50 \times 10^{-4}$ and for $\Phi_{Cl^-} = 17 \times 10^{-4}$;the ratio $\Phi_{NH_3} / \Phi_{Cl^-}$ is 3:1 (for $Cr(NH_3)_5Cl^{+2}$ the ratio is 30:1.)

Adamson's rules (20) 1 and 2 predict ammonia aquation to be preferential: These seem to be only mildly applicable in this case. In contrast, the result at 647 nm produced $\Phi_{Cl^-} > \Phi_{NH_3}$, in opposition to the Adamson's rule order and more like thermal dissociation.

1.2.2.2- cis-$Co(en)_2Cl_2^+$ (21,22) : For the cis compound the reactions are more complex than for trans. The interpretation of product distributions is complicated because of a second photoreaction of cis-$Co(en)_2(H_2O)Cl^{2+}$. After correction for secondary photolysis, it can be shown that cis-$Co(en)_2Cl_2^+$ gives $\Phi_{Cl^-} = 0.0024$ with 70 - 75% of trans aquo product while 25 - 30% is cis aquo product. Study of the 2°C reaction shows that cis-$Co(en)_2Cl(H_2O)^{2+}$ photoisomerizes to trans with a yield 0.0042. The trans aquo isomer appears to be photoinert. It should be noted that the 2°C reactions do not include further aquation(22).

1.2.2.3-cis and trans $Co(en)_2(NH_3)Cl^{2+}$: Pribush et al. (23) also examined these species using 488 nm radiation in acidic media. The resulting quantum yields for ammonia substitution (14.8×10^{-4} and 2.06×10^{-4}) and chloride aquation (2.96×10^{-4} and 3.1×10^{-4}) for trans-$Co(en)_2(NH_3)Cl^{2+}$ and cis-$Co(en)_2(NH_3)Cl^{2+}$ respectively, suggest that photolysis rules are similar to those for Cr(III) amines. A product isomer analysis for trans-$Co(en)_2(NH_3)Cl^+$ gave 80 - 82% trans $Co(en)_2(H_2O)Cl^{2+}$ and 18 - 20% of trans-$Co(en)_2(NH_3)Cl^{2+}$. For cis-$Co(en)_2(NH_3)Cl^{2+}$

the results show that Φ_{NH_3}/Φ_{Cl^-} was 0.66 while product analysis shows the presence of four products with an 80/20 ratio of cis to trans-$Co(en)_2(NH_3)H_2O^{3+}$ and likewise trans to cis-$Co(en)_2(H_2O)Cl^{2+}$ (with large error). These results show that the yield for chloride aquation is about the same as for the trans complex while for ammonia aquation, yields in the cis complex are sharply reduced. This last observation is to be expected since ammonia is now not on the axis predicted to be labilized by Adamson's rules. The overall situation is more involved of course than for the trans isomer. Labilization of the N - end of the axis activates one end of an ethylenediamine ligand. Following a previously proposed mechanism they suggest a) recoordination and hence no net reaction occurs or b) edge displacement of ammonia takes place, leading to the observed main isomer, trans-$Co(en)_2(H_2O)Cl^{2+}$ the scheme is shown in figure 1.2. A third possibility, that of edge displacement of chloride, is considered to be unlikely in view of its remote position.

1.2.3 Cyanide complexes: It is now useful to give information on Co(III) complexes with different behavior, especially $Co(CN)_6^{3-}$ (24). Unlike Co(III)-amines, this ion luminesces and reacts with higher quantum yield.

Also the family $Co(CN)_5X^{3-}$ ($X = Cl^-$, Br^-, I^-) (25,26,27) gives a higher yield than the corresponding pentammines. $Co(CN)_4SO_3X^{4-}$ (28) ($X = SO_3^{2-}$, OH^-, or H_2O)

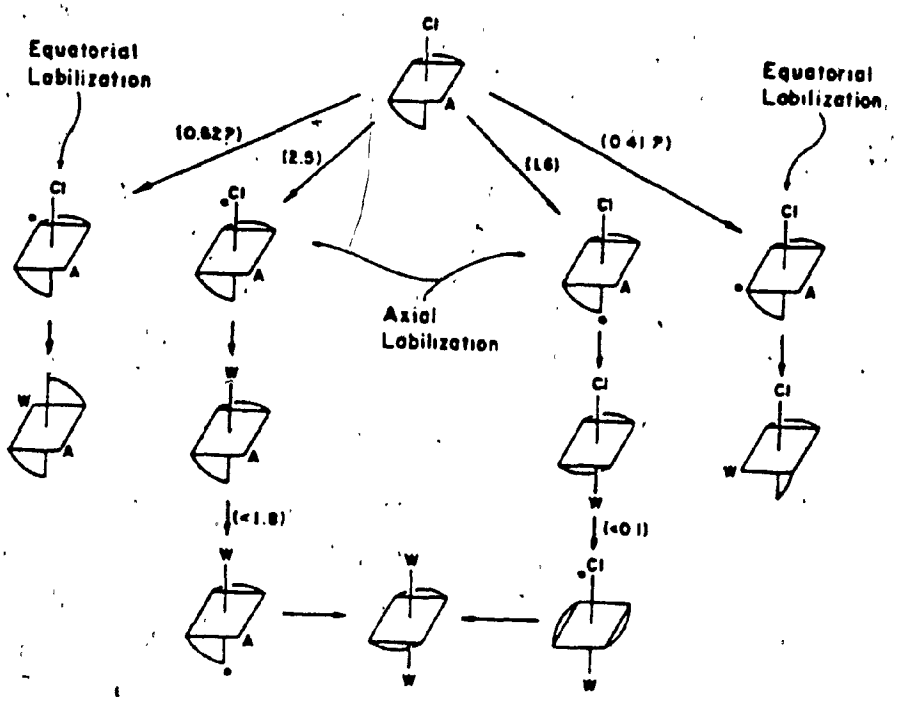

Figure 1.2 Expected Photolysis products for cis-$Co(en)_2(NH_3)Cl^{2+}$ assuming either axial or equatorial ligand labilization from ref. (23)

complexes are of considerable interest because their excited state reactivity pattern shows an important difference from their ground state behaviour.

1.2.3.1- The photophysical and photochemical behavior of $Co(CN)_6^{3-}$: In solution, there are three principal bands found in the absorption spectrum (24). At 50,000 cm^{-1}, there is a very intense band with (ε_{max} = 1.6 x 10^4). Two weak bands appear at 32,100 cm^{-1} (ε_{max} = 180) and at 38,600 cm^{-1}(ε_{max} = 160). These are presumably the LF bands. Mingardi and Porter (24) found another weak band at 18,500 cm^{-1} which could be seen only in the crystal because it is masked by the tail of the more intense UV band in solution. The extinction coefficient at the band maximum is approximately 0.01. It is assigned as a triplet. The emission spectrum of crystalline $K_3Co(CN)_6$ was measured by the same workers. A broad band with a maximum at 14,400 cm^{-1} and a half width of about 2,000 cm^{-1} was observed in the crystal at 4.2 and at 77 K. The luminescence is distinctly visible as a red glow. As we mentioned earlier on assigning the absorption band of $Co(CN)_6^{-3}$ the weak absorption band is assigned as $^3T_{1g} \longleftarrow A_{1g}$ (18,500 cm^{-}). The emission may be assigned to the reverse transition Stokes shifted. An investigation of the photochemical behaviour of $Co(CN)_6^{3-}$ has been carried out by Moggi et al. (25). Excitation was performed by using 254, 313 and 366 nm radiation. The photochemical experiments were carried out in the media of 1 x 10^{-2} N aqueous H_2SO_4, pH

5.5, and pH 7.5 buffer solutions. In all experimental conditions (except in the case of the pH 7.5 buffered solutions irradiated at 254 nm) photoreaction is the simple aquation reaction:

$$Co(CN)_6^{3-} \xrightarrow[H_2O]{h\nu} Co(CN)_5H_2O^{2-} + CN^{-1} \text{----------(1.2.11)}$$

The quantum yield of the photoaquation reaction was found to be 0.31 ± 0.03 at 25°C, independent of the wavelength of irradiation, reaction medium and complex concentration. This value is in fair agreement with the quantum yield obtained by Adamson and Sorper (26) who excited at 370 nm an aqueous solution of the complex. At 50°C and 75°C quantum yields of 0.35 and 0.38 were obtained.

1.2.3.2-$Co(CN)_5Cl^{3-}$, $Co(CN)_5Br^{3-}$, $Co(CN)_5I^{3-}$:

The photochemical behaviour of aqueous solutions of these complexes was studied by Adamson and Sorper (26,27). They observed a progressive change in the absorption spectrum of the irradiated solutions terminating in that of $Co(CN)_5H_2O^{2-}$. This indicates that light causes the aquation of X^- ion.

$$Co(CN)_5X^{3-} \xrightarrow[H_2O]{h\nu} Co(CN)_5H_2O^{2-} + X^- \text{----------(1.2.12)}$$

For $Co(CN)_5Cl^{3-}$ and $Co(CN)_5Br^{3-}$ photoexcitation was performed with 370 nm radiation corresponding to ligand field band excitation. For $Co(CN)_5I^{3-}$, 370 and 550 nm radiation was used, which corresponds to the tail of a charge transfer band (ε_{max}= 330 nm : ε_{max} = 3630) and to a ligand field(500 nm, ε_{max} = 87). The quantum yield values

obtained by Adamson and Sorper(26,27) for photoaquation of $Co(CN)_6^{3-}$ and $Co(CN)_5X^{3-}$ complexes at 370 nm decrease in the order $I^- < CN^- < Br^- < Cl^-$. The authors noted that this order is not the one of the spectrochemical series, but is the order of increasing difficulty of oxidation of the ligand. This suggests a reaction via a redox pathway.

1.2.3.3-trans- $Co(CN)_4(SO_3)X^{n-}$ (X = SO_3^{2-}, OH^-,or H_2O)

These complexes were studied by Wrighton et al. (28) at wavelengths of 254, 313, 366 or 434 nm. The thermal aquation of trans-$Co(CN)_4(SO_3)_2^{5-}$ was sufficiently rapid to compete with photochemical reaction. The electronic spectra in the UV -visible region for trans-$Co(CN)_4(SO_3)_2^{5-}$ show bands at 317 and 380 nm. trans-$Co(CN)_4SO_3(H_2O)^{3-}$ shows bands at 363 and 380 nm and $Co(CN)_4SO_3H^{2-}$ bands at 260 and 370 nm. The photoreaction under irradiation of a LF band at 366 nm and a CT band at 260 nm for these sulfito complexes are summarized by the following steps:

$$\text{trans-}Co(CN)_4(SO_3)_2^{5-} \xrightarrow[OH^-]{h\nu} \text{trans } Co(CN)_4(SO_3)OH^{4-} + SO_3^{2-} \qquad (1.2.13)$$

$$\text{trans-}Co(CN)_4(SO_3)OH^{4-} \xrightarrow[OH^-]{h\nu} Co(CN)_4(OH)_2^{3-} + SO_3^{2-} \qquad (1.2.14)$$

$$\text{trans-}Co(CN)_4(SO_3)(OH_2)^{3-} \xrightarrow[H_2O]{h\nu} Co(CN)_4(OH_2)_2^{-} + SO_3^{2-} \qquad (1.2.15)$$

$$\text{trans-}Co(CN)_4SO_3(OH_2)^{3-} \xrightarrow{h\nu} \text{reduction to Co(II)} \qquad (1.2.16)$$

Reactions (1.2.13) and (1.2.14) are carried out at pH 13 whereas (1.2.15) and (1.2.16) were in 0.01 $HClO_4$. Mechanistic discussion for the observed photoreactions must account for the wavelength dependent quantum yield, the specific effect of the sulfito group, the photoreduction to yield Co(II) and the suppression of the initial rate of disappearance of $Co(CN)_4(SO_3)_2^{5-}$ upon addition of Na_2SO_3. Substitution via a CT state should yield a preferential loss of the sulfito group since the primary step would be homolytic cleavage of $Co-SO_3$ bond. Invoking the CT excited state adequately accounts for increase in quantum efficiency upon 254 nm excitation relative to 313 nm irradiation for aquo and hydroxo complexes. In contrast to CT excited states, ligand field excited states are thought to yield only substitution chemistry analogous to other Co-CN systems.

1.3 The role of solvents in photoreactions of metal complexes:

Our studies, in common with a number of others, indicate that the solvent can play a significant part in determining photoreaction yields. This is both an opportunity and a problem. It offers an opportunity since it provides an additional parameter against which to test mechanistic hypotheses. It is a problem because the effect of the solvents can be quite subtle and it is not easy to vary only one solvent parameter at a time.

In this introductory section, we review five roles which may be played by solvents in reactions of the type studied here. A possible example of each of these roles is given. Unfortunately, the problem is underlined by the fact that we cannot be sure of the assignment in these examples.

1.3.1 Cage effect (29)

A chemical reaction in the liquid phase is significantly affected by transport processes in the solvent that control the movement of reactants toward or apart from each other. On the one hand, there is the uncontrolled statistical molecular motion leading to large overall displacements on a longer time scale which are described as a diffusion of the reactants in a quasicontinuous solvent medium with the appropriate boundary conditions at the reaction surface. From this one obtains a

steady state diffusion controlled reaction rate constant which in its simplest approximation, is inversely proportional to bulk shear viscosity of the solvent (30).

This phenomenon is important to the reaction of short lived species. When radicals or similar hot species are formed, surrounding solvent molecules tend to cage them together. The probabilty of a recombination back reaction is inversely related to the rate of diffusional separation. The homogeneous recombination of halogen atoms in various solvents is well described as a function of viscosity. A systematic study of this effect for iodine photodissociation was carried out by Noyes (31) and co-workers using solvents of various viscosity and with variation of the excitation wavelength. They observed a decrease of photodissociation quantum yield with increasing wavelength, i.e. decreasing excess energy available for conversion to kinetic energy of the separating atoms and increasing viscosity of the solvent. It was not clear, however, whether other solvent parameters were of importance.

In consequence, viscosity dependent quantum yield may be interpreted as evidence for a cage effect and reactive intermediates susceptible to recombination. The exact correlation between this effect and (Φ) remains controversial despite numerous studies especially in the field of organic photochemistry (32). For this reason various data processing procedures were investigated. Zink et al. (33) applied Noyes theory (34,35), originally developed to treat the scavenging of photoproduct radical

pairs in solution, to the charge transfer photoreaction of tris(dibenzyldithiocarbamato)iron(III) with halogenated hydrocarbons. According to this treatment, (Φ) should depend linearly on $\eta^{-0.5}$, which indeed was found to be the case in some studies (36). A possible example of a simple and classical cage effect is found in the photolysis of $Co(NH_3)_5Br^{2+}$ in the region 300 nm > λ > 254 nm (8).

1.3.2 Analog of the effect of the solvent polarity on ionic thermal reaction:

Although the bridge between thermal reaction and photochemical reaction is ambigious, still we could find commonground between both subjects in terms of initial and final (or transition) states. What follows is an example for the simple role of solvent polarity on both thermal and photochemical reactions. Recently solvolysis of trans dichlorobisethylenediamineCo(III) has been studied by Groves and Wells (37) in a mixture of water propan-2-ol. They found a plot of log(rate constant) against Grunwald-Winstein Y factor was linear. The Y parameter is a well documented measure of the local polarity of the solvent system and its ability to solvate a developing charge in the transition state (38). Values for the Grunwald-Winstein Y values were calculated for water + propan-2-ol. from the rate data of Robertson and Sugamori (39). Y represents the effect of the solvating power of the solvent on the process (initial state)$\longrightarrow$(transition state) for an I_d type such as solvolysis of t-butylchloride where the

extension of the C-Cl bond in the transition state to form separate ions is virtually complete in water + alcohol mixture. Groves and Wells (37) suggested that linearity in the plot of log(rate constant) versus Y values supports the view that there is considerable heterolytic extension of the Co-Cl bond in the transition state for solvolysis in these mixtures.

In contrast, they found only a non-linear plot for log(rate constant) against the reciprocal of the dielectric constant. Incidentally, minima in the transition state parameter observed at mole fractions of propan-2-ol where the decrease in the partial molar volume of propan-2-ol has a minimum suggest that solvent structure has considerable influence on the rate. A free energy cycle applied to the process (initial state) $\longrightarrow$ (transition state) in water and in the solvent mixture show that it is The change in the solvation of the transition state which is the dominant effect. The above study illustrates the best known solvent polarity effect. No quantified photo-chemical case is a clear parallel. However, some studies have produced results which might be interpreted similarly.

In one study by Langford and Tipping (40), photo-solvolysis of $Cr(NH_3)_6^{3+}$, $Cr(NH_3)_5Cl^{2+}$, $Cr(CH_2CH_2NH_2)_5Cl^{2+}$, $Cr(CH_3CH_2CH_2NH_3)_5Cl^{2+}$ was carried out in water and DMSO. Phosphorescence of $Cr(NH_3)_6^{3+}$ is completely quenched in base but the loss of NH_3 is not. In the pentamines

both NH_3 and Cl^- are lost. They suggested the photosolvolysis arose in the quartet excited state and not the phosphorescence doublet. This was interpreted in terms of a tetragonal distortion model of quartet behaviour . Solvent effects were different for NH_3 and Cl^- loss. In the case of NH_3, yield increased slightly in DMSO. In contrast, DMSO, which has a small Winstein Y, suppresses Cl^- loss. If the key to the reaction is quartet tetragonal distortions, a solvation requirement, parallel to the above transition state requirement, could account for the suppression of Cl^- loss.

1.3.3 Reaction controlled by Nucleophilicity and solvent orientation:

Photonucleophilicity is interesting because important differences from nucleophilicity in a thermal reaction may arise. In thermal reaction, a nucleophile may lower the barrier for substitution by the stabilization of the transition state through new bond formation. A nucleophile in photoreaction may be involved with an excited state which lies at an energy well above the thermal substitution barrier. In that case, it may play a role in the selection of relaxation channel rather than in lowering a barrier. Nevertheless, this selection may result from bond formation. In photoreactions, the decays from a high energy state can lead to non-equilibrium effects not operating in the pseudo equilbrium model of transition state theory. A notable example is the problem of solvent reorientation. A

nucleophile must form a bond to an excited state to provoke substitution. The time for reorientation of a solvent molecule such that the nucleophilic group is correctly directed, can be the rate determining process.

Wong and Kirk (41) studied the photosolvation of trans-$Cr(NH_3)_2(NCS)_4^-$ and trans-$Cr(en)_2(NCS)F^+$ in various water methanol, ethanol, acetonitrile, ethyleneglycol, glycerol and acetone mixtures and in aqueous solutions of polyvinylpyrolidone. They found that the quantum yield for thiocyanate loss from $Cr(en)_2(NCS)F^+$ to be fairly independent of solvent, while for thiocyanate loss from trans-$Cr(NH_3)_2(NCS)_4^-$ it is large. At higher concentrations of organic solvent, specific reductions of quantum yield were observed. They claimed that for negative ions the water in the solvation sphere is not appropriately oriented for nucleophilic substitution and must rotate in order to substitute.

Another similar study was done by Cusumano and Langford (42) using trans-$Cr(NCS)_4(NH_3)_2^-$ and trans-$Cr(en)_2(NCS)_2^+$ in the solvents H_2O, DMSO, DMF, CH_3CN, CH_3NO_2 and water- glycerol mixtures. They found that the quantum yield for the reaction of cation complex is a linear function of the Guttman donor number of the solvent parameter which closely parallels Winstein's Y. This supports an associative mechanism for photosubstitution at Cr(III) which had been suggested on the basis of stereochemistry and of course a role for a solvent nucleophile.

Cusumano and Langford (42) claimed that nucleophilic attack on a very short lived species is indicated by the fact that the reaction of the otherwise similar anion correlates only with solvent fluidity (reciprocal of viscosity). They suggested that a solvent molecule which is correctly oriented toward the metal center can achieve rapid nucleophilic attack. They didn't find any significant temperature dependence in the reaction of the cation. Thus, they argue that photonucleophilic attack is not an activated process analogous to thermal nucleophilic attack. They claim the role of a good nucleophile appears to be to select the reactive relaxation route.

1.3.4 Local environmental effect on the probability of absorption leading to selectivity.

The assumption that a unique chemical species is involved in all photochemical and photophysical process may be an over simplification. At any instant, a variety of solvent arrangements obtain about dissolved transition metal complexes. Only if the interconversion rates between these solvates are rapid compared to reaction rate is it appropriate to speak of a single solvated chemical species in the usual statistical manner. Conti and Forster (43) have observed phenomena attributed to multiple solvates of $Cr(CN)_6^{3-}$ in H_2O at room temperature with interconversion rates apparently less than 10^7 s^{-1}. In these experiments emission was pumped at different wavelengths in the red edge of the $^4T_2 \longleftarrow {}^4A_2$ absorption band. The existence of

more than one species with interconversion times in excess of the ^2E lifetime was inferred from the excitation wavelength dependence of emissions. The different excitation wavelength dependence of τ also has been observed in a mixture of two solvents. Since water is a quencher of $Cr(CN)_6^{3-}$ phosphoresence, the longer lifetime in 80% glycerol-water is to be expected. If long wavelength excitation in the mixed solvent selects solvates with higher proportions of water in the solvation sphere, the lifetime should approach that found in aqueous solution. Much, if not all, Cr(III) photochemistry originates in $^4T_2$ while the lifetime of solvates of $^4T_2$ is not known, The $^4T_2$ lifetime is likely to be much shorter than the ^2E lifetime. If solvate relaxation is slow enough, in some cases to lead to multiple ^2E lifetimes, multiple solvates should also prevail on the time scale appropriate to $^4T_2$ reactions . It is then possible that photochemical and photophysical measurements at different wavelengths do not pertain to the same species. Also, comparison of direct and photosensitized processes may be misleading if one solvate is preferentially excited or is a more efficient acceptor in energy transfer.

1.3.5 Solvent perturbation of Hamiltonian for state to state crossing:

According to "Hollebone theory" (44,45) specially Cr(III) octahedral complexes the medium must provide a quadrupole operator to couple the asymmetric stretch mode to the asymmetric buckle mode. This coupling is thus required for $^2E \longleftrightarrow {}^4A_2$ if ΔV is 3 (ΔV is the change of the vibrational angular momentum quntum number).

The thermal substitution reaction of trans-$Cr(NH_3)_2(NCS)_4^-$ is quite sensitive to deuteration of the amine ligands. This was attributed to the role of H - bonding of the N—H moiety to the solvent (46). The selection of trans solvent molecules for interaction with a medium gives a quadrupole perturbation. Lifetimes of this complex in various media can be understood from this point of view. The fastest relaxation occurs in water and other hydroxide solvents. Good H - bonding acceptors which are large molecules (and subject to some steric crowding limits) are intermediate. The longest lifetimes are associated with poor H - bond acceptors like CH_3CN and CH_3Cl.

1.4 Magnetic circular dichroism:(47,48)

A brief introduction to MCD spectroscopy is given here because MCD spectra are used in chapter (4) to improve the precision of our understanding of spectra of Co(III) complexes employed in this work:

The Faraday effect in its simplest form may be expressed by the equation

$$\phi = VHl \qquad \text{----------(1.4.1)}$$

where ϕ is the angle of rotation of plane of polarization of a linearly polarized beam when it travels through a sample of thickness l, parallel to magnetic field H , and V is the Verdet constant characteristic of a given substance and a function of concentration, temperature, and frequency. An compact generalization of equation (1.4.1) is:

$$\hat{\phi} = \phi - i\theta = \frac{\pi}{\lambda} l\,(\hat{n}_- - \hat{n}_+) = \int_0^l V\, H(l)\, dl \text{---------(1.4.2)}$$

$\hat{\phi}$ is the complex magnetic rotation whose real part (ϕ) is rotation and imaginary part (θ)is the ellipticity.

$\hat{n}_-$ is the complex refractive index for left circularly polarized (l.c.p) light and n is the complex refractive index for the right polarized (r.c.p) light.

$\hat{n}_-$ is defined by $\hat{n}_- = n_- - iK_-$ while similarly, $\hat{n}_+ = n_+ + iK_+$ In these equations, K corresponds to the absorption index. In order to extract useful chemical information from the Faraday effect, it is necessary to relate the experimentally observed quantity.(θ,ϕ)to molecular properties. This can be done by calculating ($K_- - K_+$) directly using conventional time dependent perturbation used in calculating the

absorption coefficient. The electric field vector of a circularly polarized light wave travelling in the positive z direction is:

$$\vec{E_{\pm}} = 1/\sqrt{2}\,(\vec{i} + \vec{ij})\,E_o \exp\,[2\pi i\nu(t - n_{\pm} z/c) \quad \text{--------(1.4.3)}$$

where the subscripts + and - denote r.c.p and l.c.p respectively, $\vec{i}$ and $\vec{j}$ are unit vectors along the x and y axes of a right handed coordinate system. Further, proceding in the manner of refrence (49), the energy of interaction between the light wave and a molecule is given by $-\vec{m}.E_{\pm}$ where $\vec{m} = \sum_i e_i \vec{r_i}$ is the electric dipole operator, following the derivation of ref. (49,50), we obtain the absorption coefficient α associated with a transition from state a to a higher state j

$$\alpha_{\pm} = \frac{4}{hc}\,(N_a - N_j)\,f(\nu,\nu_o)\,|\langle a \mid m_{\pm} \mid j\rangle|^2 \quad \text{----------} \quad (1.4.4)$$

where N_a and N_j are the numbers of molecules per unit volume in state a and j respectively, $f(\nu,\nu_o)=(E_a - E_j)/h$ is a frequency function defining the absorption line $\int(f/\nu)d\nu = 1$ and $m_{\pm} = m_x \pm i m_y$.

α is defined in the usual way from the Beer-Lambert law as:

$$I = I\,e^{-\alpha l} = I\,e^{-4\pi\nu K/c} \quad \text{----------(1.4.5)}$$

Since we are dealing with an electric transition, in most cases $N_j \simeq 0$, it then follows from equations 1.4.2,4 and 5 that for transition $a \longrightarrow j$

$$\theta = \frac{1}{4}(\alpha_- - \alpha_+) = \pi^3/ch \sum_{a \longrightarrow j} N_a\, f(\nu,\nu_o)[\,|\langle a|m_-|j\rangle|^2 - |\langle a|\,m_+|j'\rangle|^2\,] \quad \text{-- (1.4.6)}$$

where the sum is over all degenerate components of the

transition.. If a constant magnetic field, H_z is applied along the z axis, the wave functions and energy levels of the system are perturbed, the perturbing energy being

$$- \mu_z H_z = (L_z + 2S_z) H_z \quad \text{----------(1.4.7)}$$

where μ_z, is the z-component of the magnetic dipole moment operator, is the Bohr magneton and L_z and S_z are the z-component of the total orbital and spin angular momentum operators respectively, measured in a unit of $h/2\pi$. By the use of perturbation theory, explicit expressionsforthe energy and wave function of any state $|k\rangle$ may be obtained correct to first order in the magnetic field

$$E_k = E_k^\circ - \langle k^\circ | \mu_z | k^\circ \rangle H_z \quad \text{----------(1.4.8)}$$

$$|k\rangle = |k^\circ\rangle - \sum_{j \neq k} \frac{\langle j^\circ | \mu_z | k^\circ \rangle H_z | j^\circ \rangle}{E_k^\circ - E_j^\circ} \quad \text{----------(1.4.9)}$$

Assuming a Boltzmann distribution, the following equation may be obtained

$$N_a = N_a^\circ \exp [-(E_a - E_a^\circ)/kT]$$
$$= N_a^\circ [1 + \langle a^\circ | \mu_z | a^\circ \rangle H_z/kT] \quad \text{----------(1.4.10)}$$

where in the last expression the exponential has been expanded and only the first power in H_z retained. This approximation will hold good provided

$\langle a^\circ | \mu_z | a^\circ \rangle H_z/kT << 1$, a condition which is generally met in practice except at very low temperatures. Finally if we require an explicit description in terms of absorption lines, a form for $f(\nu, \omega)$ must be assumed, for laurentian lineshape:

$$f(\nu, \nu_\circ) = \frac{2}{\pi} \frac{\nu^3 \Gamma}{(\nu_\circ^2 - \nu^2)^2 + \nu^2 \Gamma^2} \qquad (1.4.11)$$

The $(2/\pi)$ is a normalizing factor where Γ is the approximate linewidth at half height. Equation (1.4.11) has the virtue that it will be possible to write explicit algebraic expressions for both θ and ϕ, If Gaussian shape is used, it would not be possible to write such explicit algebraic expression.

Recalling that $\nu_\circ = (E_a - E_j)/h$ and using equation (1.4.8) we obtain

$$\nu_\circ = \nu_\circ^\circ - H_z/h \left[\langle j^\circ | \mu_z | j^\circ \rangle - \langle a^\circ | \mu_z | a^\circ \rangle \right] \equiv \nu_\circ^\circ - H_z \nu_\circ' \text{------} \qquad (1.4.12)$$

where $\nu_\circ^\circ = (E_j^\circ - E_a^\circ)/h$ substitute (1.4.12) into equation (1.4.11) and expand $f(\nu, \nu_\circ)$ in power of H_z again retaining terms through first order. The result is

$$\frac{\pi}{2} f(\nu, \nu_\circ) = \frac{\nu^3 \Gamma}{(\nu_\circ^2 - \nu^2)^2 + \nu^2 \Gamma^2} + \frac{4 \nu_\circ^\circ \nu_\circ' H_z (\nu_\circ^2 - \nu_j^2)\, \nu^3 \Gamma}{\left[(\nu_\circ^2 - \nu_j^2) + \nu^2 \Gamma^2 \right]^2} \qquad (1.4.13)$$

It can be shown that retention of terms only through the left hand side is justified provided $\nu_\circ' H_z \ll \Gamma/2$. Since the left hand side of the inequality is the Zeeman splitting, the expansion to the first order is seen to be valid only if the Zeeman splitting is much less than the line width. If we substitute equations (1.4.9, 10, and 13) into equation (1.4.6) and keep only terms linear in H_z, the final result is

$$\theta = - \frac{8\pi^2}{3ch} H_z N \left[f_1 A + f_2 (B + C/kT) \right] \text{-------} (1.4.14)$$

where N $(\equiv N_a d_a)$ is the total number of molecules per unit volume in the ground state a, d_a is the corresponding degeneracy of this state and

$$A = 3/d_a \sum_{a \rightarrow j} [\langle j|\mu_z|j\rangle - \langle a|\mu_z|a\rangle \; Im \langle a|m_x|j\rangle \langle j|m_y|a\rangle] \quad (1.4.15)$$

$$B = 3/d_a \sum_{a \rightarrow j} Im \{ \sum_{k \neq a} [\langle k|\mu_z|a\rangle / (E_k - E_a)] [\langle a|m_x|j\rangle \langle j|m_y|k\rangle - \langle a|m_y|j\rangle \langle j|m_z|k\rangle] + \sum_{k \neq j} [\langle j|\mu_z|k\rangle / (E_k - E_j)] [\langle a|m_x|j\rangle \langle k|m_y|a\rangle - \langle a|m_y|j\rangle \langle k|m_x|a\rangle] \} \quad (1.4.16)$$

$$C = 3/d_a \sum_{a \rightarrow j} \langle a|\mu_z|a\rangle \; Im \{ \langle a|m_x|j\rangle \langle j|m_y|a\rangle \cdots \quad (1.4.17)$$

Let us take up discussions of the terms A, B, C and the basic requirement for a molecule to exhibit each term.

1) A terms: The basic requirement for a molecule to exhibit an A and C terms is that there must be a non zero magnetic moment in either the ground state a or in the excited state j . This in turn requires that one or more of these states must be degenerate. The symmetry requirement for such degeneracies is that the molecule must possess at least a threefold symmetry axis. The A terms are characterized by its S-shaped bands and results when the excited state is degenerate. This is illustrated in figure (1.3) for both energy level and the shape of MCD spectra.

2) C terms: Figure (1.4) shows the effect of the magnetic field on a molecule for which the ground state a is degenerate to á and a. This mean the lower state a is more populated than the upper state a at any finite temperature.

This unequal population is more pronounced at low temperatures. The resultant line shape of the C term is given in figure 1.4c.

3) **B terms:** The B term is temperature independent. Such a characteristic can be used to differentiate them from the C term. The B term arises from the mixing of the ground and two or more excited states by the magnetic field. In order to simplify this, let us look again to equation (1.4.16) in which the dominant contribution to the B terms comes from the second summation where we are considering only three states. In the absence of a magnetic field the promotion of an electron to states j and k is independent of the state of polarization of incident light provided that the molecule is not optically active and absorption observed at resonance $E_k - E_a = h\nu$ and $E_k - E_j$ as presented in figure (1.5b). If however, there are off diagonal matrix elements in the magnetic moment between the states j and k, then these states are mixed bythe magnetic field. The magnetic field causes each state to acquire the same characterstics of the other. Now there will be differential absorption of the left and right circularly polarized component in figure (1.5c). This differential absorption results in an MCD band, which for allowed transitions, passes through their maximum values at frequencies corresponding to zero field resonance frequencies of transition k_a, k_j. The preferential absorption of left and right circularly polarized component will, however, be

different for two transitions as in figure(1.5c). Consequently, if a positive MCD band is observed at k_a, than a negative band will be observed at j_a.

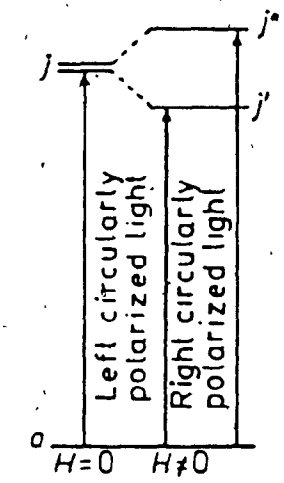

(a) Energy level diagram

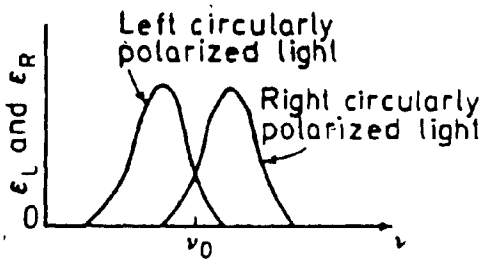

(c) Absorption for $H \neq 0$

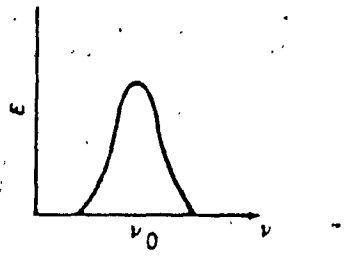

(b) Absorption for $H = 0$

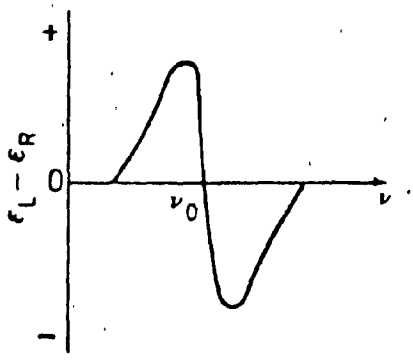

(d) Resultant *A* term

Figure 1.3 Illustration of the A term. a) Energy level diagram for an electronic transition to a degenerate j. b) Absorption in the absence of a of a magnetic field. c) Absorption of left and right circularly polarized light in a magnetic field. d) Resultant A term MCD curve.

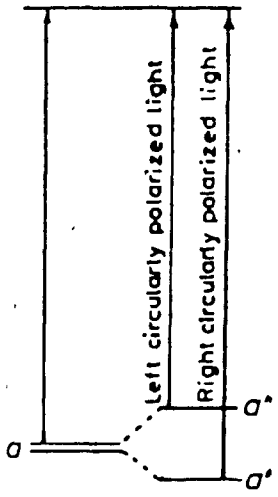

H=0 H≠0

(a) Energy level diagram

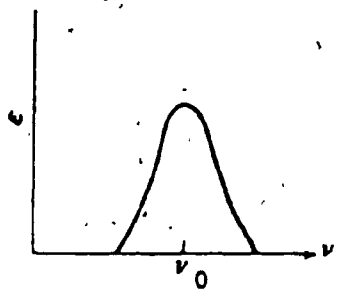

(b) Absorption for H=0

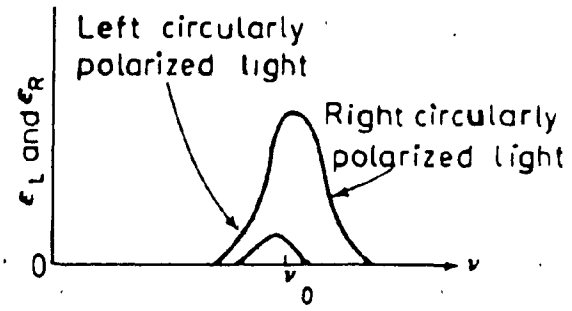

(c) Absorption for $H \neq 0$

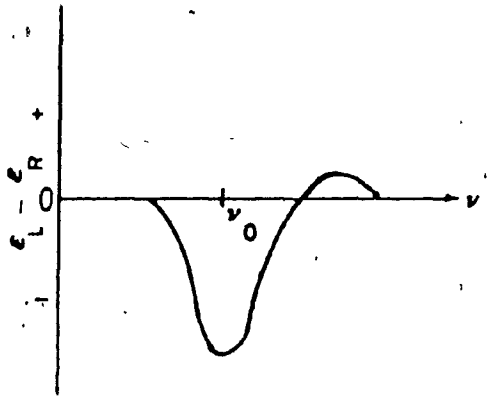

(d) Resultant C term

Figure I.4 Illustration of the C term; a) Energy level diagram for an electronic transition from a degenerate ground state a to a non-degenerate state j. b) Absorption in the absence of a magnetic field. c) Absorption of left and right circularly polarized light in magnetic field . d) Resultant C term MCD curve.

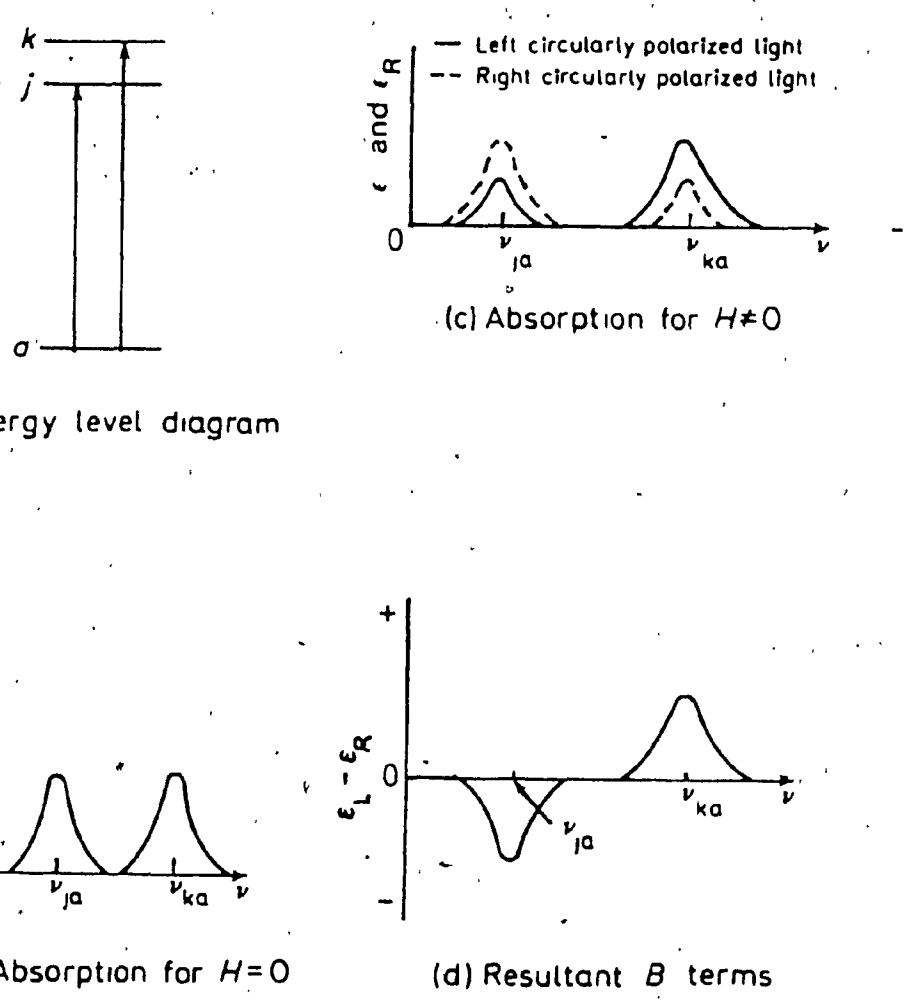

Figure I.5 Illustration of the B term. a)Energy level diagram for electronic transitions to two non-degenerate states j and k. b) Absorption in the absence of a magnetic field. c)Absorption of the left left and right circularly polarized light in a magnetic field. d) Resultant B term MCD curves

1.5 Picosecond Laser Spectroscopy

1.5.1 Introduction:

In the evolution of tools for flash photolysis the normal mode laser with a relatively low power and long duration output was superseded by the Q-switched laser with peak power output of 5×10^8 W and duration limited to about 10^{-8} s. Picosecond pulses are generated by a third model of lasers known as "mode locked".

These latter can operate, at a duration as short as 4×10^{-13} s and with a power of more than 10^{10} W. These ultrashort pulses have found extensive applications in optical non-linear studies, plasma physics, optical radar and other physics and engineering disciplines, as well as in molecular relaxation.

1.5.2 Mode locked lasers

In this context mode-locked (51) means that a periodic train of picosecond (10^{-12} s) light pulses is emitted by the laser. The question is to find out how the laser generates a train of picosecond light pulses. The lasers consist of a solid rod of active medium, either Neodymium-doped YAG (Yt-Al-garnet) or glass or ruby crystal, with the ends polished optically flat and parallel, and a Q-switch cell which contains a saturable dye. These elements are located in a cavity defined between two dielectric-coated mirrors which are accurately aligned as shown in figure (1.6). These elements form the laser cavity with overall

optical length L. The laser rod is surrounded by a helical flashlamp. When the flashlamp discharges, the light is absorbed by the rod and a population inversion of energy levels results. That is, there are more ions in the excited state than in the ground state. (shown in Figure 1.7). As a result of spontaneous fluorescence from some small number of these excited states, the emitted photons will stimulate the other excited states to emit with the same phase and direction. Naturally, there is also absorption from ground state unexcited centers, but since there are more centers in the excited state than the ground state, there is a net increase or amplification of light at the wavelength of the lasing transitions. It is important to note that this is not the main transition associated with absorption from the flashlamp (see Figure 1.7). So far, this is, of course, only a binary lasing action, an action which gives the meaning of the acronym LASER, namely, light amplification by stimulated emission of radiation where the flashlamp pumped laser rod is considered an amplifier for light in a certain band of wavelengths as shown in figure (1.8).

Now if we look inside the cavity, the beam passes back and forth many times, continuously sharpening the pulse and increasing the intensity, with the duration of the pulse theoretically limited by spectral band width. Upon insertion of bleachable dye with a broader absorption band than the laser line, standing waves are set up with discrete optical frequencies by the Farby Perot modes:

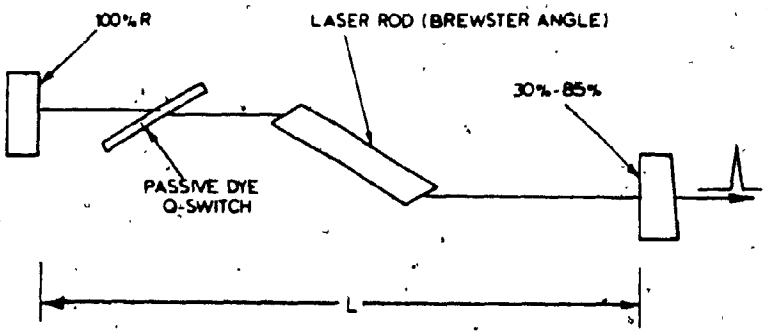

Figure I.6 Elements of a passive dye laser including geometrical arrangement of the laser rod (Brewster angle), passive dye Q-switch, and mirror of reflections to eliminate extraneous reflections in the laser cavity.

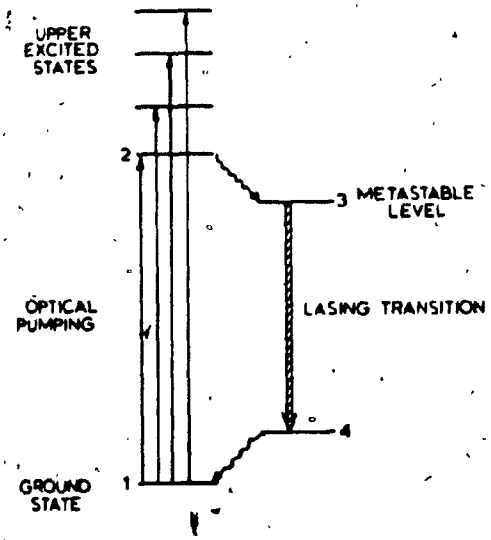

Figure I.7 Energy level diagram of a four-level laser (i.e. Nd:glass).

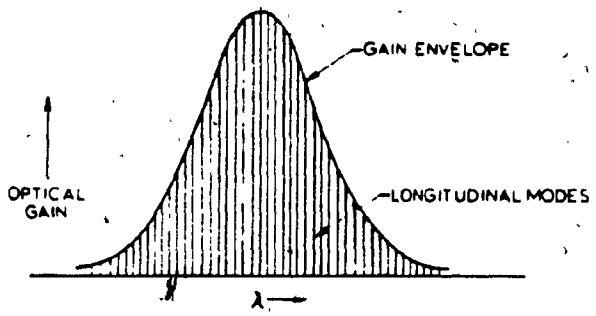

Figure I.8 Distribution of the optical gain of the active mediun over a band of wavelengths

$$\nu_n = \frac{nc}{2L}$$

where L is the optical separation of mirrors and c is the velocity of light. This arises because light absorption ``saturates'' the dye and allows transmission which briefly transmits the light nearly in phase with itself. For typical lasers where there are 10^6 modes oscillations within the cavity, the adjacent mode separation is given by $\Delta\nu$ $\nu_n - \nu_{n-1} = c/2L$. Computer calculations show that the pulse is sharpened after each successive pass with the maximum achieved after 15 passes. Although the saturable absorber provides a method for sharpening the pulses and separates them by c/2L, no unified model provides sufficient information with respect to the formation of the broad envelope. Normally, the modes of the laser oscillate in random fashion without any set phase relationship. The locking of the phase is provided by bleachable dye modulation of the frequencies ($\nu_o + \Delta\nu$, ν_o and $\nu_o - \Delta\nu$) of the cavity interferometer and coupled until the modes defined by total band width are coupled.

1.5.3 Single Picosecond Pulse Operation(52):

The first high intensity single pulse instrument was by Vuylstoke (53). He constructed a laser with a mirror having 100% reflectivity at low incident light intensity, but not near maximum pulse intensity. The front switched rapidly to zero reflectivity, dumping the pulse in less than the optical cavity round trip time and yielding a

single pulse of high power. An alternative method for extracting single pulses from a mode locked train utilized a spark gapped to 10 kV. The gap is adjustable so that one can select the most intense pulse to initiate a discharge. A high voltage pulse, generated by discharge, is used to increase the voltage on a partially energized polarizing Pockels cell so that a 90° change of polarization is generated for about 5 ns. A single pulse is thus transmitted which has a high intensity and duration as short as 2 ps. With the addition of a 25 cm long amplifier a single picosecond pulse with as much as 1 J of energy is generated (53).

1.5.4 General description of apparatus used:

The apparatus is the Nd/YAG picosecond spectrometer system of the Canadian Center for Picosecond Laser Flash-Photolysis (see figure 1.9). The main parts of this apparatus are the following lasers:

a) Oscillator: A Quantel YG 402G gives 30 picosecond mode locked pulses at the rate of 10 pps. The fundamental output wavelength is at 1064 nm and the maximum energy per ps pulse 2.5 mJ

b) Pulse selector: The pulse trains go to the pulse (2-3 mJ) selector which in this case is the PF 302 from Quantel consisting of:

1- antireflection coated Glan-Taylor prisms(cross pola-

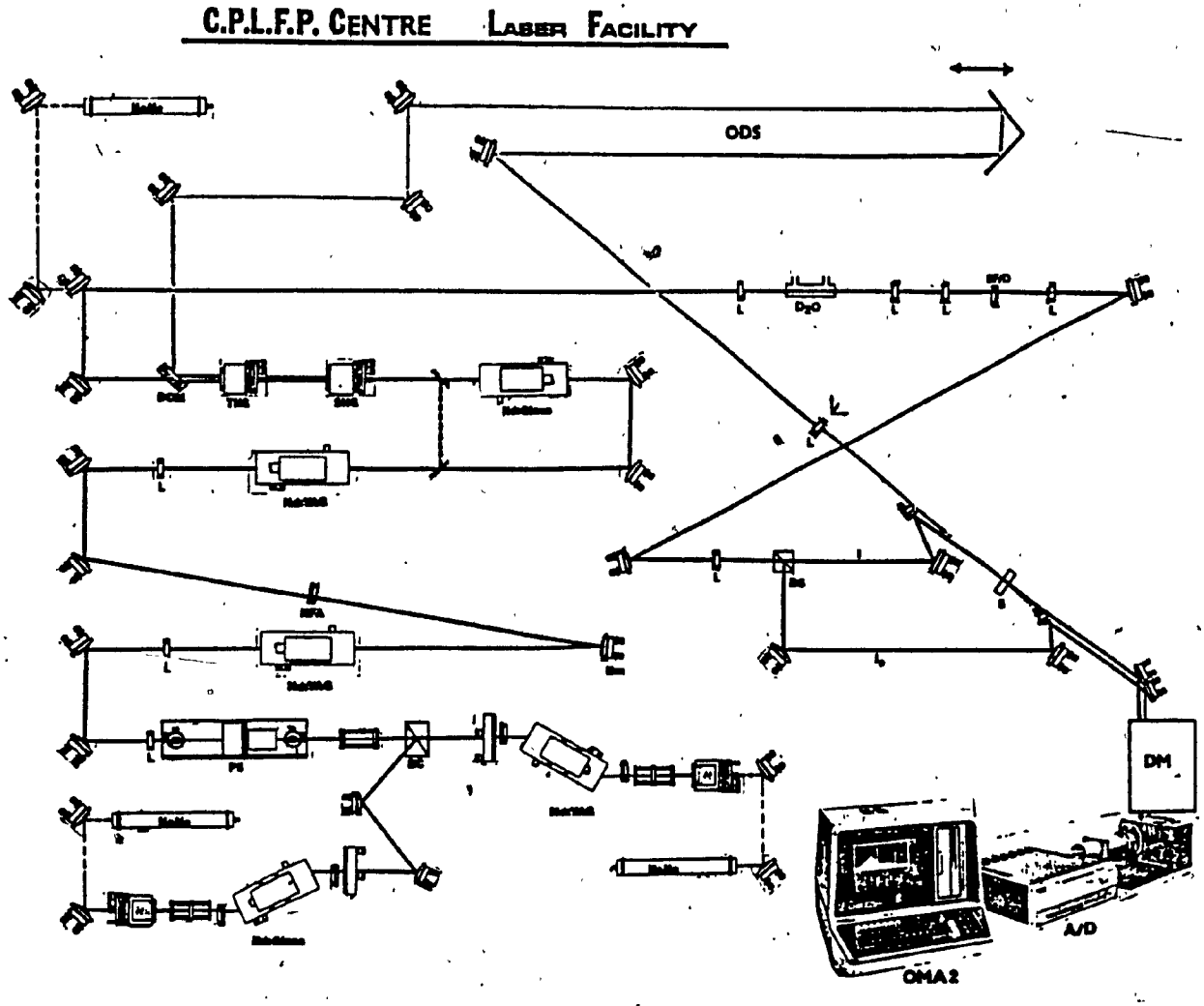

Figure 1.9 Block diagram of Canadian Picosecond Center

rizer).

2-three terminal, double crystal Pockels cell (a half wave plate at 3600 volts).

3- in conjunction with the Pockels cell, a photodiode detector and the fast switching electronics. The PF 302 is a pulse slicer intended to be used on 10 Hz mode locked laser systems. The slicer allows the selection of a single pulse from a mode locked train. A voltage applied to the z axis of KD^*P crystals make them birefringent. It is thus possible to obtain a path difference equal to half a wavelength when the voltage applied is (see figure 1.10)

$$V_{\lambda/2} = \frac{\lambda}{2\, n^3 r_{63}}$$

where λ = laser wavelength

n = ordinary index of KD^*P = 1.47

r_{63} = 25 10^{-10}

This optical path difference makes the Pockels cell equivalent to a half-wave plate for light propagating along the crystal axis. The PF 302 is equipped with two crystals in parallel . The Pockels cell, combined with two crossed polarizers(high quality Glan-Taylor prisms) acts as a shutter, open or closed, depending upon whether or not a high voltage is applied. After the selection of the pulse from the train it is subjected to a two step amplification. The first amplified is a Quantel SF 410-07 with a 7 x 115 mm Nd:YAG rod while the second is an SF 410-09 with a 9.35 x 115 mm Nd:YAG rod. After the amplification of the beam, it passes through a second harmonic generation cell of KDP which is used to change the fundamental wavelength 1064 nm

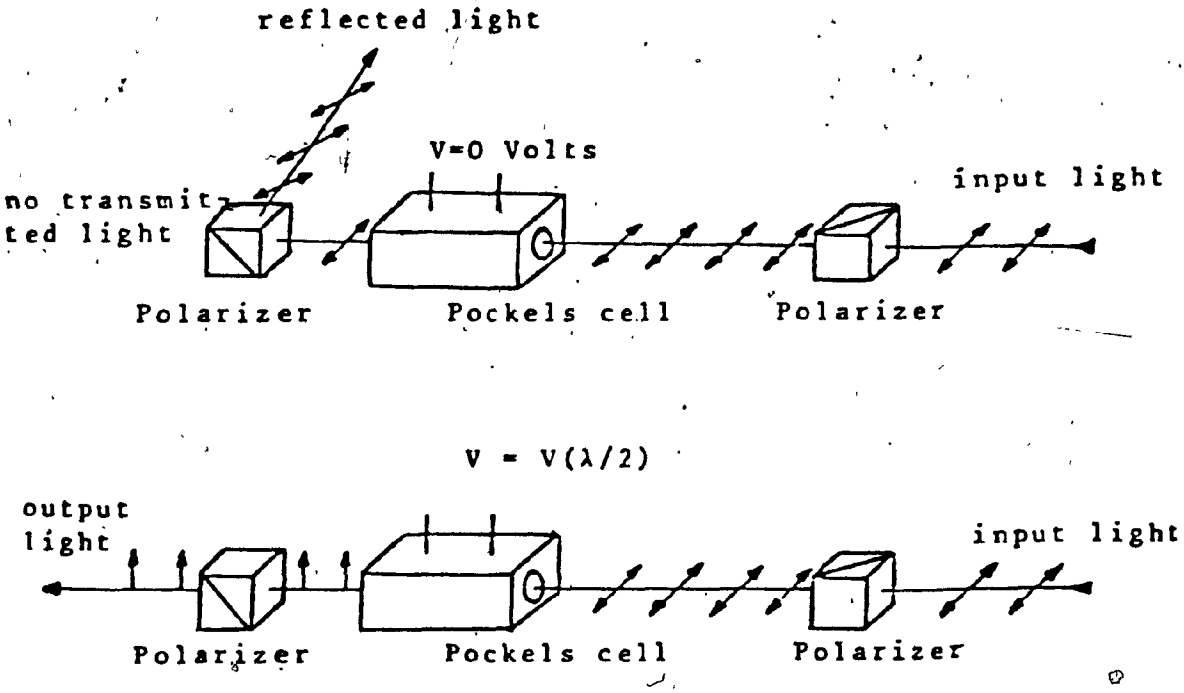

Figure 1.10 Illustration of the pulse slicer function with two different applied voltages on the Pockels cell.

to 532 nm. This is followed by a third harmonic generator of KDP used to combine 1064 and 532 nm to give 355 nm light. The frequency doubler is composed of 21 mm x 21 mm x 35 mm type I crystal of highly deuterated KDP, installed in a refractive index matching cell. The third harmonic generation is similar to Frequency Doubler Type I, except it employs a 21 mm x 21 mm x 35 mm KD*P crystal which is dry mounted. The amplified single pulse of 1064 nm light with an energy of 15 to 50 mJ and pulse width 4 to 8 ps is frequency doubled using the type I KDP (Potassium dihydrogen phosphate) angle tuned crystal. The interaction that generates the second harmonic is due to the non-linear polarization vector, P_{nl}, defined by the relationship

$$(P_{nl}) = d_{ijk} E_j E_k$$

where E_j and E_k are the components of the resultant electric field and d_{ijk} is the linear piezoelectric constant related to the susceptibilty of KDP by the equation

$$\chi_{ijk} = 2\, d_{ijk}$$

In KDP the non-vanishing coefficients after matrix evaluation are $d_{14} = d_{25} = d_{36}$. The second harmonic can finally be expressed as

$$P_E(I) = -d_{14} E^2 \sin \phi$$

Tuning the angle (ϕ) gives a maximum convergence to green (530 nm) light. Here, the power output of the green light is proportional to the square of the incoming 1060 nm energy. With a type I KDP cyrystal, the emerging beam I (1060 nm) and I' (530 nm) are orthogonal to each other. Conversion to green does not time broaden the pulse. After

generation of 530 nm, it enters the third harmonic generation in which the generated 530 nm pulse and 1060 nm combine by a process similar to the above to give 355 nm. This technique does not convert all the 1062 nm light but leaves a part which is focused into a 20 cm cell containing 50% H_2O and 50% D_2O (by volume). The focusing of a high intensity light beam into a Raman active fluid results in the generation of a transient birefringence producing stimulated Stokes and anti-Stokes Raman signals. This technique produces a "super broadened" continuum in which the blue light is delayed with respect to the red component. Under these conditions no time broadening is observed so that one obtains a "White light" source having the same time resolution as the laser pulse with a wave length range 400 to 600 nm. This is used as a spectroscopic probe light.

1.5.5 Some systems which have been studied:

Picosecond flash photolysis provides a means to investigate the kinetics of excited state transients, but still the simple interpretation of spectra is complex. Two short case histories are instructive before attempting a new system.

1.5.5.1- Cr(III) complex $^4T \longrightarrow {}^2E$:

Investigations searching for the $^4T_{2g}$ state of Cr(III) has attracted the attention of several people. These efforts have generally led to upper limits for the $^4T_{2g}$ lifetime. Castelli and Forster (54) and Yardely and Beattie (55) have reported $^4T_{2g}$ lifetimes to be less than 100 ns and later 2 ns for various Cr(III) complex ions. The first partial success was a study by Kirk et al.(56) using second harmonic Nd pulses at 530 nm to excite several chromium complexes; $Cr(acac)_3$ (acac = acetylacetonate ion), $Cr(NCS)_6^{3-}$, and trans-$Cr(NH_3)_2(NCS)_4^-$ (Reineckate ion). All these have small extinction coefficients at 530 nm (100 M^{-1} cm^{-1}), Thus no GSB (Ground state bleaching) is observed. However, they did find ESA (Excited state absorption) in the spectra of all three compounds. The risetime of ESA was not longer than the 5 ps duration of the pump pulse. The ESA of $Cr(acac)_3$ decayed with a lifetimes of 1.5 ± 0.3 ns. The excited state lifetimes of Reineckate and the hexathiocyanato complexes were found to be longer than 5 ns, too long for the apparatus. The spectrum of the ESA of Reineckate ion matched an ESA spectrum at -196, reported by Ohno and Kato (57)and identified by them on the basis of lifetime, as originating from the phosphorescence of the ^2E state. The lifetime data are 0.28, 26, 79 ns, for $Cr(acac)_3$, $Cr(NCS)_6^{3-}$ and Reineckate ion, respectively. The data support the conclusion that the ESA spectra are attributable to the ^2E state. The

spectrum was found to be the same whether measured at short delay (14 ps) or at long delay, 1 ns. Unless the ESA spectra of $^4T_2$ and ^2E are fortuitously the same, "the grow in" of the ^2E takes place in a time comparable with, or less than, the duration of the pump pulse.

A similar study of Cr(III) complexes by Le Sage et al. (58) used several different solvents. Transient absorption spectra were observed when $Cr(NCS)_6^{3-}$, R^- (Reineckate ion), and trans-$Cr(en)_2(NCS)_2^+$ in various solvents were excited by picosecond laser pulses at 530 nm. According to the data, both R^- and trans-$Cr(en)_2(NCS)_2^+$ showed a noticeable solvent dependence of ESA energy (shifted towerds the blue in water), whereas the symmetric complex $Cr(NCS)_6^{3-}$ did not. The intensities of the transient absorption band for R^- and $Cr(NCS)_6^{3-}$ were comparable, independent of solvent, and approximately two times less intense than that for trans-$Cr(en)_2(NCS)_2^+$. These results suggest $^4T \longrightarrow {}^2E$ intersystem crossing yields are close to unity. Le Sage et al. (58) were unable to detect a change in any of the transient absorption spectra with time again giving no limit of spectra for the quartet itself. But, risetimes were found to vary. The most significant variations in the risetimes were found for R^- which varied from less than 6 ps in H_2O to 29 ps in DMF. The risetimes of R^- in H_2O appeared to be faster than in D_2O but both of these risetimes are fast and close to the temporal width of the laser pulse. In general, they found that ESA risetimes for both R^- and trans-$Cr(en)_2(NCS)_2^+$ are

fastest in hydroxylic solvents and slower in aprotic solvents. No such solvent trend was found for symmetric $Cr(NCS)_6^{3-}$. The risetime in high viscosity glycerol-water mixtures was not significantly different from less viscous solvents. This could be interpreted either by assuming that the bulk viscosity does not interfere with the difficulty of solvation shell rearrangement because of the presence of few glycerol molecules in the solvation sphere of the complex ion or because motions are too local to correlate with bulk viscosity. The ESA risetimes are assumed to be governed by the rate of intersystem crossing from the quartet manifold.

1.5.5.2- Singlet-triplet versus electron transfer in metal porphyrins:

Recent studies by Serpone et al. (59) on four Osmium-porphyrin complexes, Os(OEP)LL' [OEP = Octaetyl-porphyrin] are similarly illuminating. They used a picosecond laser flash-photolysis system with a double beam, mode-loked Nd:glass system delivering a 6-ps (fwhm) pulse. For the four compounds $[Os(OEP)[P(OMe)_3]_2$, Os(OEP)-O_2 [Me = methyl, py = pyridine and O_2 = dioxo], their initial excit-ed state S_1,decayed in < 8 , 50, 36 and 13 ps repectively while triplet state liftimes were found to be 6.2, 16, 5.5 and 6 ns respectively. The compounds showed an interesting variation in electronic energy state order. Two of the compounds have (d,π^*) lowest energy excited

states. They are the octaetylporhinatobis(trimethylphosphite)osmium (II), $Os(OEP)[P(OM\text{-}e)_3]_2$ and the carbonyl-(octaethylporphinato)pyridine osmium (II), Os(OEP)CO(PY). The other two compounds, the methoxonitrosmium (octaethylporphinato)osmium(VI), $Os(OEP)O_2$, have (π,π^*) lowest excited states. The absorption spectra of these latter two compounds are also of the "hyper" type. That is, they show an extra allowed absorption band not due to transitions between porphyrin ring orbitals. In these compounds the acceptor π^* orbitals of the axial ligands (l_{π^*}) are low enough in energy for the (π, l_π^*) transition to appear in the visible-near uv absorption spectrum. The lowest energy $^3(\pi, \pi^*)$ excited state of $Os(OEP)O_2$ is probably mixed with a higher energy $^3(\pi, l_\pi^*)$ state. It is worth noting that there may be little difference between an Os(II) compound with strong axial bonding due to strong π-acceptor ligands. In this sense, Os(VI) in $Os(OEP)O_2$ can be effectively thought of as analogous to Os(II) because the empty metal d orbitals are mixed with the filled P_x, P_y orbitals of the trans oxygen ligands. A general picture for the results shows that radiationless decay of the (π, π^*) states of the porphyrin are as in other aromatic molecules. Excitation from the ground state (S_0) to any singlet state (S_x) quickly (1 ps) relaxes to the lowest excited singlet (S_1) which undergo intersystem crossing to the lowest triplet state T_1 (rate constant k_2) in competition with radiationless decay (k_1) and fluorescence (k_f) back to S_0. In turn, T_1 can decay via nonradiative

transitions to S (k_3), which can phosphoresce (k_p) and back by intersystem crossing to $S_1(k_{-2})$. It was reported that the porphyrin complexes do not fluoresce. Hence k_f is insignificant, and the decay S_1 is determined by $\tau(S_1) = (k_1 + k_2)^{-1}$. The phosphorescence quantum, ϕ_p, for complexes with lowest excited states $^3(\pi,\pi^*)$ was reported as 3×10^{-3} (77K) for Os(OEP)NO(OMe) and $5\ 10^{-3}$ (300) for $Os(OEP)O_2$ (2). Since the triplet yield, $\Phi(T_1) = k_2/(k_1 + k_2)$ should be substantialy higher than these values in a complex containing the heavy atom, the low observed values for ϕ_p imply $k_p << k_3$. Additionally, k_{-2} is probably negligible because the energy gap $E(S_1) - E(T_1)$ is much greater than k_BT, the Boltzman energy (60). As a result, it is expected to observe two transient decays. One corresponds to S_1 decaying to S and T_1 with $\tau(S_1) = (k_1 + k_2)^{-1}$; the second corresponds to T_1 returning to the ground state with $\tau(T_1) = k_3^{-1}$.

Looking to the excited state absorption along series $Os(OEP)[P(OMe)_3]_2$, Os(OEP)CO(PY), Os(OEP)NO(OMe) and $Os(OEP)O_2$ one finds that it occurs at 690, 715, 600 and 675 nm, respectively. The main absorption band in the excited states are expected to be due to four orbital transitions $a_{1u}(\pi)$, $a_{2u}(\pi) \longrightarrow e_g(\pi^*)$. In the ground state the relevant orbitals red shift along the series. Although it might be expected that the excited states of the four molecules were of the same nature, it was found that there is a red shift from $Os(OEP)[P(OMe)_3]_2$ to

Os(OEP)CO(PY) and also from Os(OEP)NO(OMe) to Os(OEP)O_2 but that the excited state absorbance of the former two are to the red of those of the latter two. It was predicted that $\pi \longrightarrow \pi^*$ transitions will have different energies in (d, π^*) excited states from those in (π, π^*) excited states. Also, transitions of a different nature are possible in the two types of excited states. Serpone et al. (59) believed that the variation of excited state absorbance among the four molecules provides evidence for assignment of the energy excited states of the four Os(OEP)LL' complex, but, it took ps time resolution to gather the evidence.

1.5.6 The needs for picosecond spectroscopy:

The wavelength dependence of the quantum yield for photosubstitution of Co(III)-amine complexes over the envelope of the lowest lying spin allowed ligand field band has been described (19,61). The interpretation of this phenomenon led to postulation of photochemical or photophysical processes that discriminate on a very short time scale. Previously, no explicit information on the lifetimes of Co(III)-amine complex excited states had been available against which to test such a hypotheses. This circumstance stands in contrast to the situation with the analogous low spin d^6 configuration complexes of Rh(III) or hexacyanocobaltate(III) where weak emission with lifetimes in the range of 10 to 40 ns has been described in the case of Rh(III) (62). The emitting state has been assigned as the lowest ligand field triplet in these cases. It would

appear that the corresponding lifetime in Co(III)-amine complexes is too short for an emission to be observed or that such an emission is located too far to the red for the detectors that are usually employed. We have, therefore, initiated picosecond flash photolysis studies to try to locate short lifetime states which can be recognized via excited state absorption.

Chapter 2

2.1 Materials:

Starting materials were reagent grade and used without further purification. Deionized doubly distilled water was used. Supplier and grade are tabulated as follows:

table 2-I

Supplier and the grade of the compounds used

Compound	Company	Grade
Ethylenediamine	Aldrich	high quality
Etheylene glycol	Baker	Analyzed reagent
Dimethylsulfoxide	Anachemia	Spectral grade
Dimethylformamide	Baker	Analyzed reagent
Nitromethane	Fischer	Spectral grade
Hydrogen Peroxide 30%	Baker	Analyzed reagent
Cobalt(II)chloride-hexahydrate	Mallinckrodt	Analyzed reagent
Diphenylcarbazide	B.D.H	Analytical Grade
Sodium Nitrite	J.T.Baker	Analytical

2.2 Preparation of complexes

2.2.1 Preparation of $[Co(NH_3)_5Cl](NO_3)_2$ (63)

Twenty five grams of (0.47 mol) ammonium chloride was dissolved in 150 ml (about 2.2 mol) of concentrated (14.7 M) aqueous ammonia in a 1l Erelenmeyer flask. The solution was continuously agitated while 50 g (0.21 mol) of

finely powdered Cobalt(II)chloridehexahydrate was added in small portions, each portion being dissolved before the next was added. A yellow pink precipitate of hexaminecobalt(II)chloride formed with the evolution of heat. All subsequent operations had to be performed in a hood. To the slurry, 40 ml (0.39 mol) of 30% hydrogen peroxide was added with vigorous swirling (or mechanical stirring to the solution) as a thin stream from a buret. This results in a vigorous exothermic reaction with effervescence. When the effervescence had virtually ceased, a deep red solution of the aquopentamine salt had formed. To this 150 ml (1.8 mols) of concentrated hydrochloric acid (12 M) was added slowly. During the neutralization, the temperature of the reaction mixture rose, and the purple product precipitated, leaving a pale blue-green supernatant solution. The mixture was heated for 15 minutes on a steam bath, cooled to room temperature, and filtered by suction. The precipitated product was washed with several portions of ice cold water totaling 100 ml, followed by an equal volume of cold 6 M hydrochloric acid. An alcohol wash followed by an acetone wash facilitated drying which was accomplished by heating the product at 100° to 110° C for 1 to 2 hours. The yield was 48 g. The product was pure enough for most further synthetic work but could be recrystallized as follows with about 46 g recovery. The solid was dissolved in 450 ml. of 1M aqueous ammonia by warming gently on the steam bath, after which the clear

solution was poured (hood) into 450 ml. of concentrated (12 M) HCl. After heating for 45 minutes the complex salt $[Co(NH_3)_5Cl]Cl_2$ was isolated as above. This product was converted to the nitrate form by preparing a saturated solution of the above complex and adding concentrated nitric acid with cooling to 0° C. The absorption spectra agreed with that in the literature (4).

2.2.2 Preparation of trans-$[Co(en)_2Cl_2]NO_3$:

Krishamurthy's method (64) was used by dissolving 20 g of Cobalt(II)chloridehexahydrate in 20 ml of water, and 80 ml of ethylenediamine (30%) was added to it cautiously with stirring. Then, the solution was cooled in an ice bath to 0-5° C and 15 ml of H_2O_2 (30% ml) was added slowly, 1 ml at a time, in the beginning. After the complete addition of H_2O_2, the solution was warmed gently to about 60° - 70° C for about 15 - 20 minutes. Then 40 ml of concentrated hydrochloric acid was added to the solution with stirring and the solution was evaporated with occasional stirring until its volume was reduced to two thirds of the original. After cooling the solution in an ice bath, 30 ml of ethanol was added and it was cooled for another 10 minutes. The green crystals were filtered, washed with ethanol and dried in a vacuum desiccator. The yield was 12 g. The chloride was converted to nitrate by passing through an anion exchange resin in nitrate form. The nitrate precipitated after addition of alcohol and cooling to 0° C. The absorption spectrum agreed with that in reference (4).

2.2.3 Preparation of cis-$[Co(en)_2Cl_2]ClO_4$

The chloride salt of this compound was prepared using Blair's method (65) to convert 8 g of trans-dichloro(bisethylenediamine)cobalt-(III)chloride by evaporating a neutral solution to dryness on a steam bath. The unchanged trans form could be washed out with a little cold water, then the transformation could be completed by the evaporation. (It should be repeated that this should be done not more than two or three times, however, as decomposition takes place). The yield was 6.5 g. It may converted to the perchlorate salt by the addition of concentrated perchloric acid to a nearly saturated solution and cooling to 0° C. Again the identity of the sample was confirmed by the agreement of the absorption spectrum with that in reference(74)

2.2.4 Preparation of cis-$[Co(en)_2(NCS)Cl]NO_3$

To prepare this complex, the literature method (66) was modified. trans-$[Co(en)_2Cl_2]Cl$ 20 g was dissolved in 30 ml of warm water and a solution of potassium thiocyanate (6.8 g in 15 ml of water) was slowly added with constant stirring. Gentle heating was applied until the resulting paste dissolved, producing a purple solution which was immediately placed in an ice bath and allowed to cool for 2 hours. A marked decrease in yield resulted from overheating during the first stage of the reaction. The yield was

5 g. The precipitate of cis-$[Co(en)_2(NCS)Cl]NCS$ was changed to the nitrate form by preparing a saturated solution of the above complex and adding concentrated nitric acid followed by cooling below 0° C. Absorption spectra agreed with that in reference (71)

2.2.5 Preparation of trans-$[Co(en)_2(NO_2)_2]NO_2$:

We have used a similar method to that used for preparation of cis-dinitrobisethylenecobalt(III), a slight modification. Trans-dichlorebis(ethylenediamine)cobalt(III)-chloride 30 g dissolved with magnetic stirring in 150 ml cold H_2O. When the salt was dissolved, the solutionwas cooled to about -12° C in an ice/ salt bath and 114 g of powdered $NaNO_2$ added over 1 or 2 minutes while stirring fairly rapidly. The solution changed from green to red and before all the salt had been added was bright orange to brown. Slight heating of this solution changed it to yellow crystals of the trans dinitro product. Again the identity of the sample was confirmed by the agreement of the absorption spectrum with the reference (71).

2.4 Light intensity measurement:

For wavelengths 457,488 and 514 nm, the light source was a Coherent 6W Ar-ion laser operated well below rated current. For experiments in the range 570-622 nm, the Ar laser pumped a Coherent 590 dye laser filled with rhodamine 6G. Light intensity was monitored using a Coherent 210

power meter which was calibrated in the manner described by Kido and Langford (68). At 488 and 514 nm, Reinecate Actinometry (70) measured the intensity and calibrated the power meter. Readings were taken before and behind the cell and compared to readings taken before and behind the same cell filled with distilled water. (The absorbance calculated for solutions examined this way were in good agreement with those by conventional spectroscopy.)

2.4 Photolysis Procedure:

In order to minimize corrections for ligands released thermally, runs were normally conducted at 9° C for trans-$Co(en)_2Cl_2^+$ and 6° C for cis-$Co(en)_2Cl_2^+$ while cis-$Co(en)_2(SCN)Cl^+$ was run at 0° C. Solutions were prepared to the limit of ready solubility and then filtered through a 0.45 μm millipore filter. A small volume (10.0 ml) jacketed polarimetric cell of 10.0 cm path length was used for irradiation. It was thermostatted at the desired temperature (± 0.1° C) with circulating water. All the runs photolysis were carried out with absorbance more than one.

2.5 Analytical Procedure:

2.5.1 Chloride ion determination: The chloride ion released in the photoreactions(or in the dark reactions) was followed by mercury (II) titration using 0.016 M $HgNO_3$ solution standardized against NaCl. The indicator was diphenylhydrazine. A residual of starting material was removed by ion exchange in order to avoid further reaction.

Thus, both photolyte and control solutions were passed through 7 - 8 g of (Dowex HCR) cationic exchange resin. The released chloride was washed from the column with 15 ml of distilled water.

2.5.2 Thiocyanate ion determination: Free thiocyanate was determined by adding an aliquot of irradiated (or dark control) solution to the fourfold excess volume of reagent containing 0.1 ferric nitrate in 0.5 M perchloric acid. The absorbance due to the resulting ferric thiocyanate complex was measured ($\varepsilon = 4.3 \times 10^3$ at 450 nm) (70).

2.5.3 Ammonia measurement: Free ammonia released was measured directly for both irradiated and dark solution by the pH method (69). In this method, the acid used in controlling ionic strength is used according to the following reactions

$$NH_3 + H^+ \longrightarrow NH_4^+$$

The pH meter (four digit precision meter fabricated in the Concordia science workshop) was easily calibrated using acid solutions of concentration near experimental conditions for photochemistry. The change of free H^+ concentration, ΔC_H was then calculated

$$\Delta C_H = C_H \ (1 - 10^{-\Delta pH})$$

The only important precaution is to ensure that an adequate time is allowed for readings to stabilize.

2.6 The Conventional UV-visible absorption and MCD spectra measurements:

All conventional spectra were measured by using a Perkin-Elmer 557 spectrophotometer. The MCD spectra were measured using a custom built spectrometer (its schematic diagram is shown in the fig 2-1) Which uses in sequence a xenon 150 watt lamp, Cary 14 monochromator, Glan-Taylor polarizer, Hind's internationl Piezo-optical polarizer, Walker Engineering 2.2 T electromagnet, and Hamamatsu 955 photomultiplier detector. The phototube DC current is kept constant by a controlling feed-back circuit. The AC signal representing the 50 kHz MCD differential absorption is decoupled at the preamplifier (mounted in the phototube socket), filtered and amplified by a PAR Model 124 lock-in amplifier. The output is digitized by a 12 bit A/D converter linked to a Motorola Exorcisor II which automatically scans the spectrometer through the desired signal to noise quality conditions. Baseline and spectrum data files are subsequently merged digitally and the resulting spectra plotted displayed on a digital X-Y recorder.

The magnetic field was calibrated using the conversion factor of 0.6 A/kG given by the manufacturer and /or by measurement of standard $Co(H_2O)_6^{2+}$ solution using the value of molar ellipticity per unit field of $[\theta]^{510}_{nm}$ $= -6.1 \times 10^{3-}$ deg cm^2 d mol^{-1} G^{-1}. The molar absorptivities are given in M^{-1} cm^{-1}, and magnetic

ellipticities , $[\theta]_M$, in deg cm^2 d $mol^{-1}G$ which are calculated from the equation $[\theta]_M = 100\theta/b$ MH where θ is the ellipticity measured directly in degrees [$\theta = 3300(A_R - A_L)$], b is the path length in centimeters, M is the molar concentration, and H is the magnetic field in units of gauss. All MCD measurements were made with magnetic field parallel to and in the direction of the light beam.

In the assignment of MCD spectra the location of the zero was set by selecting "lock" frequencies where the signal is taken to be zero. The locks in these spectra are set at the long wavelength end where absorption spectra features have been exhausted. The other lock wavelength is set at the minimum point in the conventional absorption spectrum between "B" terms associated with the singlets. The correctness of the choice of lock points is indicated by the agreement of the peak frequencies of the B terms which are assigned to the singlets with the frequencies assigned to the same singlets in the ordinary absorption spectra.

Baseline corrections of these MCD spectra were carried out with the routine MERGE. It's role is as follows:

1- Subtract baseline file from data file correcting for both baseline offset and rotation using two "locking" energies.

2- Permit resetting of calibration points and number of points in the final data.

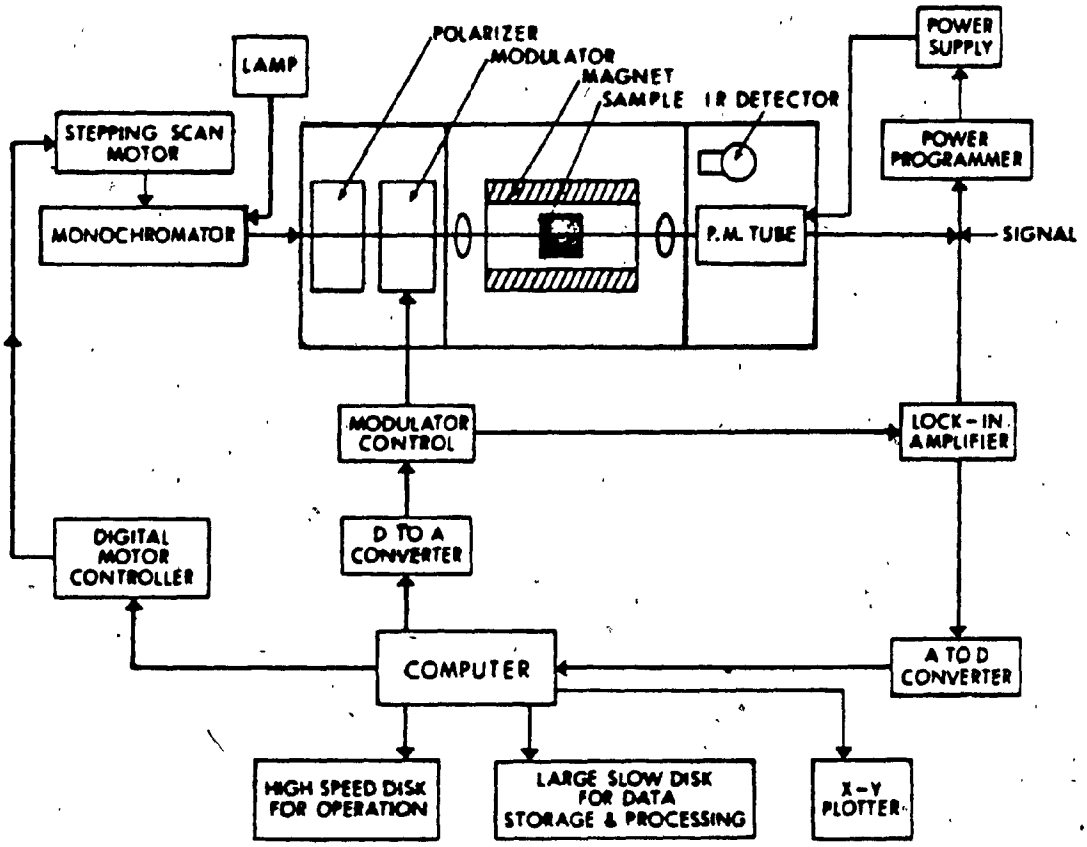

Figure 2.1 Block diagram of Magnetic Circular Dichroism Spectrometer (MCD)

For the present spectra a slit width of 0.8 mm and a scan rate of 5 cm^{-1}/s were used with a gain of 20 mV.

Solutions were prepared by weighing into small beakers (to the nearest 0.01 mg) an amount of the solid salt about three to four times the quantity needed to prepare solutions for conventional spectroscopy. A few mls of ultrapure water (millipore system) were added and the beakers warmed gently until all the salt was dissolved. The MCD spectra were recorded immediately.

2.7 Transient Spectra Measurement:

Before any run was recorded we had to find the 0 on the time scale between the exciting pulse and probe by using a cell containing Toluene and a cross polarizer so that the fundamental beam passed through the cell to induce birefringince. This event took 1-2 ps. The moment at which the probe pulse could be detected by the OMA was considered the 0 of the scale.

Most of the samples were prepared with an absorbance of 0.65 at 355 nm in a 2 mm cell. For each run 10 - 20 shots were recorded for excited sample and blank and than averaged. The results presented are the average absorbance change spectrum (ΔA) and the curve at ± 1 standard deviation for the set.

Chapter 3

Results

3.1 Photolysis

3.1.1 Photolysis of $Co(NH_3)_5Cl^{2+}$:

This work is an extension of studies by Pribush et al. (18) who used 488 nm Ar-ion laser light and work by Langford and Vuik at 514 nm and 647 nm. The full wavelength dependence has now been examined for both Cl^- and NH_3 yield. Optimum conditions were used, keeping the absorbance more than 2, the extent of photolysis at < 10%, temperature was 25° C (thermal reaction rate constant = $6.7\ 10^{-6}\ s^{-1}$ at 25° C). The quantum yields are collected in table 3-1. They are shown graphically as quantum yield versus wavelength in figure 3.1 .

3.1.2 Photolysis of cis-$Co(en)_2Cl_2^+$ and cis-$Co(en)_2(NCS)Cl^+$:

The whole first ligand field absorption band was covered in the photolysis including wavelengths 488,514,573, and 600 nm. Optimum conditions for the experiment were maintained. The temperature was 2° C(since this ion has a high thermal reaction rate $k = 2.5 \times 10^{-4}\ s^{-1}$ at 25° C). The absorbance was kept above 2, and the extent of photolysis < 20%. Quantum yields for the different wavelengths are collected in Table 3-II. They are shown graphically as quantum yield versus wavelength in figure (3.2). The absorption spectrum also appears in the figure.

The uncertainty is the standard deviation in 3 - 4 runs.

Tests of the effect of both intensity and concentration on thequantum yield have been conducted. These results showed that neither the concentration nor the intensity have an effect on the quantum yield of substitution of the chloride as shown in table (3-II)

3.1.3 Photolyses of trans-$Co(en)_2Cl_2^+$:

The photolyses include the wavelengths 458 , 488, 573, 600, and 622 nm. These cover the whole ligand field region and may be including the tail of a charge transfer band. The experiment was conducted under optimum conditions temperature 9C (thermal solvolysis has a rate constant of 4.0×10^{-7} at 24° C) and absorbance was one. It was specially diffcult at longer wavelengths to try to reach absorbance 2. The extent of photolysis was kept <10%. The quantum yield for uptake of H^+ was measured (usually assumed to measure cleavage of a Co-N bond on ethylenediamine) at a temperature of 15° C in order to get a fast steady reading on the pH-meter. Stated uncertainties represent ±0.5 standard deviation on a set of 3-5 runs. Data are collected in Table 3-3. they are graphically presented as quantum yield versus wavelength in figure (3.4). The absorption spectrum also appears in the figure (3.4).

3.1.4 Solvent and temperature dependence:

The response of the quantum yield to different sol-

vents was examined. These solvents are nitromethane, dimethylsulfoxide (DMSO), dimethylformamide (DMF) and various glycerol-water mixtures. All the conditions which were used for aqueous photolyses were preserved, except for the cases of DMSO, DMF, where the photolyses was conducted at 15C . The data for glycerol-water mixtures are collected in Table 3-IV and presented graphically in figure (3.4). The data for nitromethane, DMSO, and DMF are found in Table 3-V. Photolyses at different temperatures were carried out at 600 nm using both cis and trans $Co(en)_2Cl_2^+$. The data are collected in table 3-IV. They are presented as log(quantum yield) versus reciprocal temperature plots in figure (3.5,3.6). Pseudo-activation eneries were estimated from least squares fit of slopes to these plots as -3472 ± 147 cal mol^{-1} for the cis isomer and -3300 ± 107 cal mol^{-1} for the trans isomer.

Table 3-I

Quantum yield for photochemical ligand substitutions of $Co(NH_3)_5Cl^{2+}$ at 25° C in neutral aqueous solution with 25 ml cell. The concentration of the complex is 0.01 M

Wavelength nm	Ligand substituted	laser power mW	time hour	Quantum Yield 10^4
488	Cl^-	200	2	16.7 ± 0.5a(3)
				17.1 ± 1.2 b
	NH_3	200	2	55 ± 2.6 a (3)
				50 b
514	Cl^-			51 ± 1.3 c
	NH_3			50
573	NH_3	200	2	20.9 ± 2.4 a (4)
600	Cl^-	125	2	12.8 ± 0.9 a(3)
	NH_3	125	2	23.6 ± 0.9 a(3)
622	Cl^-	80	2	10.9 ± 1.0a(3)
	NH_3	80	2	9.1 ± 0.6a(3)
647	Cl^-			9.6 c
	NH_3			1.3 c

a) this work b) Pribush et al. (23) c) Langford and Vuik (19)
Number in parenthesis indicate number of independent runs.

Table 3-II

Quantum Yield for substitution in cis isomers at 2C°

The concentration of the complex is 0.005 - 0.01M

a) cis-$Co(en)_2Cl_2$

i) Cl^- substitution

wavelength nm	Laser power mW	time hr	Quantum Yield 10^4	
488	180-270	1-2	27±3	(4)
514	270	1-1:30	27 ± 2	(3)
573	130	1:30	16 ± 2	(3)
600	245	1	13 ± 2	(3)

ii) H^+ as measure of ring opening

wavelength nm	Laser power mW	time hr	Quantum Yield 10^4	
488	250	1	4.8	(3)

iii) effect of the concentration on the quantum yield of Cl^-

Wavelength nm	Conc. M 10^3	laser power mW	time hr	Quantum Yield 10^4
514	5.7	270	2	30
514	3.4	270	2	28

iv) effect of intensity on the quantum yield of Cl^-

Wavelength	conc	laser power	time	Quantum Yield
nm	M 10^3	mW	hr	10^4
488	5.2	180	2	28
488	5.2	270	1	30

b) cis-$Co(en)_2(NCS)Cl^+$

Wavelength	Ligand substituted	laser power	time	Quantum Yield
nm		mW	hr	10^4
488	NCS^-	255	1	26 ± 2 (3)
	Cl^-	255		4.3 ± 1 (3)
600	NCS^-	250	1	12 ± 1 (3)
	Cl^-			< 10^{-4}

Number in Paranthesis represent number of independent runs.

Table 3-III

Quantum yield for substitution of trans-$Co(en)_2Cl_2^+$ for 10% photolysis at 8° C in. The concentration of the complex is 0.005 - 0.01 M

a) Cl^- substitution

wavelength nm	Laser power mW	time hr	Quantum Yield 10^4
457.9	125	2	11.5 ± 0.5 (4)
488	190-225	2	8.44 ± 0.2 (5)
514	115	2	5.3 ± 0.6 (3)
573	110	2	8.04 ± 0.5 (3)
600	225	1	7.2 ± 0.2 (3)
622	160	1	7.0 ± 0.5 (3)

b) H^+ uptake as a measure of en ring opening

wavelength nm	Laser power mW	time hr	Quantum Yield 10^4
488	250	1	5.8 (3)

Number in parenthesis indicate number of independent runs

Table 3-IV

Quantum Yield for photosolvolysis of cis-$Co(en)_2Cl_2^+$ in water glycerol mixtures. Irradiation time, 1 hr, laser power 250 mW and temperature 0° C.

% Glycerol (by volume)	Quantum Yield $Cl^- \ 10^4$	Receprocal viscosity $1/\eta$ (a) 10
0	27 ± 3 (4)	11.20
10	22 ± 1 (3)	8.67
20	16 ± 2 (3)	6.48
30	9 ± 2 (3)	4.64
40	< 9 (3)	2.52

a) values from reference (73)

Number in parenthesis reprsent the number of independent runs

Table 3-V

Quantum Yield for photosolvolysis of cis-$Co(en)_2Cl_2^+$ in different organic solvent at 488 nm, 1 hr irradiation; 250 mW laser power.

Solvent	Quantum Yield $Cl^- 10^4$	
water	27 ± 3	
10% Nitromethane	29 ± 2	(2)
dimethylsulfoxide	< 0.1	(3)
N,N dimethylformamide	4 ± 2	(3)

The number in parenthesis represents the number of independent experiments.

3.2 MCD spectra:

The spectra of the four compounds are presented in figures (4.2,3,4,5) pages 100 - 103. Assignments are indicated on the figures and in table (4 - IV) page. The signal to noise ratio in these spectra is only sightly lower than the pen width indicates. Thus, the inflections indicating the presence of A terms are readily identified. However, this qualitative resolution does not entirely carry over into definition of band centers. The bands are broad, as expected, and it is very diffcult ! These spectra are to be compared with early MCD spectra. reported by McCaffrey et al.(74). The error bars shown in ref. (74) indicated that, as expected, developments in signal recording and processing have allowed for much improved signal to noise in the current spectra. Thus, the spectra of ref. (74) do not reveal the A terms assigned in the figures. This lack of resolution also causes two problems. In the spectra of the cis dichloro ion, the lock point implied by the published spectrum (it is not explicitly stated) does not correspond to the minimum in the absorption spectrum. This leads to the assignment of two negative B terms which do not match peaks of the absorption spectrum. If the lock is placed at the minimum, the result is a single positive B term which does match the peak in the absorption spectrum. The negative features are revealed here to be a part of A terms. Similarly, there is a lock problem in the spectrum of the chloropentamine

complex shown in ref. (74). At the low energy end, the spectrum is brought to zero at too long a wavelength. The rough constancy of the spectrum from about 16.5 kK to 13 kK shows that the last peak shown in ref.(74) is an artifact. The modification of the lock point has the consequence of changing the first B term to a positive term. The resulting peaks agree with the absorption maxima from the conventional spectra within the uncertainty. Conventional absorption spectra determined with the present samples were in excellent agreement with earlier reports. These spectra are summarized in the table only.

The treatment of the spectra are conventional first order (75). All parameter assignments are derived using the MCD spectra as input data. Values of the Racah B parameters are derived from the singlet-singlet splittings and values of C from the singlet-triplet splittings. The Octahedral splittings parameter is then fit. Only in the case of the trans dichloro complex where one triplet is missing was a general iteration used. The state energies and the values of ligand field parameters are given in Table (4-III). To help understand the discussion the figures are placed in chapter 4.

The transient spectra of Co (III)-amine complexes

The four compounds $Co(NH_3)_5Cl^{2+}$, cis-$Co(en)_2Cl_2^+$, cis-$Co(en)_2Cl_2^+$, and trans-$Co(en)_2NO_2^+$ were tested for their response in transient absorption spectroscopy. These spectra are presented in figures 5.1, 2, 3 , 4 and 5. The first three showed discrepancy for any transient, and all apparent peaks were within the noise and cannot be taken as transient absorbance. The ground state also has a low extinction coefficient. Even with the highest possible concentration we found only (i.e. only 1% of the ground state are excited). The last two compounds, cis-$Co(en)_2(NCS)Cl^+$ and trans-$Co(en)_2(NO_2)_2^+$, do show transients. These spectra were recorded at several probe delay times. The lifetimes of these transients were calculated from the first order rate equation by plotting log(A) versus time delay of the probe beam. For cis-$Co(en)_2(NCS)Cl^+$ and trans-$Co(en)_2(NO_2)_2$ rate constants were $12 \times 10^9\ s^{-1}$ and $5 \times 10^9\ s^{-}$ respectively.

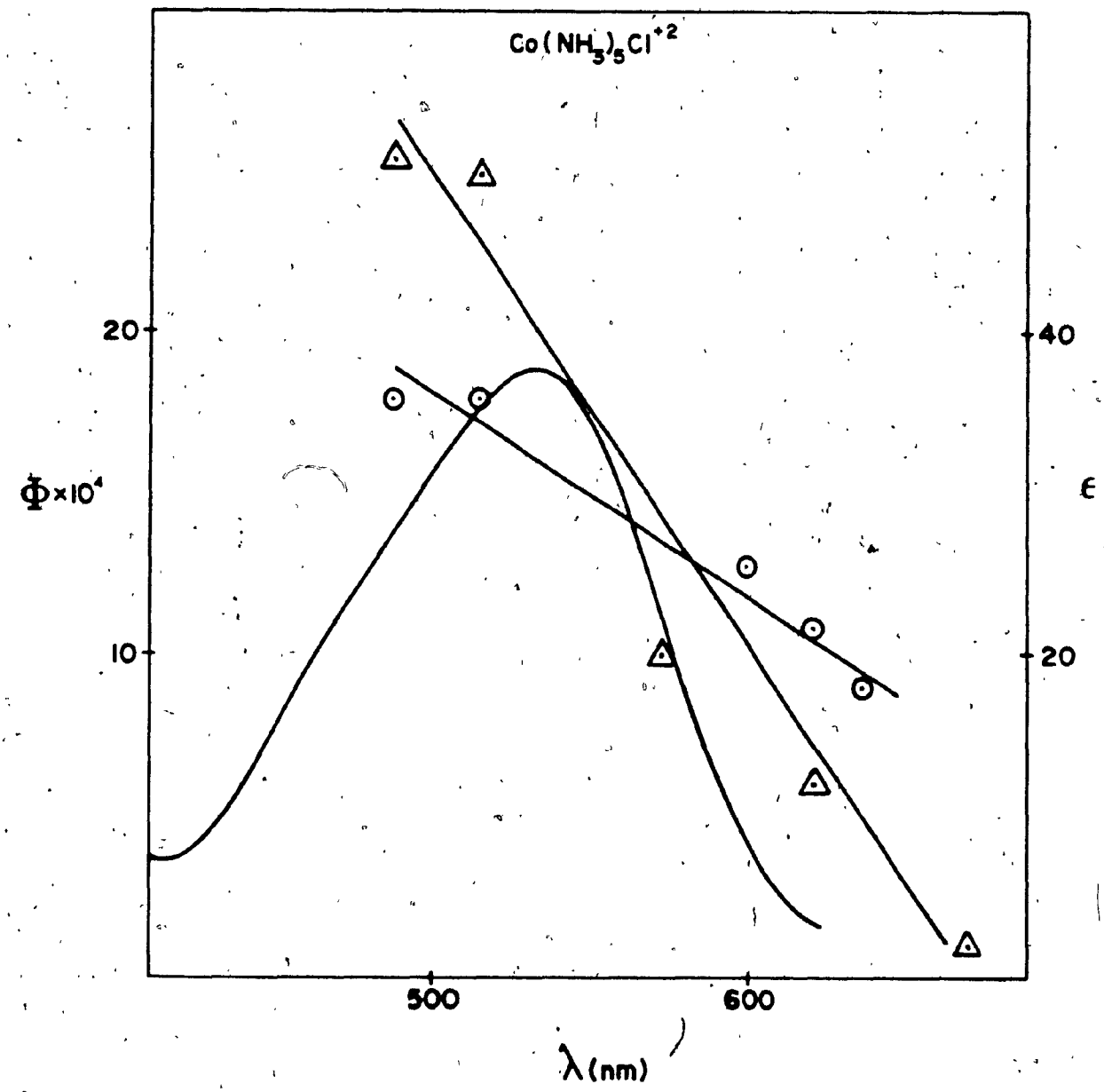

Figure 3.I Quantum yield behaviour for the photochemical ligand substitution of $Co(NH_3)_5Cl^{2+}$ at different irradiation wavelengths.

△- Ammonia substitution

⊙- Chloride substitution

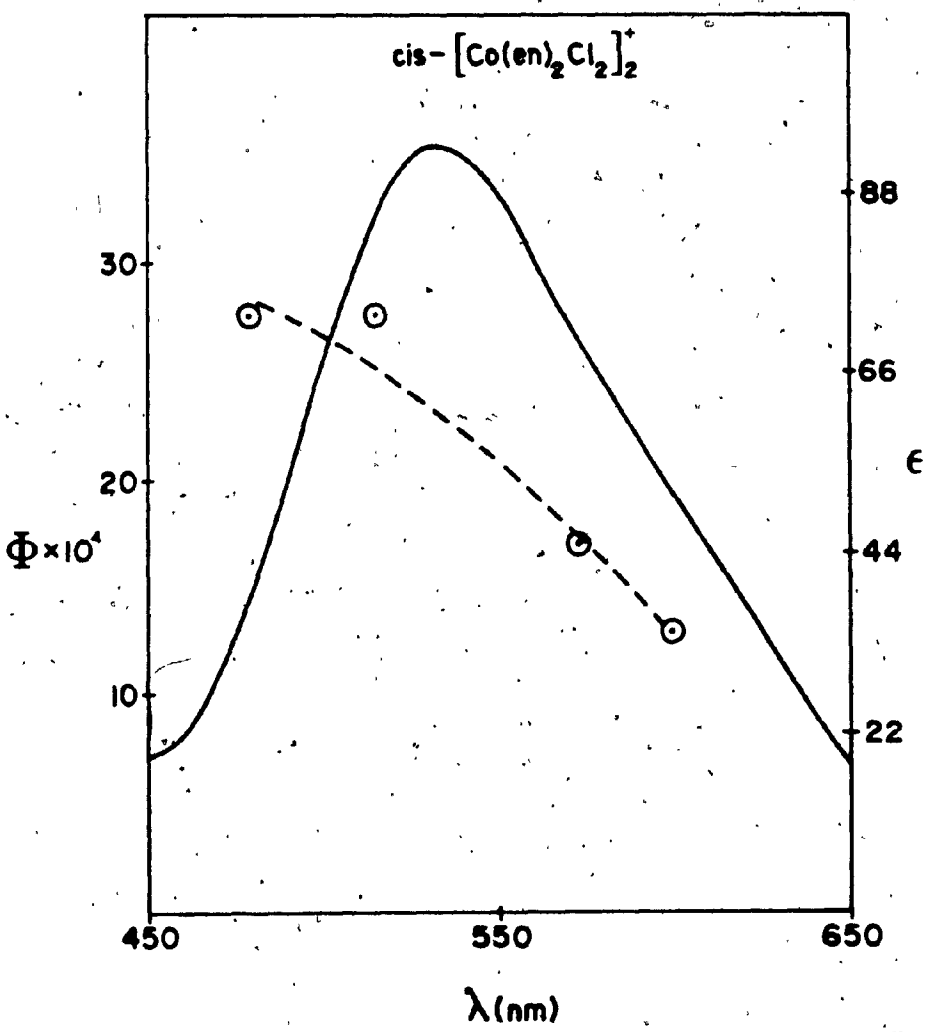

Figure 3.2 Quantum yield profile for photochemical Cl^- substitution versus different irradiation wavelengths of cis-$Co(en)_2Cl_2^+$.

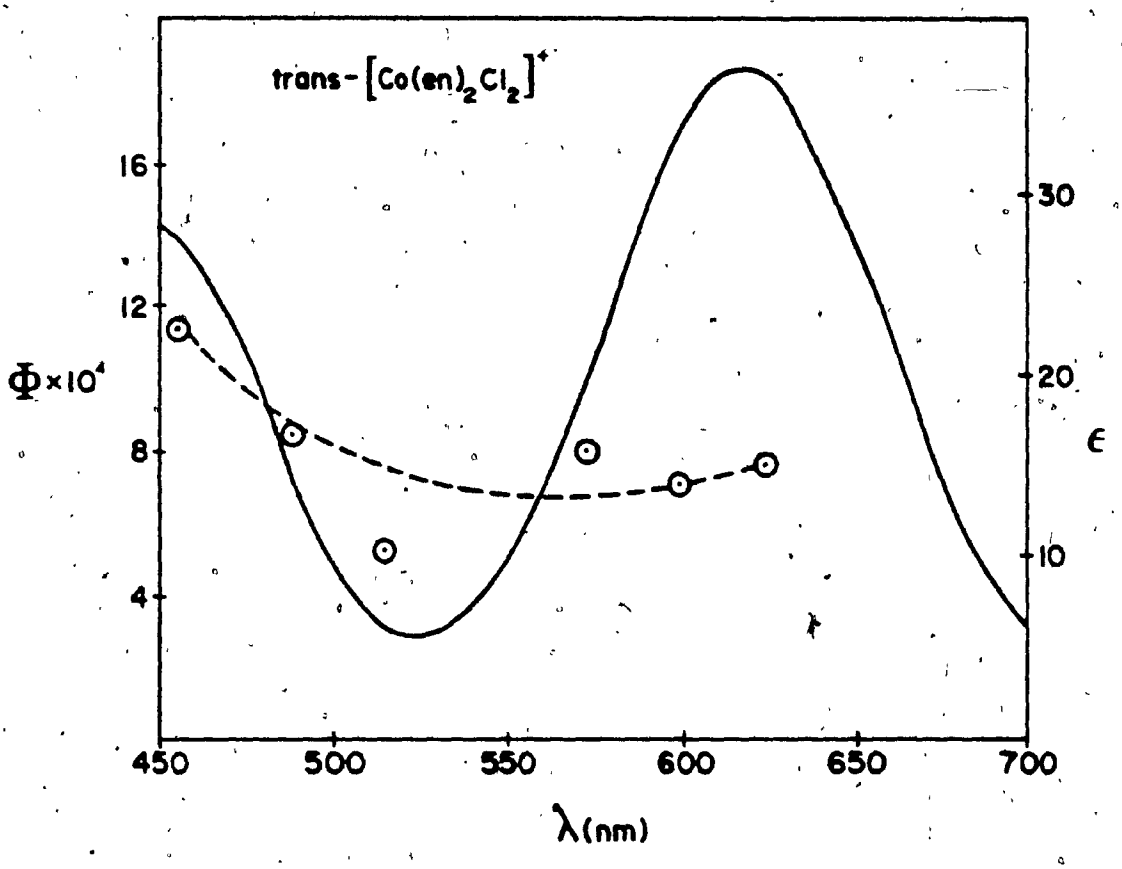

Figure 3.3 Quantum yield profile for photochemical Cl^- substitution at different wavelength of trans-$Co(en)_2Cl_2^+$.

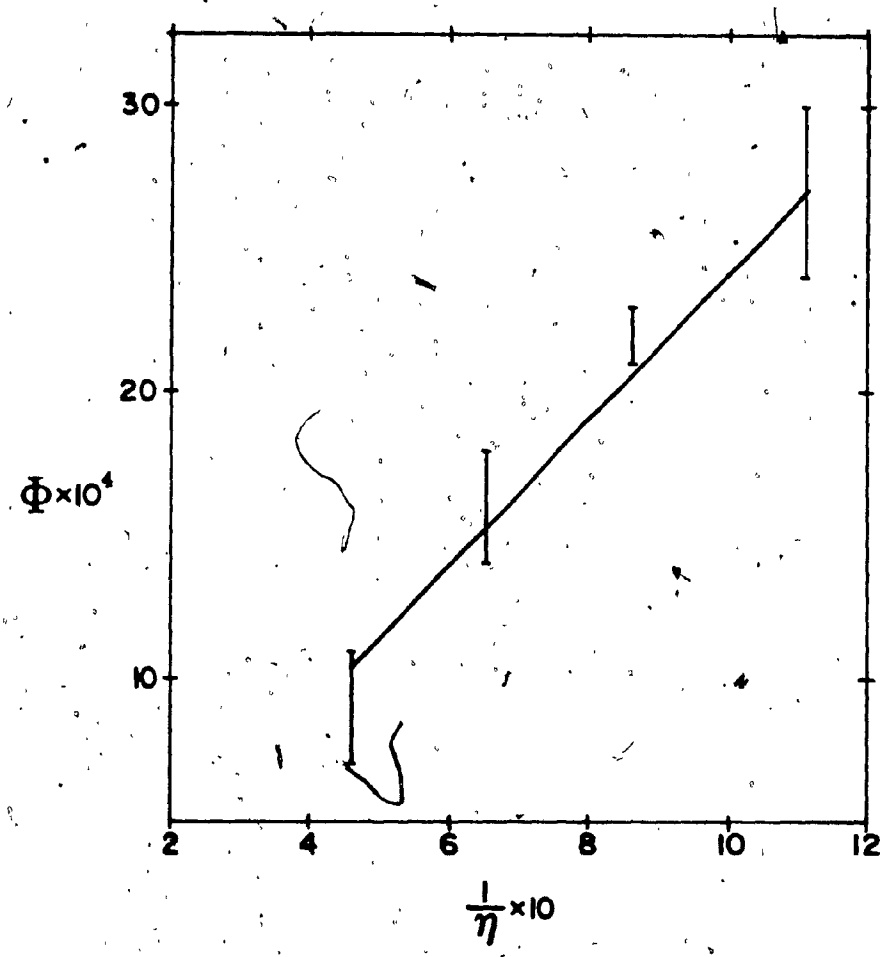

Figure 3.4 Relationship between the quantum yield for the Photosolvolysis of cis- $Co(en)_2Cl_2^+$ in water-glycerol mixture and viscosity coefficient (η)

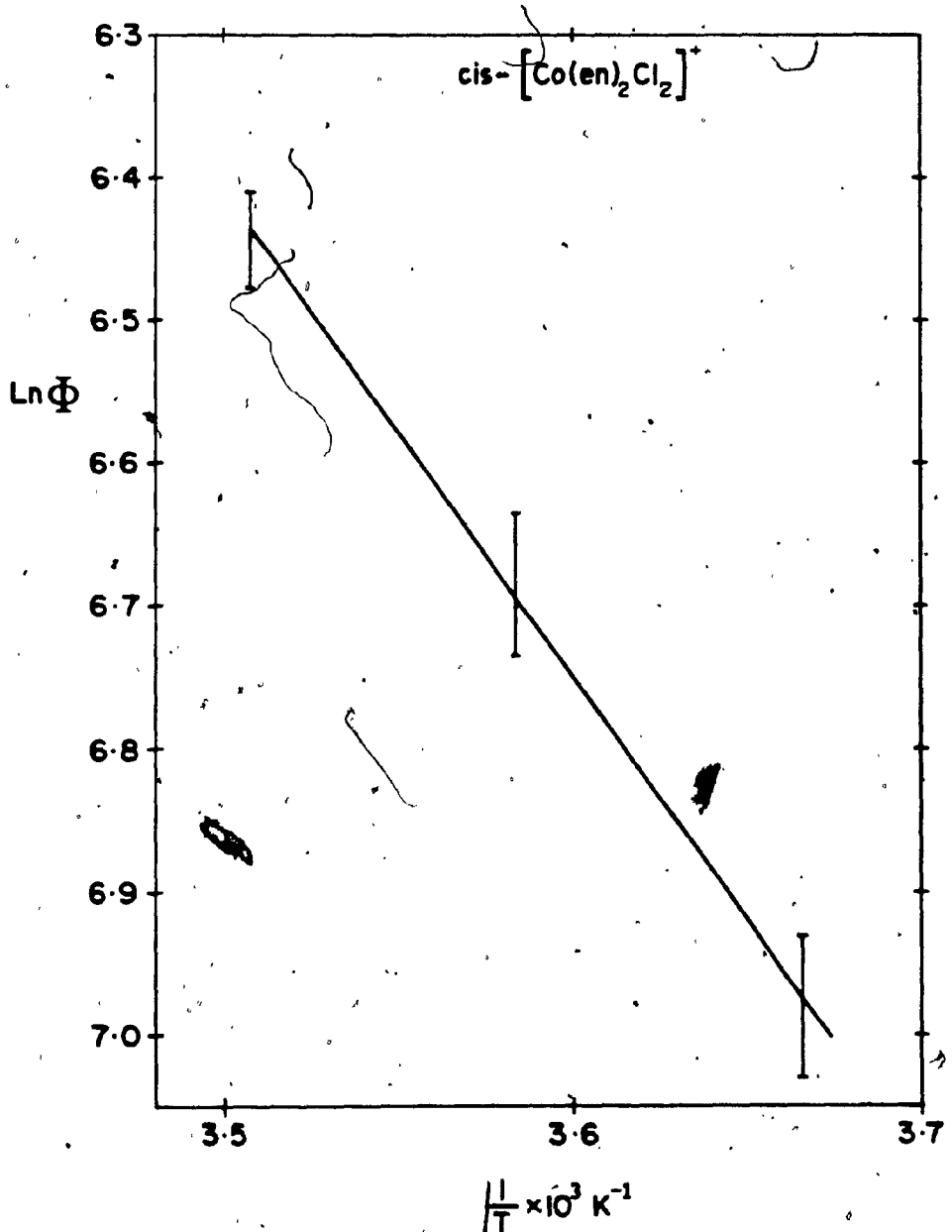

Figure 3.5 Plots of log(quantum yield) versus I/T of cis-$Co(en)_2Cl_2^+$

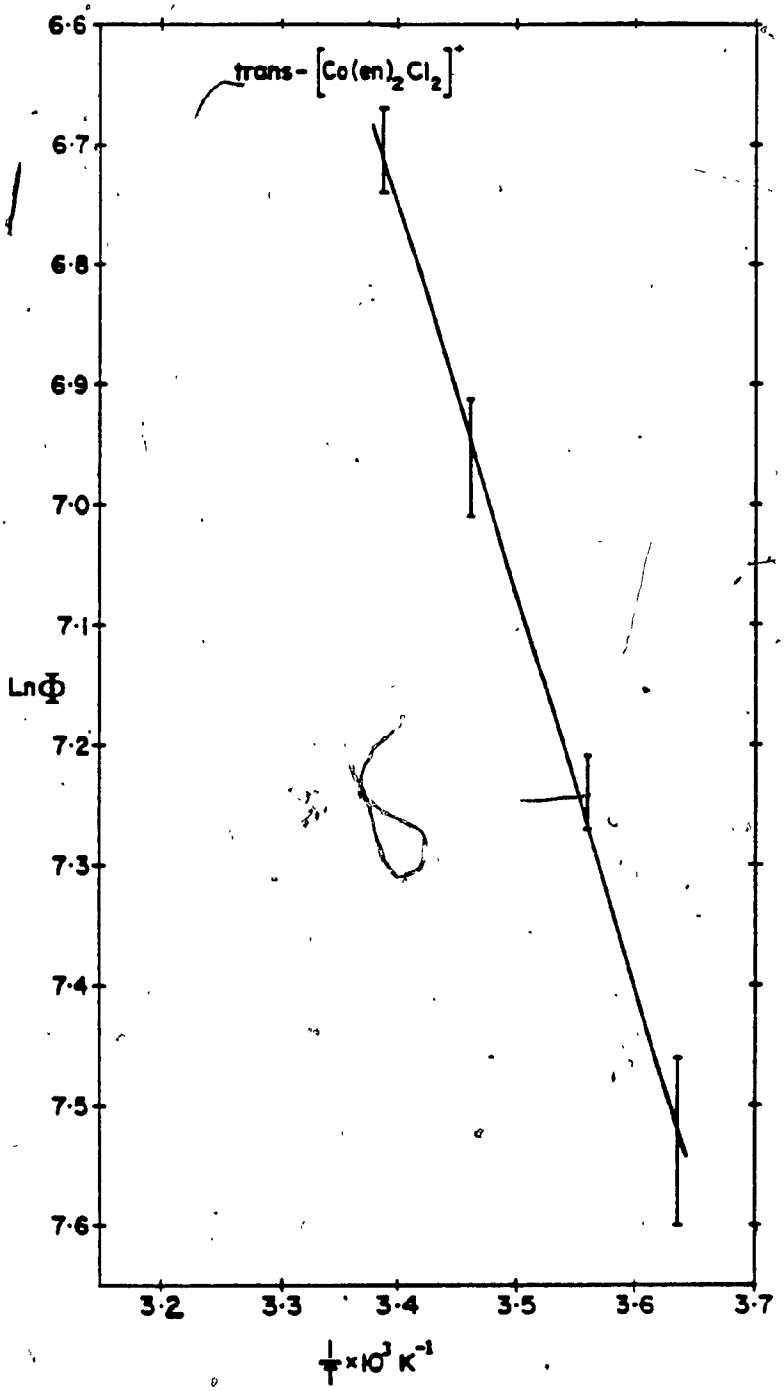

Figure 3.6 Plots of log(quantum yield) versus I/T of trans-$Co(en)_2Cl_2^+$.

Chapter (4)

Theoretical Background of d^6 Spectra

4.1 Tanabe-Sugano Diagram for O_h (78):

The calculation of all the energy levels of a d^n configuration including both interelectronic repulsions and crystal fields of intermediate strength is a problem of considerable difficulty. It has been carried out only for certain relationships between the parameters of interelectronic repulsion. The results are presented in the form of the Tanabe-Sugano diagrams (shown in figure 4.1). In these diagrams the energies of the levels of a d^n system are plotted as a vertical coordinate in units of the interelectronic repulsion parameter B while crystal field strength is the horizental coordinate (units Dq/B). By convention , the overall splitting of a single electron under octahedral field is set to $\Delta = 10Dq$, $Dq > 0$. The restriction on the usefulness of these diagrams lies in the fact that it requires two Racah parameters, B and C, to describe the interelectronic repulsion for a free ion d electron configuration. The diagrams can only be drawn if the ratio of C/B is specified. The diagrams have been compiled for values of this ratio which are considered most likely for some first transition series ions of the configurations concerned. The value of C/B is stated in each diagram. Fortunately, it seems likely that the form of the diagrams are not too sensitive to the ratio. Moreover , many of the results required later use only terms of the same multiplicity as the ground term. The relative

energies of these are a function of the parameter B only, and the diagram holds for any ion of the corresponding configuration within the inherent limits of the ligand field model. In these diagrams the zero of energy is always taken as that of the lowest term. Hence, when there is a change of ground term, the diagram is discontinuous. The discontinuity always takes the form of an increase in the slope of the term energies above a critical value of Dq/B.

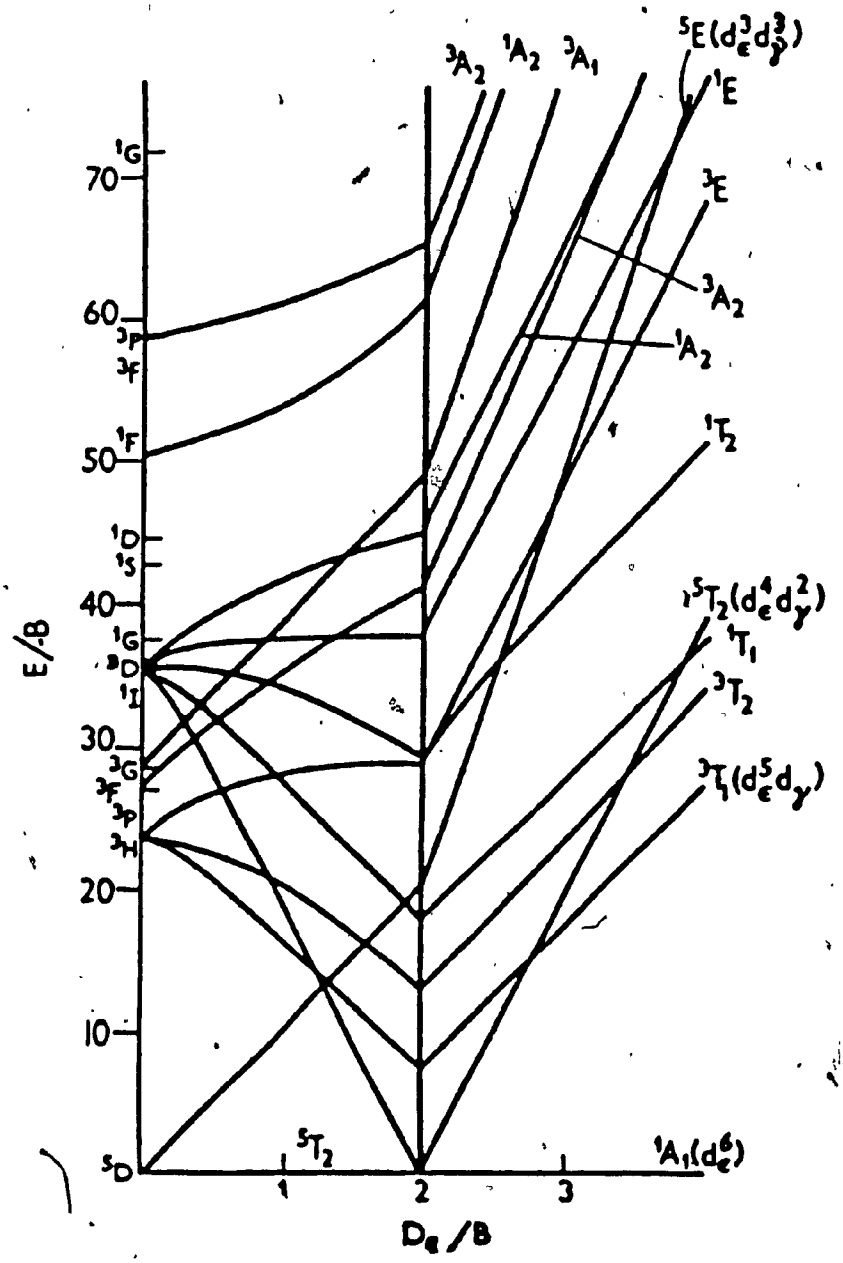

Figure 4.1 Energy level diagram (Tanabe-Sugano) for d^6 in octahedral field. C/B=4

4.2 Average Ligand Field Model

In this model all lower symmetry than octahedral complexes (D_{4h}, C_{4v}, C_{2v})are treated as pseudo octahedral. The model is calculated as octahedral energy states without taking into account the non-degeneracy of component. In order to illustrate the method we are going to apply it to $Co(NH_3)_6^{3+}$ and $Co(NH_3)_5Cl^{2+}$.

$$\Delta_{obs.}\ (Co\text{-}NH_3) = \Delta\ Co(NH_3)_6^{3+}$$

$$= 24{,}900\ kK$$

$$\Delta\ (Co\text{-}Cl) = \Delta CoCl_6^{3-}$$

$$\Delta Co(NH_3)_5Cl^{2+} = \frac{5}{6}\Delta\ Co(NH_3)_6 + \frac{1}{6}\Delta\ CoCl_6^{3-}$$

In this thesis the average ligand field method was used to account for the energy of cis-$Co(en)_2Cl_2^+$ in which holohedral symmetry was considered as D_{4h} instead of C_{2v} by taking the equatorial energy as an average of the Cl^- and the nitrogen of ethelyenediamine contributions averaged.

Once spectrosccopic states have been assigned from Tanabe-Sugano diagrams and related considerations the more detailed attempts to study the factors of structure governing photochemistry with the elements of the various states in relation to the relaxed states and the states of possible products, will require examination of a model for the wave functions from which such matrix elements may be calculated. The angular overlap model of MO's was used in the discussion by Vanquickenborne and Ceulemans (79).

4.3 Angular Overlap Analysis and Excited State Bonding in d^6 Complexes

Treatments which use the angular overlap model assign a contribution by each ligand which is additive in orbital energy (79). Within the framework of an additive angular model, one has to specify two parameters, σ_L bonding and π_L bonding for each ligand. If the contribution along each three axes is equal, the effective symmetry is O_h. If two model ligand axes (x and y) are perturbed by ligands in the same way but differently from the third one (z) the effective symmetry is D_{4h}; if all three are different, holoheder symmetry is still at least D_{2h}. It will generally be possible to select one axis (say z) which is quite different from the other two (x and y). The off-diagonal matrix element contains $(\sigma_x + \sigma_y)$. In this approximation the tetragonal case, will then be small and can neglected in the first approximation D_{4h}. Replacing σ_z by σ_{ax} and $\sigma_x = \sigma_y$ by σ_{eq} the preturbation matrix equation (4.3.1) can be expressed by means of the average axial and equatorial parameters.

	z^2	yz	xy	$x^2 - y^2$
z^2	$\sigma_z + \sigma_{-z} + 1/4(\sigma_x + \sigma_{-x} + \sigma_y + \sigma_{-y})$			
yz		$\pi_z + \pi_{-y} + \pi_y + \pi_{-y}$		
xz			$\pi_z + \pi_{-z} + \pi_x + \pi_{-x}$	
xy				$\pi_x + \pi_{-x} + \pi_y + \pi_{-y}$
$x^2 - y^2$	$-\frac{3}{4}(\sigma_x + \sigma_{-x} - \sigma_y - \sigma_{-y})$			$\frac{3}{4}(\sigma_x + \sigma_{-x} + \sigma_y + \sigma_{-y})$

.....(4.3.1)

If so, only diagonal elements will be non zero: the five orbitals of "d" symmetry remain unaffected in all cases and are characterized by the following energies:

$$\begin{aligned} E(z^2) &= 2\,\sigma_{ax} + \sigma_{eq} \\ E(xy) &= E(yz) = 2\,\pi_{ax} + 2\,\pi_{eq} \\ E(xy) &= 4\,\pi_{eq} \\ E(x^2-y^2) &= 3\,\pi_{eq} \end{aligned} \qquad (4.3.2)$$

At this point let us define the bond energy I(M-L) for a many electron system;

$$I(M\text{-}L) = -\sum n_i E_i \qquad (4.3.3)$$

where the summmation runs over the orbitals (bonding and antibonding) n_i is the occupation number of the i th orbital in the hexacoordinated complex and E_i is the energy of the i th orbital). The quantity I(M-L) cannot be expected to be an adequate approximation of the thermodynamic bond energy: an obvious and very important correction factor would include the global energy shifts of the relevant orbitals due to the change in their diagonal matrix elements. I(M-L) includes only spectroscopic parameters and, as such, it can be used optimally in the study of photochemical effects by considering different M-L bonds in the excited state $I^*(M\text{-}L)$. Let us consider the case of $I^*(M\text{-}L_{eq})$ in Co(III) surrounded by six π acceptor ligands . One of the excited configurations corresponds to the $d_{xy} \longrightarrow d_{z^2}$ excitation. The five ligand orbitals e_g and t_{2g} are again fully occupied, while the ligand π^* orbitals

are empty. The contribution to I^* through metal holes $d_{(z^2)}$ and $d_{(x^2-y^2)}$, is $\frac{1}{4}\sigma + 2\left(\frac{3}{4}\right)\sigma = \frac{7}{4}\sigma$. For the π interaction, the contribution comes from the metal electrons $(xy)^1(xz)^2(yz)^2$, i.e., $4\left(\frac{-1}{2}\right)\pi + 1(-\pi) = -3\pi$. It is interesting to compare $I^*(M\text{-}L)_{eq}$ and $I^*(M\text{-}L)_{ax}$ for a specific configuration and a given ligand. The population of d_z destabilzes the axial ligand with respect to the equatorial ligand by the amount $3/4\,\sigma z$. Population of $d_{x^2-y^2}$ has exactly the opposite effect. Depopulation of d_{xy} does not effect the $M\text{-}L_{ax}$ bond but it modifies the $M\text{-}L_{eq}$ bond strength by π energy units (stabilzation for π donor and destabilization for π acceptor ligands). The opposite holds true for depopulation of the (d_{xz}, d_{yz}) orbitals where the net difference $I^*(M\text{-}L_{eq})$ and $I^*(M\text{-}L_{ax})$ amount to $-(\pi/2)$ energy units. After the brief introduction of this theory and its implications we evaluate different energy states of d^6 by using the above parameter for the ground state $^1A_{1g}$

$$I = 4E(e_g)$$
$$= 2(3\,\sigma_{eq}) + 2(2\,\sigma_{ax} + \sigma_{eq})$$
$$= 8\,\sigma_{eq} + 4\,\sigma_{ax}$$

for the excited state $^1T_{1g}(E_g)$

$$d_{xz}, d_{yz} \longrightarrow d_{z^2}$$

$$= E(yz) + E(z^2) + 2E(x^2 - y^2)$$

$$2\,\pi_{ax} + 2\,\pi_{eq} + 2\sigma_{ax} + 2\,\sigma_{eq}$$

for $^1T_{1g}(A_{1g})$ states

$$d_{xy} \longrightarrow d_{x^2-y^2}$$

$$= E(xy) + 2E(z^2) + E(x^2 - y^2)$$

$$4\pi_{eq} + 4\sigma_{ax} + 2\sigma_{eq} + 3\sigma_{eq}$$

for $^1T_{2g}(E_g)$

$$d_{xz}, d_{yz} \longrightarrow d_{x^2 - y^2}$$

$$2E(z^2) + E(x^2 - y^2) + E(yz)$$

$$= 4\sigma_{ax} + 2\sigma_{eq} + 3\sigma_{eq} + 2\pi_{ax} + 2\pi_{eq}$$

for $^1T_{1g}(B_2)$

$$d_{xy} \longrightarrow d_{z^2}$$

$$= E(xy) + E(z^2) + 2E(x^2 - y^2)$$

$$4\pi_{eq} + 2\sigma_{ax} + \sigma_{eq} + 6\sigma_{eq}$$

Working backwards from these equations using an average ligand field model one could estimate values of $I^*(M - L_{ax})$ and $I^*(M - L_{eq})$. In consequence of such considerations, Vanquinborne and Ceulemans reduce Adamson's rules to one single statment i.e. the leaving ligand is the ligand characterized by the largest labilization energy $(I - I^*)$. The following table summarizes $I^*(M - L)$ values for some Co-amine complexes.

Table 4-I

Predicted and observed leaving ligand in some Co-amine complexes

Complex	$I^*(M - L)$	$I^*(M - L)$	$I^*(M - L)$
cis-$Co(en)_2Cl_2^+$	9.15	9.90	15.84
trans-$Co(en)_2Cl_2^+$	7.93		13.64
$Co(NH_3)_5Cl^{2+}$	8.48	8.93	13.11

According to Vanquickenborne and Ceulemans these values characterized the reactivity of a lowest vibrationally equilibrated excited state where spin makes little difference. The only result in our study which could be predicted from these numbers, is the ratio $\Phi_{NH_3} / \Phi_{Cl^-}$ for $Co(NH_3)_5Cl^{2+}$ but only for irradiation at 488 nm.[3] The result for the lower state populated at long wavelength like all results for dichloro ions appear to disagree. Thus, in light of this limitation of the Vanquickenborne and Ceulmans model and the problem with respect to the role of radiationless decay rates in determining Φ, discussed elsewhere by Adamson (85) (in which he noted that the ligand field strength cannot be the sole factor determining overall photoreactivity), we make no further use of this approach.

4.4 Previous analysis of Co-amine spectra:

Wentworth and Piper (4) assigned the component of splitting $^1T_{1g}$ and $^1T_{2g}$ in lower than octahehral symmetry, C_{4v} and D_{4h} (where $^1T_{1g}$ split to ^1E and $^1A_2$, and $^1T_{2g}$ to $^1B_2$ and ^1E) by adopting a certain approximation. They assigned the observed band maximum to the average of the energy of the $^1T_{1g}$ state of the parent compound and that of the ^1E state above the ground state.

In the case of the $^1T_2$ band, the splitting was not observed and their argument was that the charge transfer band overlapped with it. Table (4-II) summerizes the result for some Co-amine complexes.

Table (4-II)

Absorption spectra and band center of some Co-amine complexes ref.(4)

Complex	$^1A_1 \longrightarrow {}^1E$	$^1A_1 \longrightarrow {}^1A_2$	$^1A_1 \longrightarrow {}^1T_2$
$Co(NH_3)_6^{3+}$	21.05		29.5
$Co(NH_3)_5Cl^{2+}$	18.72	21.35	27.5
$trCo(en)_2Cl_2^+$	16.2	22.49	25.92
$trCo(en)_2(NO_2)_2^+$	17.8	22.4	masked

We will use these to discuss below the possibility that wavelength dependence arises from differential population of components which then react from non "communicating" vibrationally equilibrated states.

4.5 Spectral analysis of Co-ammine complexes by MCD spectroscopy:

The MCD bands observed are all assigned as either A or B terms. A terms arise (74) from a transition between a non-degenerate ground state and a degenerate excited state. Thus, it is expected that all of the singlet to triplet or quintet transitions in Co(III) ligand field spectra should correspond to A terms. B terms do not require a degeneracy. They involve the coupling of the states in the transition to all other states of the molecule in consequence of the perturbation produced by the magnetic field. It is therefore not surprising, and is consistent with results of ref (74), that all singlet - singlet bands are B terms. In ref. (74), it was suggested that some of the splitting corresponding to the C_{4v}, C_{2v}, and D_{4h} symmetries of the mixed ligand complexes studied here could be resolved in MCD. Especially, two B terms are reported for the T_{1g} octahedral state of the cis dichloro ion. In point of fact, the resolution of B terms exceeded the splittings that are seen in ordinary absorption spectra! This is not expected. The "derivative" shape of an A term or a C term can aid in spectral resolution of overlapping bands. However, there is no inherent reason why B terms of the same sign should show improved resolution. The resolution reported in ref. (74) appears to have been an artifact of poorer signal/noise 6.6 and slightly unfortunate choice of a lock point. Unfortunately the reference does not specify these lock points. The present argument supports the

criticism of reference (74). We assign one of these bands as B and a lower energy band as an A term. With this change, all singlets are poorly resolved and there is no basis for treatment of the spectra in an effective symmetry lower than octahedral. Therefore, we have attached O_h symmetry labels to all transitions which is equivalent to using an average field model.

In octahedral symmetry, the energies of the transitions are collected in table 2 (75). Using these expressions for the energies the octahedral ligand field splitting parameter, Δ, and the Racah electron repulsion parameters, B and C, are calculated and collected in table (III). Following the procedure discussed above, Table (IV) also shows the calculated spectra using these parameters.

The first point to note is that the A terms assigned to the lower triplets in these spectra are near the region of the spectrum of the well characterized triplet of the $Co(NH_3)_6^{3+}$ ion which has been extensively discussed recently by Wilson and Solomon (5). However, the small peaks at about 10.5 kK which have been recorded several times for halopentaminecobalt(III) ions are at much lower energy. These low energy peaks have been assigned as $^3T_{1g}$ by several authors (75). This cannot be valid if the LF parameters calculated here are correct. That there was a problem is hinted by the fact that these bands appear at an energy more than 2 kK below the triplet of the $Co(NH_3)_6^{3+}$ but do not vary with the ligand field strength of the halide

ligand. The origin of the 10.5 kK feature may be the overtone of an $-NH_2$ vibration which was identified at this energy by Wilson and Solomon from the comparison of Co and Cr amine complexes and by deuteration. (The other possibility is that the band is a "hot band" of the hypersensitive type since the singlet - triplet transition is associated with a $\Delta J = 2$ (76)).

An interesting specific feature of the -NCS complex is the reversal of the sign of the second B term compared to all the others. This is a reminder of the charge transfer mixing into this band.

We now turn our attention to the parameter table 2. The values of the orbital splitting parameter, Δ, are slightly smaller than those reported earlier (75). They are also less sensitive to the ligand field strength of the halide. This may simply reflect the low resolution of the B terms in the MCD spectra and the band centre error that arises from the need to set "lock" points to define the baseline. The fit given in Table 2 is not as good overall as is often found. This no doubt reflects the low resolution of the MCD and the great error in placing band centers. The value of the MCD spectra is in the opportunity to observe spin forbidden bands. Earlier efforts to fit LF parameters to spin forbidden bands in acidoamine complexes (e.g. ref 77) have produced rather odd values of the Racah parameters. The ratio C/B is expected to be 4 (75). Values calculated were nearer 8. This is now seen to be a consequence of the assignment of the lowest triplet at

approximately 10.5 kK. With the triplet as seen here, the expected ratio is, in fact, obtained. Thus, the MCD spectra may involve weak bands with consequent large errors in the location of band centers. Specifically the B terms are too broad for precise location of their centers.

This leads to the point of photochemical significance (5,61). The quintet appears to be located between the two singlet bands. This conclusion is established by two distinct arguments. First, and most directly, by the assignment of an A term in this region to the quintet. Second by the fitted position using the present qualitatively correct (i.e. giving reasonable C/B) LF parameters. Photochemical discussion has centered on the possibilty that the quintet might be the lowest excited state. For this to be the case in the vertical excitation of absorption spectroscopy would require a value of the Racah parameter C much too large to match expectations from simple theory. For it to be true of the vibrationally relaxed states, the energy minima would need to be more than 5 kK more removed from the absorption position for quintets than for triplets. This seem to be too large. We conclude quintets cannot be below.

Table (4 -III)

State energies and ligand field parameters

Transition Energies (75)

$E(^1T_{1g}) - E(^1A_{1g} = \Delta - C$

$E(^1T_{2g}) - = \Delta + 16B - C$

$E(^3T_{1g}) - = \Delta - 3C$

$E(^3T_{2g}) - = \Delta + 8B - 3C$

$E(^5T_{1g}) - = 2\Delta - 5B - 8C$

Parameters (kK)

Complex		B	C	C/B
$Co(NH_3)_5Cl^{2+}$	20.0	0.54	2.1	3.7
$trCo(en)_2Cl_2$	20.5	0.50	2.2	4.4
$cis\text{-}Co(en)_2Cl_2^+$	20.9	0.50	2.0	4.0
$cis\text{-}Co(en)_2NCSCl^+$	21.1	0.35	2.1	6.0

Table (4-IV)

Spectra of Co(III) d^6 complexes in approximate octahedral symmetry

Complex	Transition	Absorption	MCD	Calculated
		Kk		
$Co(NH_3)_5Cl^{2+}$	$^1T_{1g} \leftarrow\!\!- {}^1A_{1g}$	18.7	18.8(B)	18.0
	$^1T_{2g}$	27.5	27.5(B)	26.6
	$^3T_{1g}$	-	15.0(A)	13.8
	$^3T_{2g}$	-	20.0(A)	18.2
	$^5T_{1g}$	-	23.2(A)	21.2
tr-$Coen_2Cl_2^+$	$^1T_{1g} \leftarrow\!\!- {}^1A_{1g}$	19.2(b)	18.8(B)	18.3
	$^1T_{2g}$	25.0	26.8(B)	26.3
	$^3T_{1g}$	-	- (d)	13.9
	$^3T_{2g}$	-	16.2(A)	17.9
	$^5T_{1g}$	-	22.9(A)	20.9
cis-$Coen_2Cl_2^+$	$^1T_{1g} \leftarrow\!\!- {}^1A_{1g}$	19.9	20.5(B)	18.9
	$^1T_{2g}$	25.0	26.8(B)	27.3
	$^3T_{1g}$	-	15.5(A)	14.9
	$^3T_{2g}$	-	18.5(A)	18.9
	$^5T_{1g}$	-	22.0(A)	23.3
cis$Coen_2NCSCl_2^+$	$^1T_{1g} \leftarrow\!\!- {}^1A_{1g}$	19.9	20.5(B)	19.8
	$^1T_{2g}$	-(c)	25.5(B)	24.6
	$^3T_{1g}$	-	15.5(A)	14.8
	$^3T_{2g}$	-	18.5(A)	17.6
	$^5T_{1g}$	-	22.0(A)	23.7

(a) Calculated from LF parameters in table (III)

(b) Average of the two lower symmetry components.

(c) Band hidden under the CT tail.

(d) There is some indication of this band in the spectrum but the centre cannot be placed

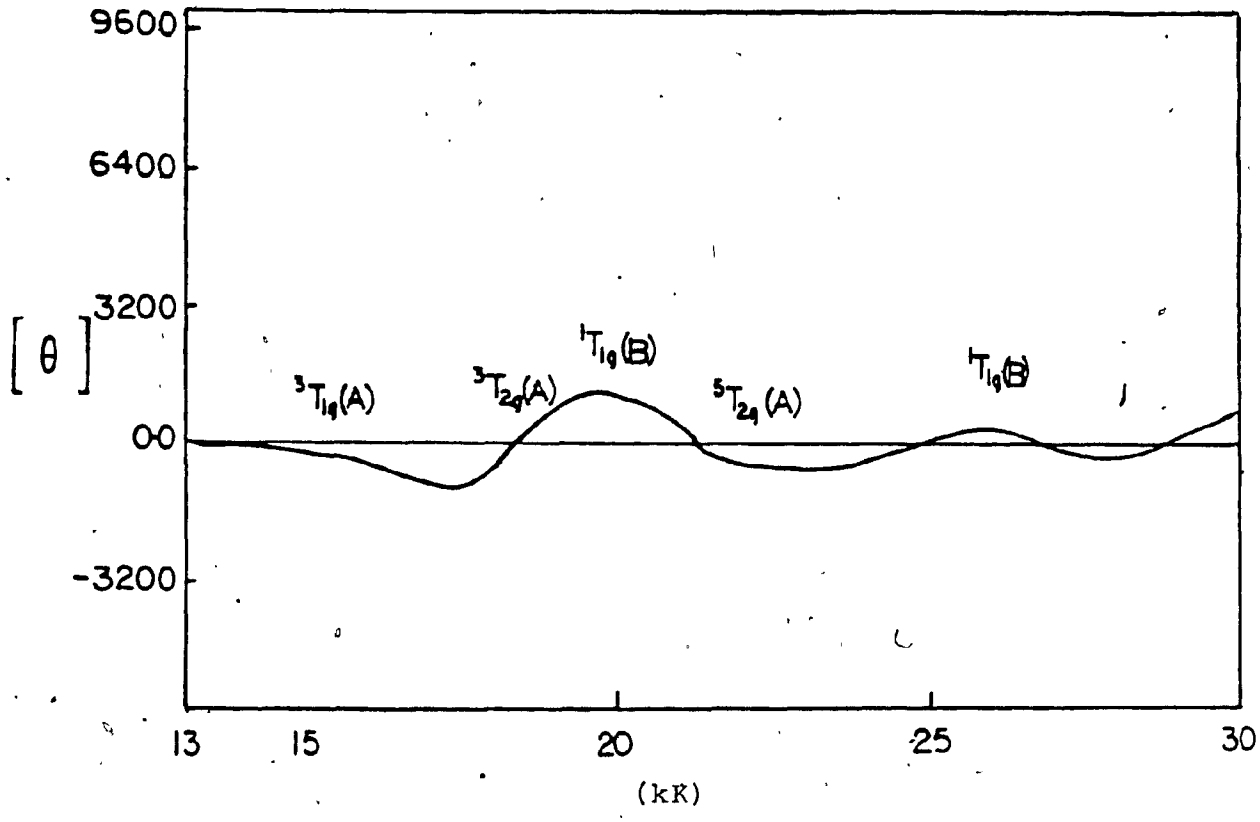

Figure 4.2 The MCD spectrum of cis-$Co(en)_2Cl_2^+$. Concentration 0.0285M. Lock points at 14 kK and 27 kK.

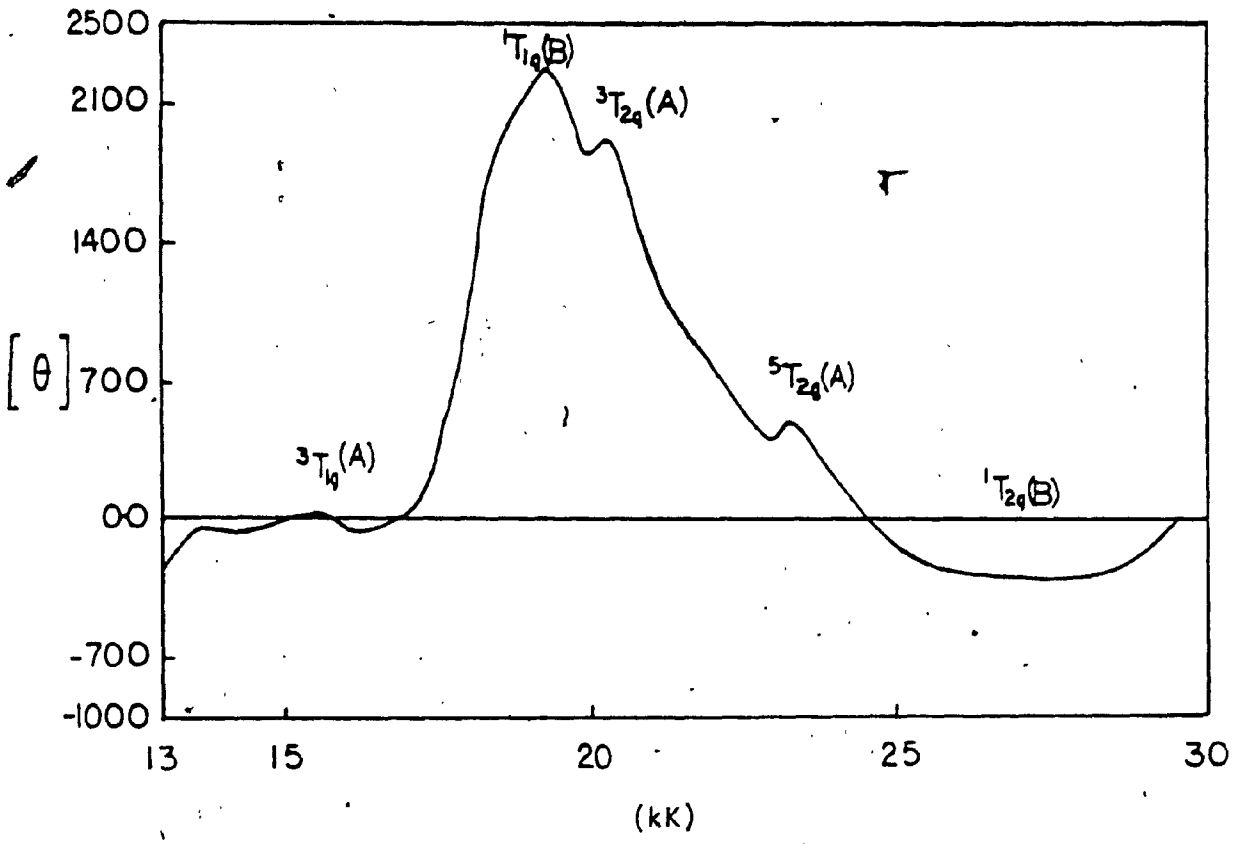

Figure 4.3 The MCD spectrum of $Co(NH_3)_5Cl^{2+}$. Concentration 0.0521M
Lock points at 13 kK and 24 kK.

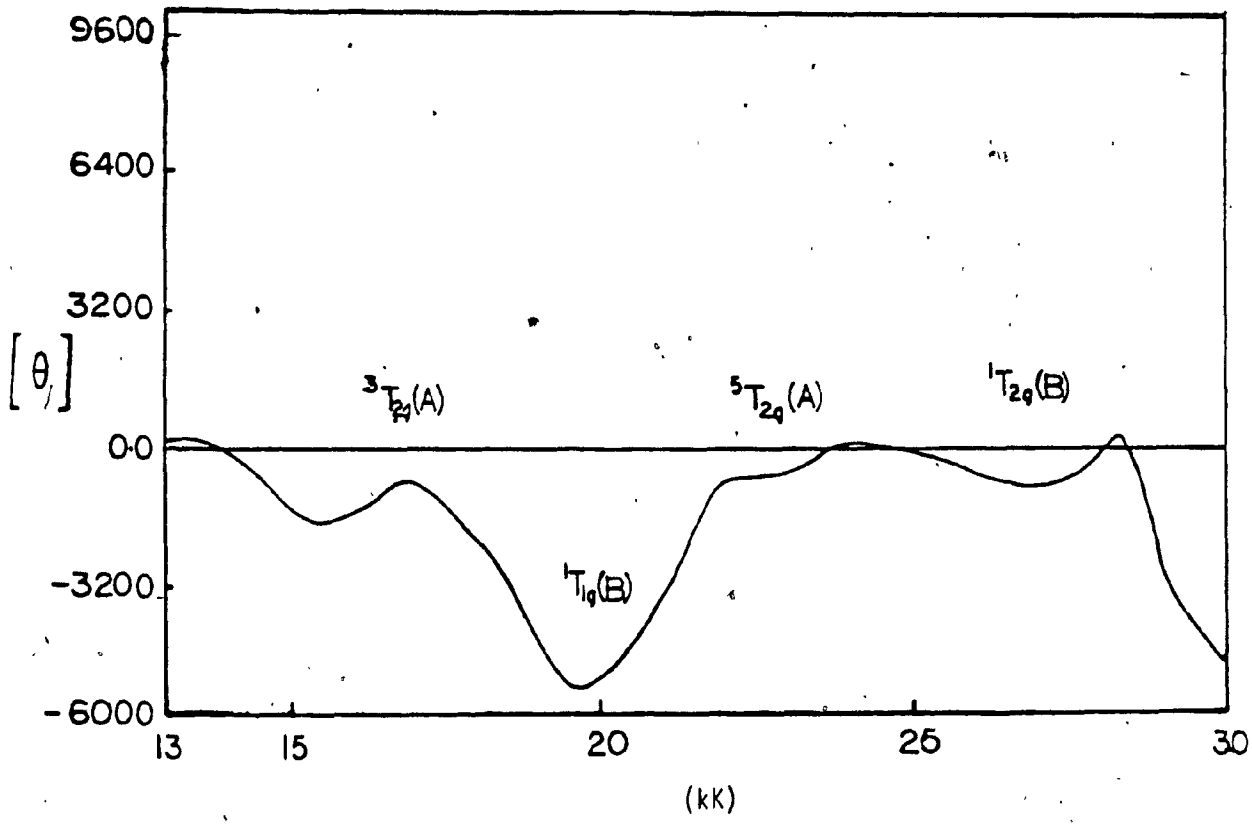

Figure 4.4 The MCD spectrum of trans-$Co(en)_2Cl_2^+$. Concentration 0.0371 M. Lock points 14 kK and 28 kK.

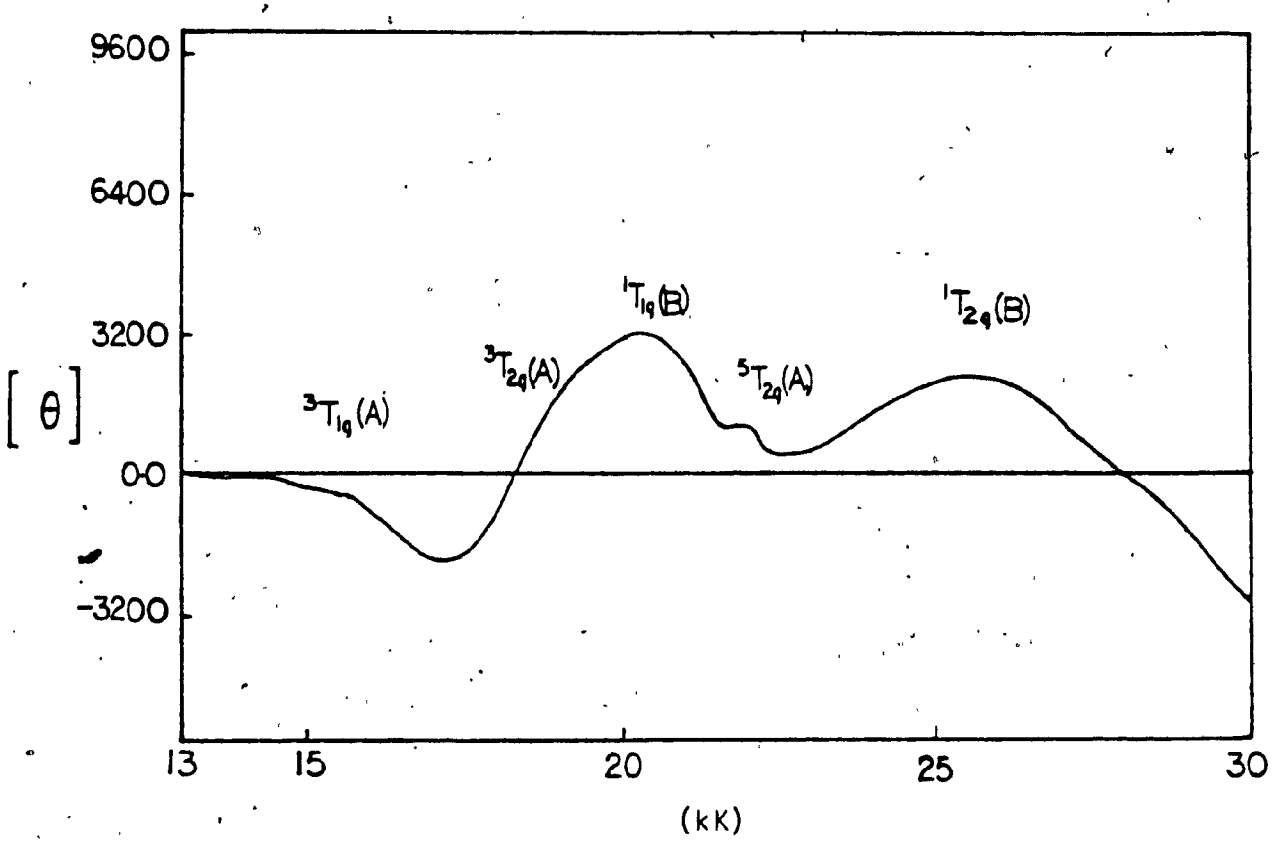

Figure 4.5 The MCD spectrum of cis-$Co(en)_2(NCS)Cl^+$. Concentration 0.018M. Lock points 14 kK and 24 kK.

Chapter 5

Discussion

5.1 Wavelength Dependence Study:

5.1.1 The photochemistry of the $Co(NH_3)_5Cl^+$:

Both chloride and ammonia yields were found to be consistent with the result of Pribush et al. (18) at 488 nm and with the results of Langford and Vuik (19) at 647 nm(Table 3.1 page 69). The issue is the behavior in between. Looking at the chloride yield along the first electronic absorption band, it was found to be falling toward a non-zero value at 647 nm . The ratio of Φ_{NH_3} / Φ_{Cl^-} which started with value 3.0 is inverted to 0.1 at 647 nm. This is easily interpreted if the NH_3 yield is approaching zero at about 647 nm. The wavelength dependence reported here shows that the relaxation processes among states determining both these reactions are prompt and occur in competition with vibrational relaxation in the original singlet manifold.

Once the significance of the initial degree of vib ronic excitation is realized, it is clear that there is nothing in the results to exclude the production of primary products with varying efficiency as a function of initial vibronic state. That is, we cannot directly distinguish prompt reaction from the initially populated singlet vibronic levels occurring in competition with full vibrational relaxation from other wavelength dependent processes invol-

ving crossing from the singlet to other states which then react, after vibrational equilibrium. An important part of the further analysis will be to begin to make a distinction. The difference in wavelength dependence of Φ between Cl^- and NH_3 yields strongly suggests that more than one state is involved in the photochemistry. Since our MCD spectra place $^5T_{2g}$ rather high, these states are taken to be $^1T_{1g}$ and the triplet states ($^3T_{1g}$ and $^3T_{2g}$) or their components in lower symmetry D_{4h} and C_{4v}. Since the ammonia Φ approaches zero at the end of the singlet region, one can argue plausibly that it is coming from a singlet, $^1T_{1g}$ which, in the case of C_{4v}, will split to A and E. In contrast, the remaining significant Cl^- yield at 647 nm suggests a significant reactivity from a lower lying state, probably the triplet. Further comment will follow the introduction of other chloro complexes.

5.1.2 The photochemistry of trans-$Co(en)_2Cl_2^+$:

Only chloride yields are measurable in this case. This complex shows different wavelength dependence from the previous one. The yields decline in the shorter wavelength region (at 457, 488 and 514 nm)whereas at the remaining wavelengths they are steady. One can argue that the tail of the CT band will cause redox initiated reaction as well as the direct photosubstitution process at short wavelength. This suggests a basically wavelength independent Φ and a reaction originating from relaxed vibronic state, perhaps one below the singlet such as the triplet

5.1.3 The Photochemistry of cis-$Co(en)_2Cl_2^+$ and cis-$Co(en)_2(NCS)Cl^+$:

Finally, looking at the results for these two complexes, one can see a similarity in their behavior. They both give evidence of a wavelength dependent process in the LF region. In the NCS^- complex we have analytical difficulties limiting measurement of the Cl^- yield but SCN^- yield declines by a factor of 3 in the same way (qualitatively) as does Cl^- aquation in the cis dichloro complexes. There is no reason to assume the approach to 4.3×10^{-4} at the end of the singlet is evidence of wavelength dependence.

5.2 The Hollebone selection rule in the photochemistry of Octahedral complexes:

In the conventional theory, the Born-Oppenheimer approximation provides the crucial separation of electronic and vibrational terms. The same mathematical convenience may be obtained through a vector decoupling procedure in tensor LF theory without any assumption concerning the vibronic coupling strength. The transition moment calculation, by either conventional or tensor technique, define the probabilities of each event to any desired order approximation. The tensorial approach, makes it clear, however, that a very limited number of vibronic coupling channels are available in most promotion and decay processes in low order perturbation calculation. If such calculations are relevant an initial vibronic states at various wavelengths can relax differently.

The test of any model, including the tensorial view of photo and decay processes just described, is its ability to predict and correlate observable events. This is only possible for low order perturbation approaches. We therefore make the major assumption that the reactions of DOSENCO (decay on selected nuclear coordinates) states will occur along the reaction coordinate determined by first order vibronic coupling of states by photon absorption.

A general procedure was formulated by Hollebone (44,45) for predicting a photoreactive coordinate:

a) The intensity of a vibronic transition is governed

by an overall octapole rule $\Delta T = 3$ where ΔT is the total angular monentum

b) Factoring this rule by tensor LF methods leads to sums of electronic and vibrational angular momentum

$$\Delta J + \Delta V = \Delta L + \Delta S + \Delta V = \Delta T = 3 \quad (1.3.1)$$

where the changes in orbital angular momentum as ΔL, spin as ΔS and ΔV changes in the vibrational angular momentum quantum number

c) By substituting known values from electronic spectra into equation (1.3.1) and vibrational angular momentum became:

$$\Delta V = \Delta T - [\Delta L + \Delta S]$$

$$= 3 - [\Delta L + \Delta S]$$

d) In the assigning of the normal mode for any ΔV, assume the ground state has an A_{1g} mode and use only those modes with non vanishing amplitude at the ligands for terminal states.

The reaction coordinated for specific events of photoexcited d^6 systems can be predicted using the general rules for transition observed in the visible region in the six coordinate Co(III) complex

	ΔJ		ΔV	Γ_V
$^1A_{1g}(^1I)$----- $^5T_{2g}(^5D)$	2	then	1	A_{1g}
$^1A_{1g}(^1I)$----- $^3T_{1g}(^3H)$	2	then	1	A_{1g}
$^1A_{1g}(^1I)$----- $^3T_{1g}(^3H)$	2	then	1	A_{1g}
$^1A_{1g}(^1I)$----- $^1T_{1g}(^1I)$	0	then	3	T_{1u}

To illustrate the scope of the theory, the final consideration will draw on different and much less straightforward experimental data. This draws attention to the importance of a capacity to understand medium effects. The first order selection rules do give an indication of factors involved in intersystem crossing processes. Consider the transition of ^2E_g states of trans-$Cr(NH_3)_2(NCS)_4^-$ to a $^4A_{2g}$ ground state (approximate O_h symmetry $^4A_{2g}$ is either a product state or the original ground state.) The rate of this relaxation is medium dependent.

5.3 The Solvent Effect on the Photochemistry of Co(III)-amine:

In reviewing the different possible roles of the solvent in chapter 1, we attempted to establish the connection between the possibilties and photoreaction mechanisms. Our results in table (3 - IV) reveal that the quantum yield is generally decreasing in series from water to different mixtures of glycerol-water to DMF and DMSO. First, we will consider the effects associated with kinetic facility of the departure of the leaving ligand. The classical treatment for the correlation of dissociation kinetics correlation with the Winstein Y parameter shows a decrease in the correct order. The correlation of Winstein Y with related thermal substitution reaction has a small slope, m, usually 0.2 (83). Thus it does not appear that this factor can account for the large changes in Cl^- yields.

A second possibility is a relation to solvent nucleophilicity. This has been illustrated in the photochemistry of $Cr(en)_2(SCN)F^+$ (41). The effect is in the correct order for DMF and DMSO, but there is no reason to assume that a modest amount of ethylene glycol can strongly effect nucleophilicity. Thus, it does not seem plausible to focus a comprehensive account on effects related to nucleophilicity. In each of these two cases, we may at best have identified a factor in the situation but do not have a comprehensive theory.

The next possibility is an analog of the effect postulated by Conti and Forster described in chapter 1.

This would explain solvent effects in terms of the variation of microenvironments as bulk composition changes. The effect on yields would arise because of changing probability of excitation in these different microenvironments. This is a reasonable suggestion and can explain wavelength dependence. Unfortunately, we have no definite information concerning the proposed microenvironment and therefore cannot fully evaluate this mechanism.

The next possibility "Hollebone theory" the excited state $^1T_{1g}$ is populated in a process vibrationally allowed by coupling with the vibration $|3t_{1u}>$. To couple the singlet and triplet in the vibrational excited state of singlet $^1T_{1g}$ is forbidden, but a fast intersystem crossing could become allowed via a quadrupole perturbation (change of angular momentum quantum number by 2) delivered by the medium. The following scheme help us to understand this case:

$$^1A_{1g}|0\ a_{1g}> \xrightarrow{h\nu} {}^1T_{1g}|3\ t_{1u}> \xrightarrow{isc} {}^3T_{1g}|3\ t_{1u}>$$

$$^1A_{1g}|0\ a_{1g}> \leftarrow$$

Fast isc may be evident in photochemistry of trans-$Co(en)_2Cl_2^+$ in which the quantum yields remain constant at longer wavelength as shown in figure 3.3. but no other effect seen in our work is consistent specifically with

Hollebone's models.

The final reasonable mechanism is the cage recombination. For the photo-aquation of $Co(en)_2Cl_2^+$ the following simplified mechanism can be suggested in order to account for the observations.

$$Co(en)_2Cl_2^+ \xrightarrow{h\nu} {}^*Co(en)_2Cl_2^+ \qquad \text{----------(5.2.1)}$$

$${}^*Co(en)_2Cl_2^+ \xrightarrow{k_2} Co(en)_2Cl_2^+ \qquad \text{----------(5.2.2)}$$

$${}^*Co(en)_2Cl_2^+ \xrightarrow{k_3} [Co(en)_2Cl\ldots\cdot Cl^-]^+ \qquad \text{----------(5.2.3)}$$

$$[Co(en)_2Cl\ldots\cdot Cl^-]^+_{cage} \xrightarrow{k_4} [Co(en)_2Cl_2]^+ \qquad \text{-------(5.2.4)}$$

$$[Co(en)_2Cl\ldots Cl^-]^+_{cage} \xrightarrow{k_5} Co(en)ClH_2O + Cl^- \qquad \text{----(5.2.50}$$

According to this mechanism, the observed photo-aquation quantum yield is given by

$$\Phi = \frac{k_3}{k_2 + k_3} \quad \frac{k_5}{k_4 + k_5} = \Phi' \frac{k_5}{k_4 + k_5} \qquad (5.2.6)$$

where Φ' is the primary cleavage yield. While a dependence of Φ' on the solvent composition cannot be definitely ruled out, the experimental results show without doubt step 4 and 5 to be the most important. The rate constant for diffusive cage escape, k_5 is expected to decrease with increasing solvent viscosity, while that of geminate recombination within the cage, k_4, should be essentially solvent independent. It is clear that the quantum yield is directly proportional in the first order of reciprocal(η). Ambiguity remains with respect to the possibility of hydrogen bonding and the effect of the charge on these results, but on balance, cage models seem adequate to the

effects observed. This means that the primary yields are larger than overall yields and wavelength dependence is associated with these large primary yields.

5.4 Effect of Temperature on the Photochemistry of Co(III)-Amines:

The hypothesis that the reactions occur in competition with vibrational relaxation has consequences for T dependence. If a reaction does not involve at least pseudo equilibrium over some vibrational degrees of freedom, the Boltzman factors which appear in experiment via apparent activation energies (E_{app}) cannot be important. Therefore, low apparent activation energies are evidence for the hypothesis of a reaction in competition with vibrational relaxation. The only way we can have a larger E_{app} and sustain the hypothesis is if the overall yield is controlled by a complex mechanism with only the primary step so fast (This is, of course, what the last section suggested).

To define quantities precisely, the temperature dependence of photoreaction is expressed as an apparent activation energy, E_{app} obtained by applying an Arrhenius type equation for quantum yield

$$E_{app} = R \frac{\ln \Phi_1 - \ln \Phi_2}{1/T_2 - 1/T_1} \qquad \text{----------(5.3.1)}$$

To find an expression for interpretation of this activation energy one must include all possible steps which could contribute to the formation of the product. If back reactions of primary products are excluded, the system is still as complex as:

$$A \xrightarrow{h\nu} A^* \quad \text{(Activation)} \quad \text{---------(5.3.2)}$$

$$A^* \xrightarrow{k_1} A \text{ primary product} \quad \text{----------(5.3.2)}$$

$$A^* \xrightarrow{k_2} A \text{ (deactivation)} \quad \text{----------(5.3.4)}$$

$$\Phi_1 \simeq \frac{k_1}{k_1 + k_2} \quad \text{--------(5.3.5)}$$

Assuming the simple case that the physical deactivating process does not depend on the temperature (which is by no means always relevant)

$$\Phi_1 = \frac{A\, e^{-E/RT}}{Ae^{-E/RT} + k_2} \quad \text{----------} \quad (5.3.6)$$

$$\ln \Phi = -E/RT - \ln(e^{-Ea/RT} + k_2/A) \quad \text{----------(5.3.7)}$$

combining equation (5.3.1) and (5.3.7)

$$E_{app} = E_a - \frac{R}{1/T_2 - 1/T_1} \ln \frac{e^{-Ea/RT} + k_2/A}{e^{-Ea/RT} + k_2/A} \quad (5.3.8)$$

Equation (5.3.8) shows that the simplest relation between E_{app} and and elementary E_a is complex. For this reason the following conideration should be taken into account.

1- Plots of ln versus 1/T should not be linear in general, but for practical reasons one can use only a small temperature variation and therefore neglects the 2nd term of equation (5.3.8).

2- In the simple case the apparent activation energy (5.3.1) is the difference $E_a - E_{app}$ increases with increasing quantum yields and may reach values of several K cal/mol for quantum yields of order 10^{-1}. For our low yields the difference will be neglegible if the simple scheme is adequate but cage effects may intervene.

3- The physical deactivating process may show an activation energy. In some cases it may be large. Returning to our results which show good linearity in reciprocal temperature, an activation energy of 6.6 K cal /mol is found for trans-$Co(en)_2Cl_2^+$ and for cis-$Co(en)_2$ a value of 6.9 K cal/mol. These values are marginal and larger than the 2-3 Kcal value found for reactions that have been associated with the picosecond processes from Cr(III) quartets (82). They are much smaller than processes associated with equilibrated Cr(III) doublets (44). They are similar to those that Rumfeldt and Sellan associated with control by elementary diffusion steps (80,81). Since the total yields here are small, there is some reason to suspect that a simple mechanism is too elementary. Ambiguous E_{app} results along with our analysis of solvent effects tend to support a complex mechanism where the initial fast (wavelength dependent) step does not determine overall yield.

5.5 The role of ring opening in the photochemistry Co(III)-amine :

The results for(Φ) in the ethylenediamine complexes (which represent the cleavage of amine group in ethylenediamine from the metal) were consistent with work done by Sheridan and Adamson (21). The ratio Φ_{Cl^-} / Φ_{H^+} was also > 1 as in the case for trans-$Cr(en)_2X_2^+$, but in the case of cis-$Cr(en)_2Cl_2^+$ the ratio was inverted from value the value also > 1 found for Co(III) (86).

Thermal and photochemical studies showed that both trans and cis are converting to trans-$Co(en)_2(H_2O)Cl^{2+}$. This means that in both cases the intermediates are the same. There is the possibilty that ligand detachment at the point of labilization is followed by a rearrangement to an intermediate of trigonal bipyramidal geometry rather than by the prompt, coordination of the solvent. Taking the result for Φ_{Cl^-} in conjunction with temperature and wavelength dependence which show at least two different pathways for reactions at cis Co(III) centers but not necessarily trans centers one finds the mechanisms suggested by Sheridan and Adamson inadequate. However, the low yield in comparison with reactivity rule expectations of cleavage of amine ligand could be explained by one of the following effects:

1- A steric effect of ethylenediamine which prevents a water molecule from effecting nucleophilic attack

2- A strain caused in the bidentate ligand which inhibits the donor atoms from acting independently.

5.6 Picosecond Spectra and Transient Assignment:

We have examined $Co(NH_3)_5Cl^+$, cis and trans-$Co(en)_2Cl_2^+$, trans-$Co(en)_2Cl_2^+$, trans-$Co(en)_2(NO_2)_2^+$, and trans-$Co(en)_2(NCS)Cl^+$. In all of these cases, excitation at 355 nm corresponds to initial population of a ligand to metal charge transfer state (LMST). In no case was transient ground state bleaching observable. This is not surprising since the ligand field bands in the visible spectrum are rather weak for exploitation in transient spectroscopy. Any change of absorbance in this region is expected to be small since typical pulse energy is 2.5 mJ. and about 1% of ground states are excited at the concentration used. In the three chloroamine complexes with only ligand pi to metal charge transfer possibilities, no excited state absorption is found in the visible spectrum (see figure 5.1,2,3). However, for both of the complexes with ligands that have potential π antibonding acceptor orbitals for metal to ligand charge transfer (LMCT), excited state absorption is observed in the visible spectrum. Figure(5.4) shows the excited state absorption spectrum of the trans dinitro complex at a probe pulse delay of 13, 46, 179 ps. The plots show the average spectrum from 10 experiments and the curves at plus or minus one standard deviation. Figure 5.5 shows the spectrum for the chloro-isothiocyanato complex at three delay times. In the second figure there is clear evidence for an initial excited state absorption in the near uv which appears with pulse and

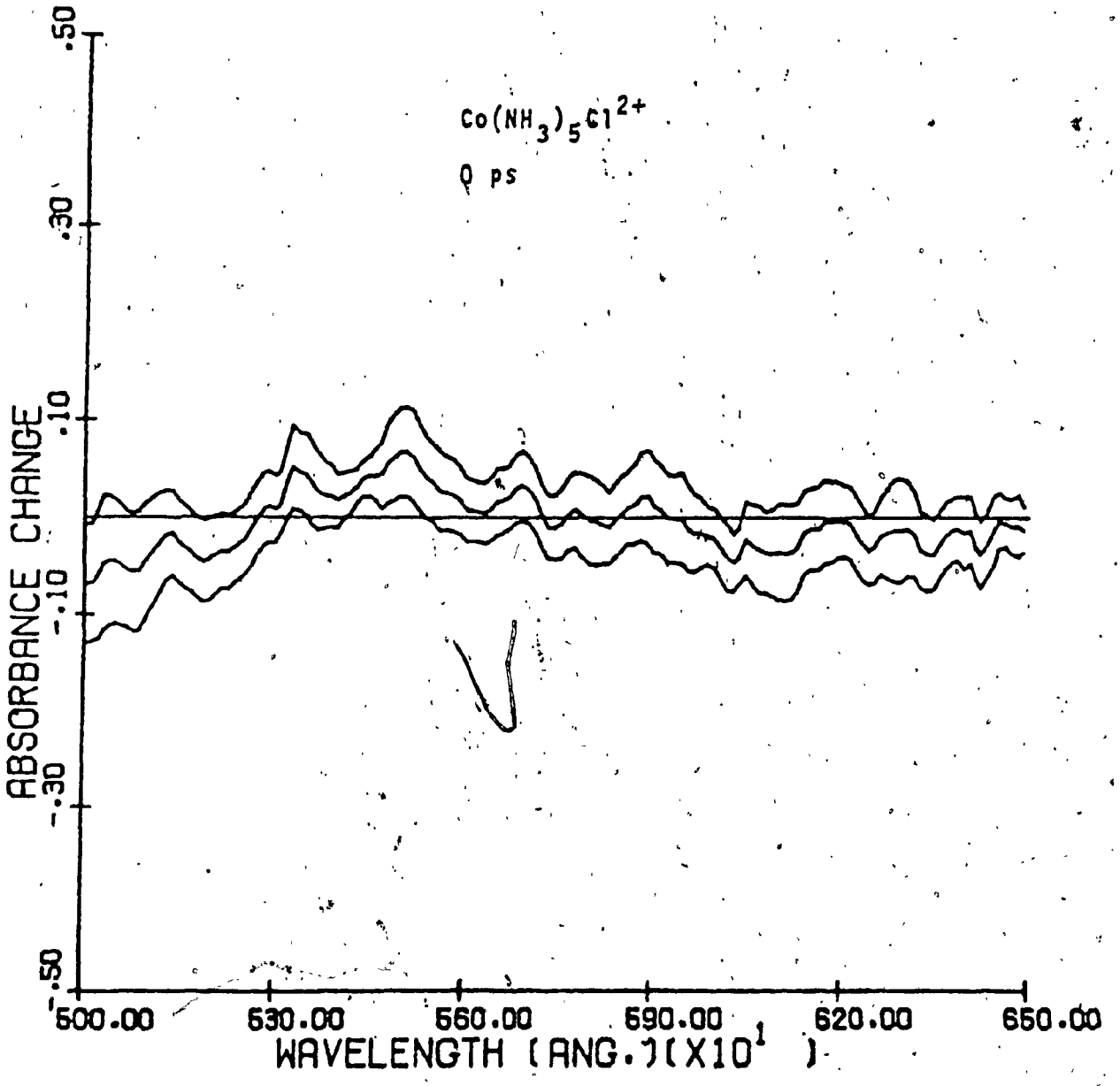

Figure 5.1 Transient absorption spectrum of $Co(NH_3)_5Cl^{2+}$ at a probe pulse delay of 0 ps

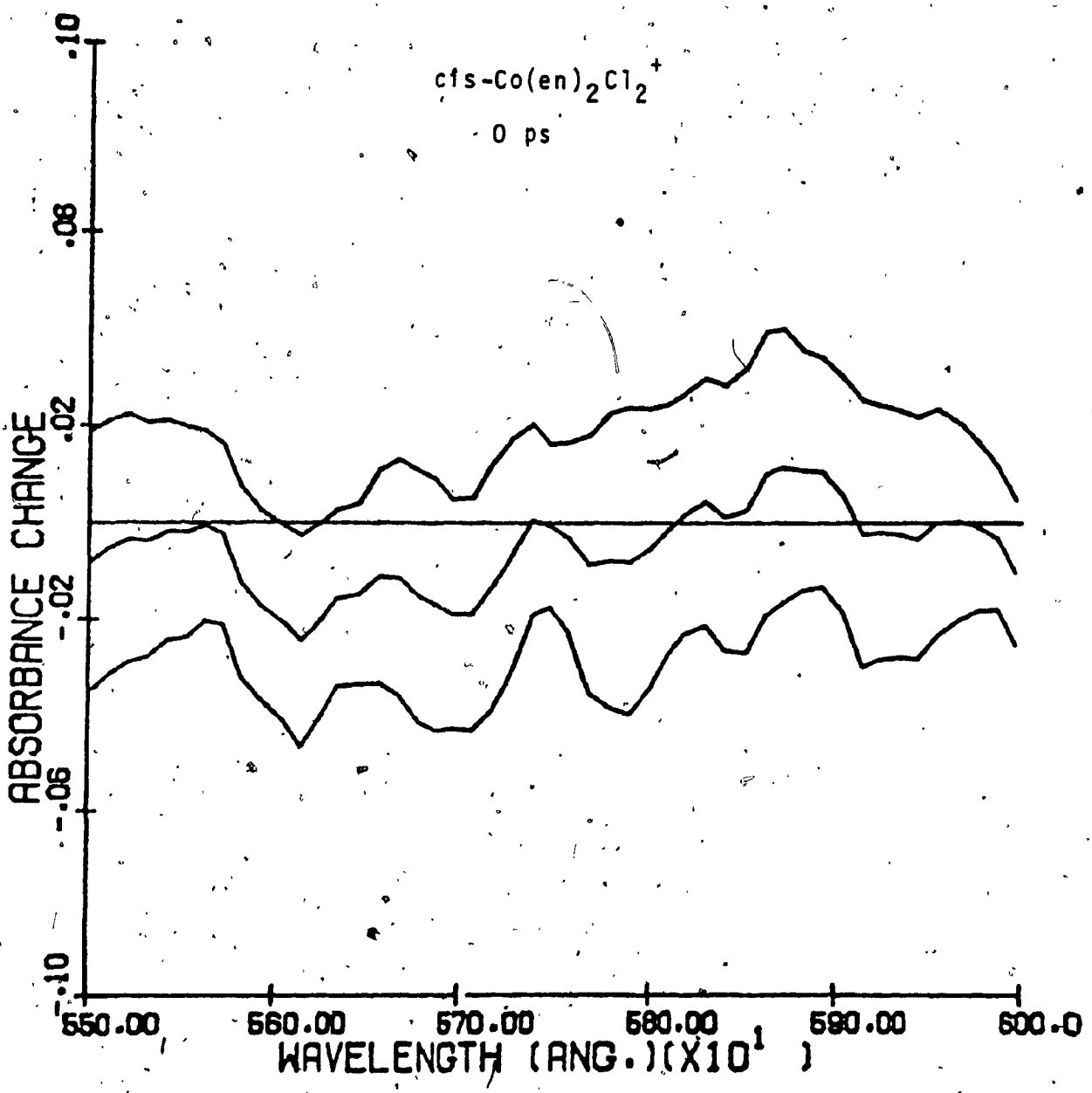

Figure 5.2 Transient absorption spectrum of cis-$Co(en)_2Cl_2^+$ at probe pulse delay of 0 ps.

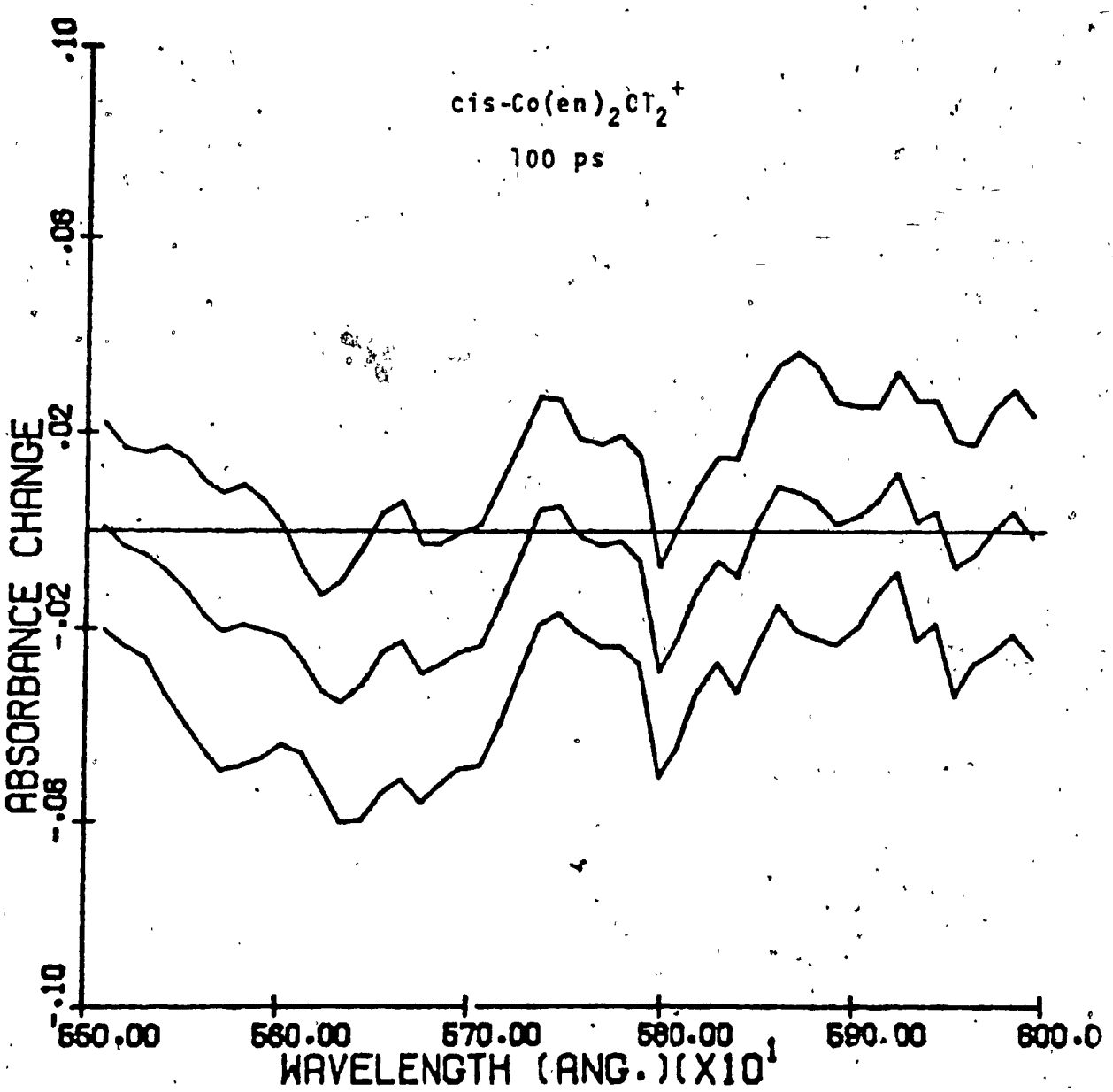

Figure 5.3 Transient absorption spectrum of cis-Co(en)$_2$Cl$_2^+$ at probe pulse delay of 100 ps.

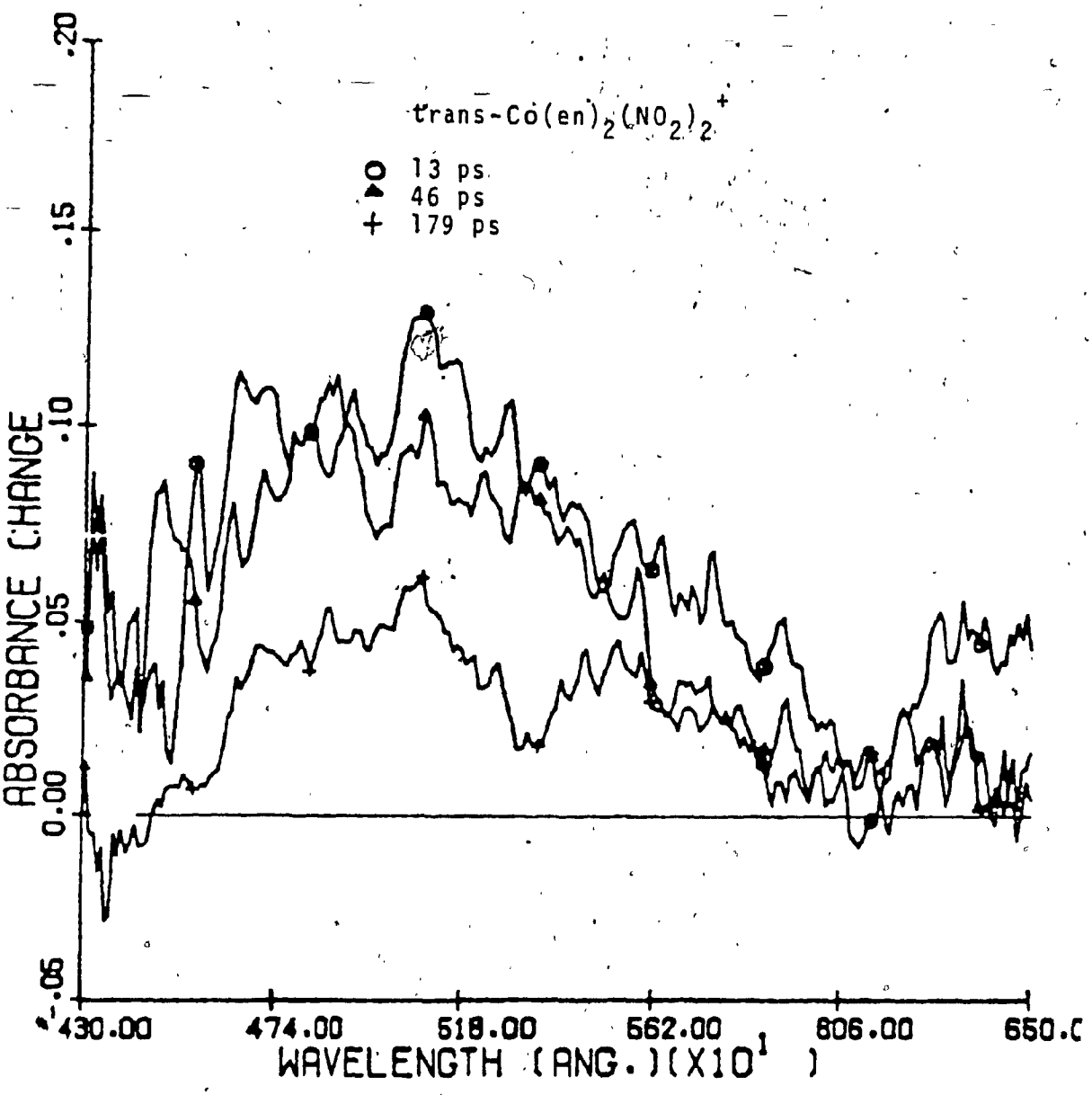

Figure 5.4 Transient absorption spectra of trans-Co(en)$_2$(NO$_2$)$_2^+$ at probe pulse delays of 13, 46, and 179 ps.

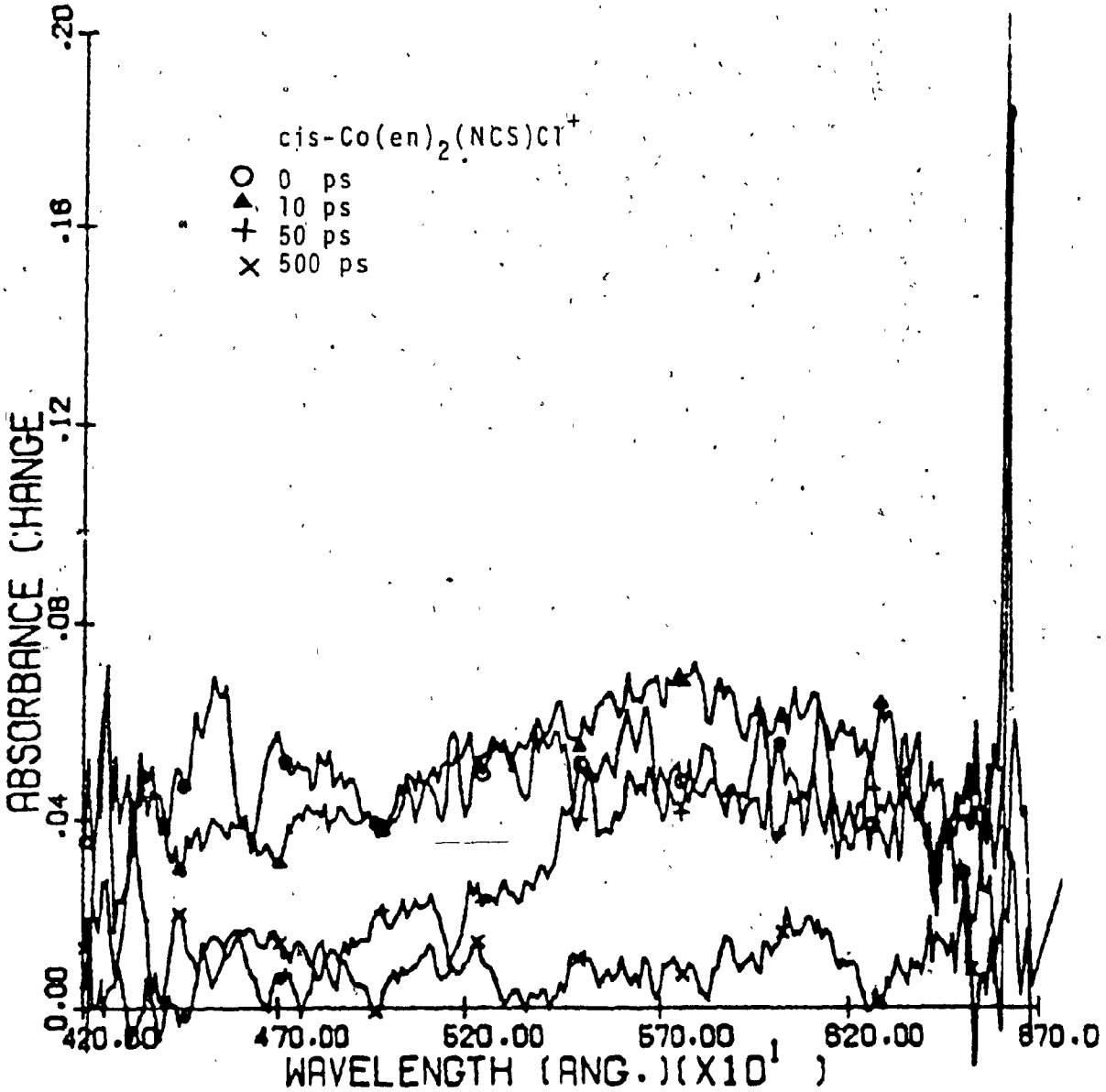

Figure 5.5 Transient absorption spectra of cis-Co(en)$_2$(NCS)Cl$^+$ at probe pulse delays of 0, 10, 50 , 500 ps.

rapidly decays in favour of the lower energy absorption centered near 605 nm which decays on a well a defined time scale with a lifetime of 120 ps. In the spectrum of the dinitro complex the evidence for the preliminary transient is less well defined but there is again a longer lived transient in the visible spectrum centered near 488 nm. This transient has a lifetime of 50 ps. Three possibilities suggest themselves as assignments for the transient:

1) A transition involving states which, in consequence of geometrical changes in the excited state, bear little relation to transitions assigned in ground state spectra.

2) A transition from the halogen or pseudo halogen formed by homolytic fission of Co-X bond to the Co(II) species produced by the same event.

3) A transition from the lowest ligand field triplet ($^3T_{2g}$ in O_h symmetry) analogous to the nanosecond state of Rh(III)amines (or $Co(CN)_6^{3-}$) (62)to a ligand based acceptor orbital (π^*) . The first possibility plagues all studies of excited state spectra. Little more can be said. The second and third possibilities can be evaluated with reasonable confidence.

The proposal that irradiation at 355 nm leads in a few picoseconds to homolytic fission is plausible. However, this assignment offers no reason for the apparent requirement for a ligand like NO_2^- or NCS^- which has a low lying π^* level. (Why shouldn't there be transient spectra

in the chloro complexes?). Furthermore, LMCT transitions in the parent Co(III) complexes which are assigned ligand π to metal e_g^* are in the uv. The optical electronegativity of the Co(III) upper sub-shell is assigned by Jorgenson (84) as 1.6-1.9. The lower sub-shell of Co(II) is assigned at 1.9. Thus, it is not clear how to account for the large shift to the red if the $.NO_2$ to Co(II) assignment is adopted. Thus, there are two problems with the proposal which we cannot resolve. The final test of this proposal may be a study of $Co(NH_3)_5SCN^{2+}$ since this complex undergoes photoisomerization to $Co(NH_3)_5NCS^{2+}$. The homolytic intermediate must exist. Dr. David Buckingham has agreed to send a sample of this difficult complex.

The remaining possibility would assign the transient ESA to a ligand field triplet to a ligand π^* transition (illustrated in fig. 5.6). It is the assignment most consistent with the interpretation given for Rh(III) and $Co(CN)_6^{3-}$ luminescence. This also provides a rationale for the apparent requirements for ligands $-NO_2$,-NCS. The relaxed LF triplet lies below the lowest (near) singlet by the sum of Racah parameter (77) plus an additional term for relaxation of the excited state which has one si antibonding electron. With Racah B = 500 cm^{-1} and C = 4B, the singlet-triplet splitting in absorption is estimated to be approximatly 4,000 cm^{-1} (i.e. 2C). This is an over estimate since geometrical relaxation should reduce repulsion. The additional "relaxation" term should be less

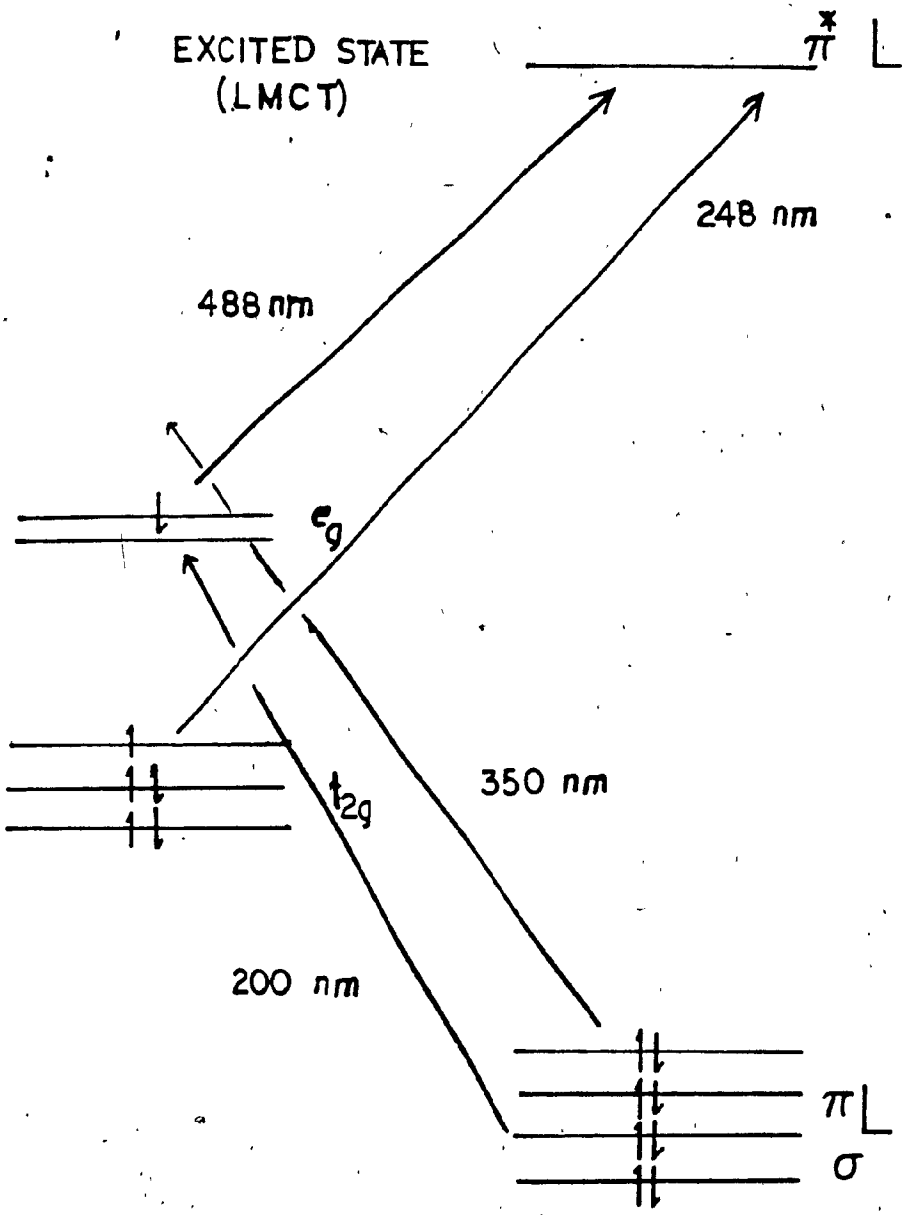

Figure 5. 6 Approximate MO diagram of Co-amine complexes

than 1/2 of the Stokes shift between absorbance and luminescence position in the Rh(III) since the , the octahedral LF splitting, is weaker for the Co(III) complexes by about 6000 - 10000 cm^{-1}. From the $Rh(NH_3)_6^{3+}$ spectra one can estimate a maximum relaxation contribution of 6,000 cm^{-1}. Therefore, the O_h symmetry $^3T_{1g}$ state in Co(III) complexes must lie, after relaxation about 10000 cm_{-1} below $^1T_{1g}$ absorption positions. Spectral analysis by Yamasaki et al. (71,72) place the first LF singlet at 23,000^{-1} for dinitro complex and at 19,000 cm^{-1} for the isothiocyanate complex. (This difference of 3,500 cm^{-1} compares favourably with a 3,700 cm^{-1} difference in positions of the corresponding transients). So according to this analysis the relaxed triplet of dinitro complex should lie between 19,400 cm^{-1} and 13,500 cm^{-1}. If 16,000 cm^{-1} is taken as a trial value, the transient absorption at 488 nm corresponds to excitation to a state at 37,000 cm^{-1} above the ground state. In the ground state spectra, there isa band a which is unique to nitro, isothiocyanato,and azido substituted complexes in Co(III) -amine systems and which occurs at 40,000 cm^{-1} in the trans-$Co(en)_2(NO_2)_2^+$ case. This band may place the ligand π^* terminal level. If so, the ligand field triplet e_g^* to ligand π^* assignment for the transient is plausible.

One can use similar arguments to those used for Rh(III) by Ford et al. (62)to calculate rate constants as shown in Jablonski diagram figure (5.7). The quantum yield for photochemical product formation from a single ex-

cited state (in the case of Co-amine our argument was the Cl^- yield is most probably from the triplet state) is :

$$\Phi = \Phi' \frac{k_p}{k_p + k_n + k_r} \qquad \text{---------(5.3.1)}$$

where k_p is an aquation rate constant, k_r and k_n are rate constants of radiative and non radiative transition.

In the case of Rh(III) the parameters are for the example of $Rh(NH_3)_5Cl^{2+}$ (62) assigned as:

$$\Phi_{rx} = 0.18 \qquad k_{rx} = 13 \times 10^6$$
$$\Phi_{isc} = 1 \qquad k_n = 50 \times 10^6$$

In the corresponding Co(III) complexes if we assume that the life times of transients are given by $1/ k_n + k_r = 120 \times 10^{-12}$ for isothiocyanato and setting $0.1 < \Phi_{isc} < 1.0$ and the value of $\Phi_{rx} = 4 \times 10^{-4}$ Table (3-II) . we substitute these values in equation 5.3.1. The result is $48 \times 10^6 < k_{rx} < 4.8 \times 10^6$. If we impose the same assumption on trans-$Co(en)_2(NO_2)_2^+$. we find that $20 \times 10^6 < k_p < 2 \times 10^6$ The values are remarkably similar to those for Rh(III). They indicate that the difference between the Rh(III) and Co(III) cases lies mainly in k_n. Of course, the wavelength dependent pathway is a separate pathway.

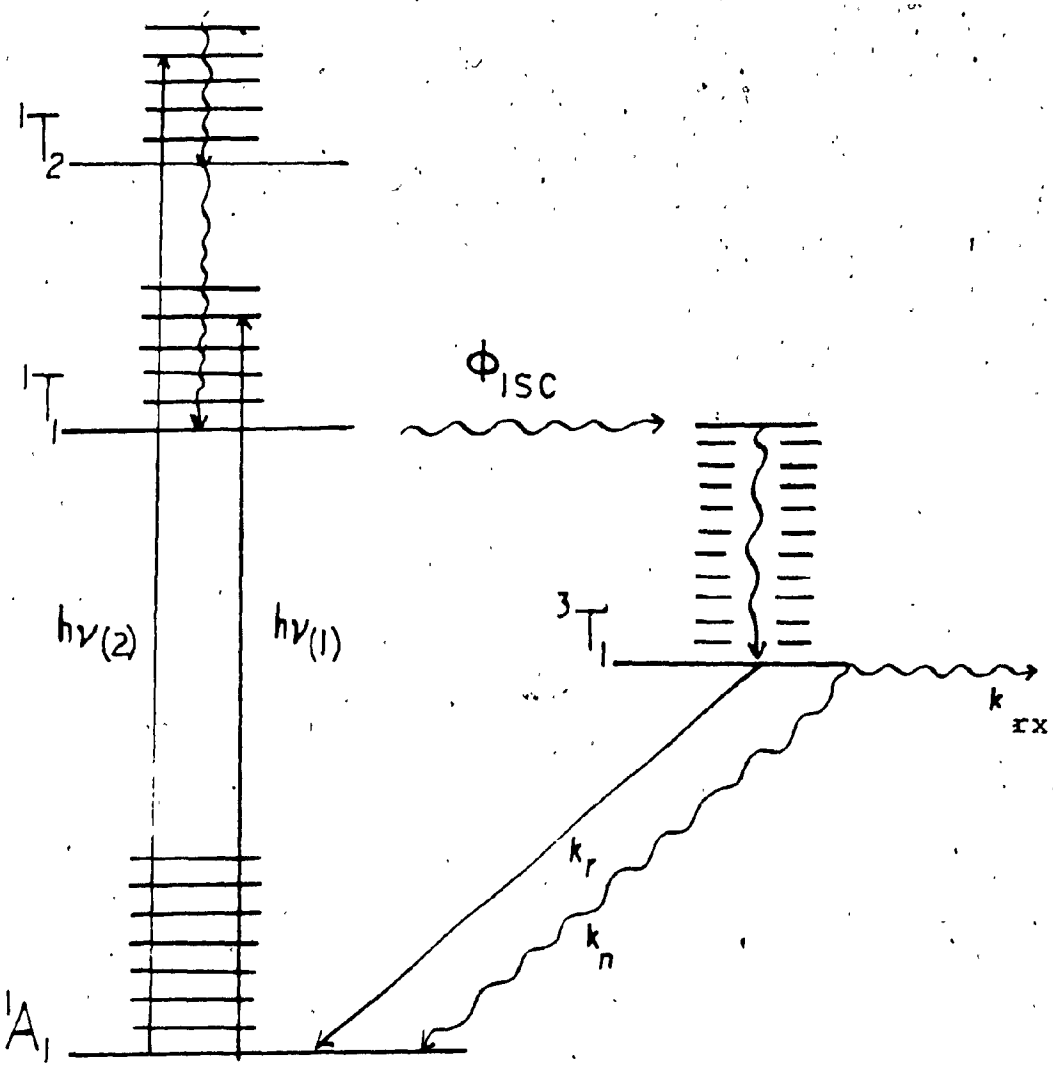

Figure 5.7 Jablonski diagram of Co-amine complexe.

5.7 Conclusion:

This study concentrated on three interrelated area: wavelength dependence of quantum yields, MCD spectroscopy and time resolved transient spectroscopy. The following conclusions have been reached:

1- The wavelength dependent yields show that aquation in the ligand field region of the electronic spectrum exhibit a) a wavelength dependence term and b) a wavelength independent part. The wavelength dependent parts have been argued to belong to initial excited states in a very fast process in competition with vibrational relaxation while the wavelength independent part is assigned to intersystem crossing to a second excited state which may react after vibrational equilibration. The most plausible labels are wavelength dependent reaction from the singlet and triplet reaction after vibrational relaxation.

2- Thr second area of study was the MCD spectroscopy of the cobalt amine complexes which showed specifically assignable A terms associated with the spin forbidden transitions. The MCD spectra of these Co-amine place the quintet at higher energy than the first singlet and it is therefore suggested that it can be neglected as a reactive state.

3- The third was a study of the lifetimes of the excited state by time resolved transient spectroscopy. This shows that the relaxed state (assigned as the triplet) has a 0.1 ns lifetime. The kinetic analysis this permits shows reactivity was similar to the triplet of

Rh(III)-amine complexes. The difference in lifetimes is for non-radiative decay lifetimes.

4- Wavelength dependence might arise from preferential population of a lower symmetry component. According to Vanquikenborne and Ceulemans (79) the A and E splitting of components of the $^1T_{1g}$ is related by the following equation:

$$E(A) - E(E) = E_T - E_c = 3(\sigma_L - \sigma_X)$$

σ_X is the ligand with a weak σ donor (Cl^-, Br^-, I^-, H_2O) while σ_L is a strong σ donor like (NH_3, en, CN). For the case of C_{4v} the E(A) state is related to the equatorial ligand while the E(E) state is related to the axial ligand. So the theory could account for a higher yield for ammonia in the case $Co(NH_3)_5Cl^{2+}$ at shorter wavelength and low yield at longer wavelength. The reverse would be true in the case of C_{2v} since E(E) is higher than E(A). Thus, the shorter wavelength radiation might populate E and favour reaction axially, contrary to what is observed for cis $Co(en)_2Cl_2^+$ complexes. The ethlynediamine yields also remain too low in this case.

5- The other theory of interest was the Hollebone theory (44,45) for decay along selected nuclear coordination. According to this both Cr-amine quartets and Co-amine singlets are expected to have the same properties since the excited state in both complexes is reacted using $|3t_{1u}>$ "buckle" mode of vibration. If the singlet excited

state is responsible for the wavelenth dependent part of the photo-aquation of Co-amine complexes and the quartet $^4T_{2g}$ is responsible for such Cr(III) chemistry as has often been argued both should have similar reactivity. Experimentally we found in cis-$Co(en)_2Cl_2$ $\Phi_{Cl^-} >> \Phi_{H^+}$ while in the case of cis-$Cr(en)_2Cl_2^{3+}$ the reverse happened. Thus, the theory is not yet helpful. Hollebone theory could explain fast intersystem crossing from the singlet to triplet state by quadrapole perturbation of the medium. for trans-$Co(en)_2Cl_2^+$ thereby explaining the absence of wavelength dependence on the absence of wavelength dependence on that case.

The final theory is that of Conti and Foster(43) which argues that the wavelength dependence is due to differences of absorption at different wavelengths arising from varying local solvent environments. If interconversion among these microenvironments is not fast compared to 10 ps, This is a promising approach to explaining wavelength dependent yields. Unfortunately, we do not know enough about solvent microenvironments to evaluate the full implications of this suggestion. The NMR tool recently introduced by Eaton et al.(87) might help in the future.

References

1- V. Balzani and V. Carassitti, Photochemistry of Coordinatination Compounds (Academic Press, New York, 1970).

2- E. Zinato In " Concept of Inorganic Photochemistry"; A.W. Adamson, P. Fleischaur, Eds.; (Wiley: New York, 1975); Chapter 3

3- V. Balzani, L. Moggi, F. Scandola, and V. Carassitti, Inorg. Chim. Acta. Rev., 1, 7,(1967).

4- R. A. D. Wentworth and T. S. Piper, Inorg. Chem., 4, 709,(1967).

5- R. B. Wilson and E. I. Solomon, J. Am. Chem. Soc., 102, 4085, (1980).

6- T. M. Dunn In " Modern Coordination Chemistry" J. Lewis and R. G. Wilkins, Eds., Interscience Publishers, New York, (1960)

7- A. W. Adamson, W. L. Watts, E. Zinatto, D. W. Watts, P. D. Fleischour, R. D. Lindholm, Chem. Rev., 68, 541, (1968).

8- J. F. Endicott, G. J. Ferraudi and J. Barbar, J. Phys. Chem., 79, 6, (1975).

9- C. K. Jorgenson, Adv. Chem. Phys. 5, 33,(1963).

10- H. Yamatara, Bull. Chem. Soc. Japan., 31, 95, (1958)

11- D. H. W. Carstens and G. A. Crosby , J. Mol. Spectroscopy., 34, 113, (1970).

12- H. B. Gray and C. H. Langford, "Ligand Substitution Processes", Eds., Benjamin, London, (1966).

13- M. F. Manfrin, G. Varani, L. Moggi and V. Balzani, Mol. Photochemistry, 1, 387, (1969).

14- J. F. Endicott and M. Hoffmann, J. Am. Chem. Soc., 87, 3348, (1965).

15- A. Haim and H. Taube , J. Am. Chem. Soc., 85, 495, (1963).

16- L. Moggi, N. Sabbatini, V. Balzani, Gazz. Chim. Ital., 97, 980, (1967).

17- A. Vogler and A. W. Adamson, J. Phys. Chem., 1, 67,(1970).

18- R. A. Pribush, C. K. Poon, and A. W. Adamson, J. Am. Chem. Soc., 96, 3027, (1974).

19- C. H. Langford and Carol P. J. Vuik, J. Am. Chem. Soc., 98,5410, (1976).

20- A. W. Adamson, J. Phys. Chem., 71, 798, (1967).

21- P. S. Sheridan and A. W. Adamson, J. Am. Chem. Soc., 3033, (1974).

22- Ref. (7) page 575

23- R. A. Pribush, R. E. Wright and A. W. Adamson, J. Am. Chem. Soc., 98, 2495, (1977).

24- M. Mingardi and G. B. Porter., J. Chem. Phys., 44, 4354, (1966).

25- L. Moggi, F. Balletta, V. Balzani and F. Scandola, J. Inorg. Nucl. Chem. 28, 2589, (1966).

26- A. W. Adamson and A. H. Sorper, J. Am. Chem. Soc., 80, 3805 (1958).

27- A. W. Adamson and A. H. Sorper, J. Inorg. Nucl. Chem., 8, 209, (1958).

28- M. Wrighton, H. B. Gray, G. S. Hammond, V. Miskowski, Inorg. Chem., 12, 740, (1973).

29- K. Luther, J. Schroeder, J. Troe, U. Unterberg, J. Phy. Chem., 84, 3072, (1980).

30- P. Debye, Trans. Electrochem. Soc., 81, 265, (1942).

31- J. Zimmerman and R. M. Noyes, J. Chem. Phys., 18, 658, (1950).

32- P. H. Liu and J. J. Zink ; J. Am. Chem. Soc., 99, 2155, (1977).

33- J. P. Leonard, Prog. Inorg. Chem., 17, 207, (1974).

34- R. M. Noyes, J. Am. Chem. Soc., 77, 2042, (1955).

35- R. M. Noyes, J. Am. Chem. Soc., 78, 5486, (1956).

36- K. Angermann, R. Schmidt, R. van Eldik, H. Kelm and F. Wastegastian, J, Inorg. Chem., 21, 1175, (1982).

37- G. S. Groves and C. F. Wells, J. Chem. Soc., Faraday Trans. 1, 78, 619, (1982).

38-J. E. Leffler and E. Grunwald "Rates and Equilbrium of organic Reactions" John Wiley and Sons, NY, (1963). page 297ff

39- R. E. Robertson and S. E. Sugamori, J. Am. Chem. Soc., 91, 7254, (1969).

40- C. H. Langford and L. Tipping, Can. J. Chem., 50, 887, (1972).

41- C. F. Wong and A. D. Kirk, Can. J. Chem., 54, 3794, (1976).

42- M. Cusumono and C. H. Langford, Inorg. Chem., 17, 2222, (1978).

43 C. Conti and L. S. Forster, J. Am. Chem. Soc.,99, 613,(1977).

44- B. R. Hollebone, C. H. Langford and N. Serpone, Coord. Chem. Rev. 39, 181. (1981).

45- B. R. Hollebone, Theoret. Chim. Acta, 56, 45, (1980)

46- N. A. P. Kane-Maguire,C. H. Langford and J. Conway, JCS. Chem. Commun., 801, (1974).

47- P. N. Schatz and A. J. McCaffery; J. Quarterly Rev. Chem. Soc., 23. 552, (1969).

48- C. Djerass, E. Bunnenberg and D. Elder, Pure and Applied Chemistry, 57, (1971).

49- L. Pauling and E. B. Wilson, " Introduction to Quantum Chemistry", McGraw-Hill, NY, (1935).

50- E. B. Wilson, J. C. Decius, and P. C. Cross, "Molecular Vibrations", McGraw-Hill, NY, (1955),section 7-9.

51- Micheal M. Malley, Picosecond Laser Techniques, In "Creation and Detection of the Excited State", Eds, W. R. Wave, Marcel Deker, Inc., NY, (1974),page (99).

52- P. M. Rentzepis, Picosecond Spectroscopy and Molecular Relaxation, in"Advances in Chemical Physics" Eds.,I. Prigogine and S. A. Rice, John Wily and Sons, NY, (1977).

53- A. A. Vuylstoke, J. Appl. Phys., 34, 1615, (1963).

54- F. Castelli and L. S. Forster, J. Am. Chem. Soc., 95, 7223, (1973).

55- J. T. Yardely and J. K. Beattie, J. Am. Chem. 94, 8925, (1972).

56- A. D. Kirk, P. H. Hoggard, G. B. Porter, M. G. Rockelly and M. W. Windsor, Chemical Physics Letters. 35, 199,

(1979).

57- T. Ohno and S. Kato, Bull. Chem. Soc. Japan., 43, 8, (1970).

58- R. LeSage, K. L. Sala, R. W. Yip, C. H. Langford, Can. J. Chem., 61, 2761, (1983).

59- N. Serpone, T. L. Netzel, M. Gouterman, J. Am. Chem. Soc., 104, 246, (1982).

60- A. Antipas, J. W. Buchler, M. Gouterman and P. D. Smith, J. Am. Chem. Soc., 100, 3015, (1978).

61- C. H. Langford and A. Y. S. Malkhasian, J. Chem. Comm., , 1210, (1982).

62- P. C. Ford, Coord. Chem. Revs., 44, 61, (1981).

63- G. G. Schlessenger, Inorg. Syn., 9. 160, (1967).

64- M. Krishnamurthy, J. Inorg. Nucl. Chem. 34, 3915, (1972).

65- J. C. Blair, Inorg. Syn., 2, 222, (1946).

66- A. Werner, Ann. 1, 386, (1912).

67- E. P. Harbulak and M. J. Albinak, J. Inorg. Nucl. Chem., 25, 232, (1963).

68- H. Kido and C. H. Langford, J. Am. Chem. Soc., 105, 1196, (1983).

69- P. Riccieri and H. L. Schlafer, Inorg. Chem., 4, 727, (1970).

70- E. E. Wegner and A. W. Adamson, J. Am. Chem. Soc., 88, 394, (1966).

71- K. Yamasaki, J. Hidaka and Y. Shimura, Bull. Chem. Soc. Japan., 50, 2624, (1977).

72- K. Yamasaki, J. Hidaka and Y. Shimura, Ibid; 49, 3060, (1970).

73- M. L. Sheely, Ind. Eng. Chem., 24, 1060 (1932).

74- A. J. McCaffrey, P. J. Stephens, and P. N. Schatz, Inorg. Chem. 6, 1614, (1967).

75- C. K. Jorgenson, "Absorption Spectra and Chemical Bonding in Complexes", Addison-Wesley, Reading, MA, 1962. Ch. 5.

76- B. R. Hollebone and M. Stillman, Chem. Phys. Letters, 66, 248, (1979).

77- V. S. Sastri and C. H. Langford, Can. J. Chem. 47, 4237, (1967).

78- Y. Tanabe and S. Sugano, J. Phy. Soc. of Japan., 9,753, (1954).

79- L. G. Vanquikenborne and A. Ceulemans Coord. chem. Rev., 48, 157, (1983).

80- R. Rumfeldt and J. Sellan, Can. J. Chem., 54, 519 (1976).

81- R. Rumfeldt and J. Sellan, ibid; 54, 1061 (1976).

82- N. A. P. Kane-Maguire and C. H. Langford, JCS. Chem. Commun., 351 (1973).

83- C. H. Langford, Inorg. Chem., 3, 228, (1964).

84- C. K. Jorgenson , Experimetia Suppl., 98, (1964).

85- C. Kutal and A. W. Adamson, Inorg. Chem., 12, 1993 (1973).

86- A. D. Kirk, Coord. Chem. Rev., 39, 225 (1981).

87- D. R. Eaton, C. V. Rogerson and A. C. Sandercock, J. Phy. Chem., 86, 1365 (1982).